HAL
open science

Cobalt complexes with N-heterocyclic ligands for catalysis

Yann Bourne Branchu

To cite this version:

Yann Bourne Branchu. Cobalt complexes with N-heterocyclic ligands for catalysis. Catalysis. Université Paris Saclay (COmUE), 2018. English. NNT : 2018SACLX075 . tel-02124429

HAL Id: tel-02124429

https://theses.hal.science/tel-02124429v1

Submitted on 9 May 2019

HAL is a multi-disciplinary open access archive for the deposit and dissemination of scientific research documents, whether they are published or not. The documents may come from teaching and research institutions in France or abroad, or from public or private research centers.

L'archive ouverte pluridisciplinaire **HAL**, est destinée au dépôt et à la diffusion de documents scientifiques de niveau recherche, publiés ou non, émanant des établissements d'enseignement et de recherche français ou étrangers, des laboratoires publics ou privés.

université PARIS-SACLAY

NNT : 2018SACLX075

ÉCOLE POLYTECHNIQUE
UNIVERSITÉ PARIS-SACLAY

Complexes de Cobalt à ligands *N*-hétérocycliques pour la catalyse

Thèse de doctorat de l'Université Paris-Saclay
préparée à l'École polytechnique

École doctorale n°571 Sciences Chimiques : Molécules, Matériaux, Instrumentation et Biosystèmes 2MIB
Spécialité de doctorat: Chimie

Thèse présentée et soutenue à Palaiseau, le 15 octobre 2018, par

Yann Bourne-Branchu

Composition du Jury :

Abderrahmane Amgoune Professeur, Université Claude Bernard Lyon 1 (– UMR 5246)	Président
Muriel Durandetti Maître de conférences, Université de Rouen (– UMR 6014)	Rapporteur
Marc Petit Chargé de recherche, Sorbonne Université (– UMR 8232)	Rapporteur
Lutz Ackermann Professeur, Georg-August Universität	Examinateur
Jérôme Hannedouche Chargé de recherche, Université Paris Sud (– UMR 8182)	Examinateur
Corinne Gosmini Directrice de recherche, École polytechnique (– UMR 9168)	Directrice de thèse
Grégory Danoun Chargé de recherche, École polytechnique (– UMR 9168)	Co-Directeur de thèse

Thèse de doctorat

Complexes de Cobalt à ligands *N*-hétérocycliques pour la catalyse

Thèse de doctorat de l'Université Paris-Saclay

préparée à

l'École polytechnique

École doctorale n°571 Sciences Chimiques : Molécules, Matériaux, Instrumentation et Biosystèmes 2MIB

Spécialité de doctorat: Chimie

Thèse présentée et soutenue à Palaiseau, le 15 octobre 2018,

par

Yann Bourne-Branchu

Composition du Jury :

Abderrahmane Amgoune Professeur, Université Claude Bernard Lyon 1 (– UMR 5246)	Président
Muriel Durandetti Maître de conférences, Université de Rouen (– UMR 6014)	Rapporteur
Marc Petit Chargé de recherche, Sorbonne Université (– UMR 8232)	Rapporteur
Lutz Ackermann Professeur, Georg-August Universität	Examinateur
Jérôme Hannedouche Chargé de recherche, Université Paris Sud (– UMR 8182)	Examinateur
Corinne Gosmini Directrice de recherche, École polytechnique (– UMR 9168)	Directrice de thèse
Grégory Danoun Chargé de recherche, École polytechnique (– UMR 9168)	Co-Directeur de thèse

"Creativity is inventing, experimenting, growing, taking risks,
breaking rules, making mistakes and having fun"

Mary Lou Cook

Acknowledgements

La plupart des gens le savent, je ne suis pas la personne la plus expressive qui soit. Ceci étant dit, les lignes qui suivront manqueront peut-être un peu de sens, et ne reflèteront probablement jamais assez à quel point je suis reconnaissant envers toutes les personnes que j'ai rencontrées, avec qui j'ai travaillé, qui m'ont aidé et soutenu au cours de ces 3 années de thèse mémorables.

Tout d'abord, je tiens à remercier les personnes qui ont dirigées cette thèse : le Dr. Corinne Gosmini, que je remercie pour m'avoir accordé cette thèse, accueilli dans son laboratoire, et fait découvrir la chimie du cobalt, ainsi que pour son écoute, et sa patience ; et le Dr. Grégory Danoun, que je remercie pour m'avoir encadré tout au long de cette thèse, pour avoir écouté mes idées et mes propositions, même quand elles allaient peut-être un peu trop loin… et pour m'avoir soutenu dans mes travaux, leurs réussites et leurs échecs.

Ensuite, je remercie les membres de mon jury de thèse, qui ont accepté d'évaluer les travaux que j'ai réalisés au cours de ces 3 années : le Pr. Abderrahmane Amgoune, qui a présidé ce jury, le Dr. Muriel Durandetti et le Dr. Marc Petit, qui ont évalué et commenté mon manuscrit, et le Pr. Dr. Lutz Ackermann et le Dr. Jérôme Hannedouche, qui ont assisté et participé à l'examen de ma soutenance de thèse.

Je remercie aussi tout les membres du LCM, avec qui j'ai pu travailler et échanger, à commencer par (même si le labo est maintenant organisé par thématique…) la team cobalt, dans le labo 8, avec Alice et Ying-Xiao, qui étaient là quand je suis arrivé, et Céline et son optimisme, qui étaient là quand je suis parti (bonne chance pour la fin de ta thèse !). Je remercie aussi Elodie, pour sa bonne humeur et son aide précieuse en matière de synthèse organique et de sécurité. Le labo 7 étant le mien, passons au labo 6, 5 et 4, sur la chimie des iminophosphoranes, avec Irene et sa playlist dont on ne se lasse jamais ! ainsi que Louis, et sa passion de la chanson française ! et je remercie aussi bien évidemment leur cheffe, Audrey, pour ses conseils, tant en chimie que lors de la préparation de ma soutenance. Je garde tout de même une pensée pour Karl, dans le labo 3, ainsi que pour les GC dont je me suis occupé pendant une partie de ma thèse. Dans le labo 2, je remercie Duncan, et son engouement à travailler sur des quantités de produit que je qualifierais de respectables. Enfin, le labo1, le labo de la chimie des lanthanides, où je remercie greg, qui a permis la mise en place de la partie chimie de coordination de cette thèse, et qui a grandement contribué aux résultats obtenus de par ses conseils et ses idées. Je remercie aussi ses étudiants : Arnaud et son légendaire pessimisme, Mathieu (Capitaine !) et nos conversations musicales, Ding *and its multiple faces*, et

Violaine et sa bonne humeur immuable, ainsi que Jules, Maxime et Valeriu, arrivés sur la fin de ma thèse et que je n'ai pas vraiment eu le temps de connaître plus. Je remercie aussi Anne-Florence, qui m'a beaucoup aidé, entre autres, pour la gestion des commandes de gaz, et Louis R., toujours vaillamment présent à son poste jours après jours. Je remercie aussi, à « l'étage du dessus », Marie, pour nos conversations, et qui a réalisé les structures cristallines, et Sophie, qui a réalisé les spectres de masses et qui m'a aidé à les analyser, ainsi que Cédric, Gilles F., Gilles O., Stéphane, Edith, Adrien, Ségolène, Svetlana, Radhika, Silvia, Zsuzsanna, et Vincent, ainsi que Christophe, Cindy, Gilles A. et Thérèse. Je remercie aussi Sukhakah et le rôle qu'il a joué malgré lui, et les étudiants que j'ai pu encadrer au cours de ces 3 années : Clément, Gustave, Hadrien, Ariane, Sara, François et Louis, ainsi que Junghan.

Si une thèse se déroule certes dans le laboratoire, elle impacte et est impactée tout autant par la vie à l'extérieur du labo. Aussi, je remercie tous ces gens que j'ai rencontré en-dehors du laboratoire pendant ma thèse (principalement *via* les fanfare, oui…). Je remercie donc les fanfares parisiennes par lesquelles je suis passé et leurs membres : la Brass de Pneu, les Zébra Rayures, le CUC et la V4, pour le temps qu'ils m'ont pris et laissé aux cours de ces 3 années ; et l'FMR Brass Band, une bonne idée, mais peut-être pas au meilleur moment (mais ça en valait la peine !).

Enfin, je remercie les gens qui étaient déjà là avant la thèse, et qui m'ont soutenu et supporté pendant. Entre autres, les membres de la CacoPhoniE, ceux qui sont passé par là avant moi, qui passeront par-là après, qui m'ont conseillé et qui m'ont supporté (pour n'en nommer que certains, Sarah, Virginie, Anne-Laure, Hugues, Debs, Sylvain, Maïlys, Camille, Célia, et j'en passe…) ; je remercie aussi François, Ishak et Loïc, les 3 indéfectibles, toujours présents après toutes ces années, et, enfin, ma famille, qui a toujours cru en moi avant et qui continuent à me suivre dans mes choix.

Résumé français

La préparation de nouvelles molécules complexes et l'optimisation de leurs conditions et voies de synthèse a toujours été un des principaux objectifs de la chimie organique. Parmi les méthodes de synthèse existante, les réactions de couplage organométalliques font partie des découvertes les plus importantes. La catalyse organométallique a dès lors connu un développement continue, conduisant à la mise au point de catalyseurs toujours plus performants et polyvalents. Si de nombreuses nouvelles réactions ont été découvertes au début en utilisant des catalyseurs à base de palladium, ruthénium ou rhodium, les problèmes liés à leur rareté et leur prix en augmentation incitent les chercheurs à développer de nouvelles méthodes catalytiques employant d'autres métaux de transition plus abondants, comme le fer, le cobalt et le nickel. S'ils sont capables de réaliser les mêmes type de réactions de couplages, leur capacité à réaliser plus facilement des transferts mono-électronique ouvre aussi de nouvelles possibilités de réactivité.

C'est dans ce cadre que ce travail de thèse a été réalisé, avec pour objectifs de mettre au point de nouvelles réactions catalysées au cobalt et de développer de nouveaux complexes de cobalt permettant, à terme, d'élargir la gamme de réactivité du cobalt.

Dans un premier temps, nous avons travaillé sur l'activation de la liaison C–N de la fonction amide par des complexes de cobalt. Cette nouvelle réactivité de la fonction amides a été mise en évidence par les groupes de Garg et Szostak en 2015, en utilisant des amides activés comme partenaire de couplage électrophiles dans des réactions de couplages catalysées par des complexes de nickel, palladium ou rhodium.

Dans le but de développer de nouvelles réactions faciles à mettre en œuvre et synthétiquement intéressantes, nous avons décider de travailler avec des *N*-Boc amides comme partenaires de couplage, et avons réussi à obtenir des résultats préliminaires prometteurs avec des couplages entre amides et bromures d'aryle, permettant de former des benzophénones dissymétriques, ainsi qu'avec une réaction d'homo-couplage d'amides, permettant la formation de benzophénones symétriques. A la suite de ces premiers résultats, nous avons réussi développer une réaction catalysée de conversion de la fonction amide activée en ester, dans des conditions douces et non anhydres. Ces conditions ont aussi une grande chemosélectivité, permettant d'utilisées des substrats fonctionnalisés. Cette réaction de couplage entre un amide et un alcool a été testée avec une large gamme d'alcool, même peu nucléophiles, et d'amides, aussi bien aliphatiques qu'aromatiques, avec de bons rendements. Cependant, cette réaction a aussi des restrictions, et est très influencé par l'encombrement stériques des réactifs. Ainsi, les alcools tertiaires ne peuvent pas être couplés.

Un des grands intérêts synthétiques de cette réaction est dû au fait qu'elle fonctionne aussi avec les amides utilisés comme groupements directeurs pour les réaction d'activation C–H, permettant leur conversion en ester avec un rendement correct et dans des conditions douces. Cette dernière application de la réaction de conversion des amides en esters trouve son utilité dans le domaine de la synthèse totale, où l'utilisation de groupements directeurs de type amide, très utilisés pour les réactions de C–H activation, peut s'avérer être un problème sur l'ensemble d'une synthèse. En effet, les amides non protégés sont peu réactifs et donc difficilement retirable d'une molécule substrat dans des conditions douces, ne touchant que la fonction amide. Avec ce nouveau pan de la réactivité des amides, il peut dorénavant être possible d'utiliser les amides comme groupement directeur pour la C–H activation, puis comme site réactif, pour des réactions chemosélective.

Dans un second temps, nous avons travaillé sur le développement d'une nouvelle famille de complexes bimétalliques, basée sur les ligands dipyrrométhènes. Tout d'abord, la synthèse du ligand ditopique 5-(4-pyridyl)dipyrrométhène a été optimisée. En effet, la synthèse de dipyrrométhènes requiert une étape de condensation, entre un aldéhyde et un pyrrole, menant au dipyrrométhane, et une étape d'oxydation, généralement réalisée avec de la DDQ, permettant l'obtention du dipyrrométhène. Cependant, cette dernière étape ne donne que de faibles rendements dans le cas du dipyrrométhène voulu. Cet oxydant a été remplacé par MnO_2, utilisé pour les oxydations ménagées et dans les réaction d'aromatisation. Ce changement de réactif a permis d'augmenter significativement le rendement de cette étape d'oxydation pour le 5-(4-pyridyl)dipyrrométhène, passant de 16% avec la DDQ, décrit dans la littérature, à 96% dans notre cas, avec un protocole expérimentale plus simple à mettre en œuvre. En effet, l'utilisation de MnO_2 permet d'obtenir le produit d'oxydation pur après une simple filtration sur Célite du milieu réactionnel. En ce qui concerne l'étape de condensation, réalisée sans solvant, à 90°C dans un large excès (12 à 14 équivalents par rapport à l'aldéhyde) du pyrrole correspondant au dipyrrométhane désiré, elle a été optimisée pour les pyrroles à hauts points de fusion et difficile à obtenir, comme le 2-phénylpyrrole. En ajoutant une très faible quantité de toluène (5 équivalents par rapport à l'aldéhyde), il a été possible de diminuer la quantité de pyrrole engagée dans la réaction à 5 équivalents. Avec ces nouvelles conditions, 3 pyridyl-dipyrrométhènes ont pu être préparés, avec différents degrés d'encombrement au niveau de la partie dipyrrométhènes : le 5-(4-pyridyl)dipyrrométhène, le 1,9-diphényl-5-(4-pyridyl)dipyrrométhène et le 1,9-*tert*-butyl-5-(4-pyridyl)dipyrrométhène.

Plusieurs tests de coordination ont été réalisés entre chacun de ces ligands et différents sels et précurseurs de cobalt. A la suite de ces tests, il a été mis en évidence que les sels de cobalt(II) se coordinent préférentiellement sur la pyridine des dipyrrométhènes substitués. A l'inverse, dans la cas du dipyrrométhène non substitué, les sels de cobalt(II) se coordinent sur la partie dipyrrine, conduisant, pour les halogénures et les acétates de cobalt(II), au complexe *tris*(dipyrrin) cobalt(III) ou, pour les acetylacetonate de cobalt(II) et (III), au complexe *bis*(dipyrrin) cobalt(III). Avec le précurseur $[Cp^*Co^{II}Cl]$, il a néanmoins été possible d'obtenir le complexe de cobalt(II) $[Cp^*Co^{II}(dipyrrin)]$, avec la partie pyridine libre.

Dans le cas du ligand 1,9-diphényl-5-(4-pyridyl)dipyrrométhène, en bloquant au préalable le site de coordination de la pyridine, avec un complexe chlorure de *bis*(bipyridine)ruthénium(II), la coordination du sel de cobalt se fait alors dans la partie dipyrrine, dans des conditions réactionnelles douces. Le complexe bimétallique cobalt/ruthénium ainsi obtenu est encore à étudier , autant pour ses propriétés luminescentes que pour ses potentielles applications en catalyse.

En ouverture sur ces travaux de thèse, il serait intéressant de croiser les 2 parties de cette thèse et d'étudier la potentielle réactivité des complexes cobalt/dipyrrine et cobalt/ruthenium/dipyrrine par rapport aux amides activés. L'utilisation de la partie ruthenium(II) ouvre la possibilité d'une activation photo-induite de la fonction amide et le développement de réactions de couplages croisés avec des amides sans excès de métal réducteur.

Contents

List of abbreviations **16**

General introduction **20**

Part I. Reactivity of cobalt catalyst with non-planar amides **25**

I.1. State of the art about metal-catalyzed coupling reactions with distorted amides 28

I.1.1. Nickel-catalyzed reactions with amides 29

I.1.2. Palladium-catalyzed reactions with amides 34

I.1.3. Rhodium-catalyzed reactions with amides 36

I.1.4. Cooperative catalysis 37

I.2. Cobalt reactivity toward non-planar amides 39

I.2.1. The choice of the amide and preliminary studies 39

I.2.2. The semi-decarbonylative reductive homocoupling of amides 42

I.2.3. The reductive cross-coupling between amides and aryl halides 45

I.2.4. The cobalt-catalyzed amide-to-ester conversion 47

I.3. Application of the amide-to-ester conversion: toward new synthetic strategy 56

I.3.1. The Resorcylic Acid Lactones 58

I.3.2. The C-H functionalization / Amide-to-ester conversion strategy 59

I.4. Conclusions and perspectives 61

Bibliography of part I 63

Part II. Development of new cobalt catalysts with dipyrromethene ligands 67

II.1. State of the art about dipyrromethene metallocomplexes 71

II.2. Synthesis and optimization of dipyrromethenes 75

II.2.1. State of the art about 5-4-pyridyl)dipyrromethenes 76

II.2.2. The synthesis of pyrroles 77

II.2.3. Study of the condensation step: synthesis of dipyrromethane 78

II.2.4. The case of the 2-phenylpyrrole condensation 80

II.2.5. Optimization of the oxidation step 81

II.3. Preliminary tests of cobalt complexation.....85

II.3.1. Coordination with 5-(4-pyridyl)dipyrromethene 85

II.3.2. Coordination with 1,9-di-*tert*-butyl-5-(4-pyridyl)dipyrromethene 88

II.3.3. Coordination with 1,9-diphenyl-5-(4-pyridyl)dipyrromethene.....91

II.4. The cobalt-ruthenium bimetallic complexes.....96

II.4.1. The choice of the ruthenium precursor 97

II.4.2. Synthesis of the bimetallic cobalt-ruthenium complex 99

II.5. Conclusions and perspectives 101

Bibliography of part II.....104

General conclusions and perspectives..... 108

Experimental part 111

List of Abbreviations

Ac: acetyl

acac: acetylacetonate

ACN: acetonitrile

Ad: adamantyl

Alk: alkyl

aq: aqueous

Ar: aryl

Benz-Icy: 1,3-dicyclohexylbenzimidazol-2-ylidene

Bn: benzyl

Boc: *tert*-butoxycarbonyl

BODIPY: boron dipyrrin

bpy: 2,2'-bipyridine

Bt: benzotriazyl

COD: cyclooctadiene

Cp: cyclopentadienyl

Cp*: pentamethyl cyclopentadienyl

Cy: cyclohexyl

d: doublet

DCE:1,2-dichloroethane

DCM: dichloromethane

dcype: 1,2-(di-cyclohexylphosphino)ethane

DDQ: 2,3-dichloro-5,6-dicyano benzoquinone

deeb: 4,4'-bis(ethoxycarbonyl)-2,2'-bipyridine

Dipp:2,6-di-isopropylphenyl

DMAP: dimethylaminopyridine

DME:1,2-dimethoxyethane

DMF: *N*,*N*-dimethylformamide

DMSO: dimethyl sulfoxide

dpm: dipyrromethene (dipyrrin)

dppf: 1,1'-ferrocenediyl-bis((diphenylphosphine)

e-D: electron donating specie

EDC: 1-ethyl-3-(3-dimethylaminopropyl)carbodiimide)

Et: ethyl

et al.: *et alii*

et coll.: *et collaborateurs*

equiv.: equivalent

FID: flame ionization detector

GC: gas chromatography

HBTU: 3-[bis(dimethylamino)methyliumyl]-3*H*-benzotriazol-1-oxide hexafluorophosphate

(Het)Ar: heteroaryl

Hex: hexyl

HRMS: high-resolution mass spectrometry

ICy: 1,3-dicyclohexylimidazol-2-ylidene

i-Pr: isopropyl

IPr: 1,3-bis(2,6-diisopropylphenyl)imidazole-2-ylidene

L.B.: Lewis base

Me: methyl

MOF: metal-organic framework

Ms: methylsulfonyl (mesyl)

Nacnac: 1,3-diketiminate

n.d.: not detected

NHC: *N*-heterocyclic carbene

NMP: *N*-methylpyrrolidinone

NMR: nuclear magnetic resonance

Nu: nucleophile

ORTEP: Oak Ridge Thermal Ellipsoid Plot

Pd-PEPPSI: ((1,3-bis(2,6-diisopropylphenyl)imidazole-2-ylidene) (3-chloropyridyl) palladium(II) dichloride

Ph: phenyl

phen: phenanthroline

PMHS: polymethylhydrosiloxane

Pin: pinacol

ppm: part per million

Py: pyridine, pyridyl

q: quadruplet

RCM: ring closing metathesis

r.t.: room temperature

s: singulet

SIPr: 1,3-bis(2,6-diisopropylphenyl)imidazolidine

t: triplet

TBAB: tetrabutylammonium bromide

TBAF: tetrabutylammonium fluoride

TBS: tributyl silyl

t-Bu: *tert*-butyl

terpy: terpyridine

Tf: trifluoromethanesulfonyl

THF: tetrahydrofuran

TLC: thin layer chromatography

TMS: trimethyl silyl

TIPS: triisopropyl silyl

Ts: toluenesulfonyl (Tosyl)

XANTPhos: 4,5-bis(diphenylphosphino)-9,9-dimethylxanthene

XRD: X-ray diffraction

General Introduction

The preparation of new elaborate molecules and the optimization of their synthesis has always been one of the major points of organic chemistry. One of the most important breakthroughs in the field of synthetic methodology was the discovery of metal-catalyzed cross-coupling reactions, by Suzuki, Negishi, Heck, Miyaura, rewarded by a Nobel Prize in 2010,[1] which allowed new synthetic disconnections. Since this discovery, organometallic catalysis underwent a continual development, leading to more polyvalent catalysts and more efficient transformations. Concerning coupling reactions, the majority of these developments were focused on the use of palladium-, ruthenium- or rhodium-based catalysts, known for their efficiency. However, these metals are also very employed in other domains, like for the construction of electronic components. These high valued applications led to an important increase of the prices of these scarce elements (Graphe 1).[2]

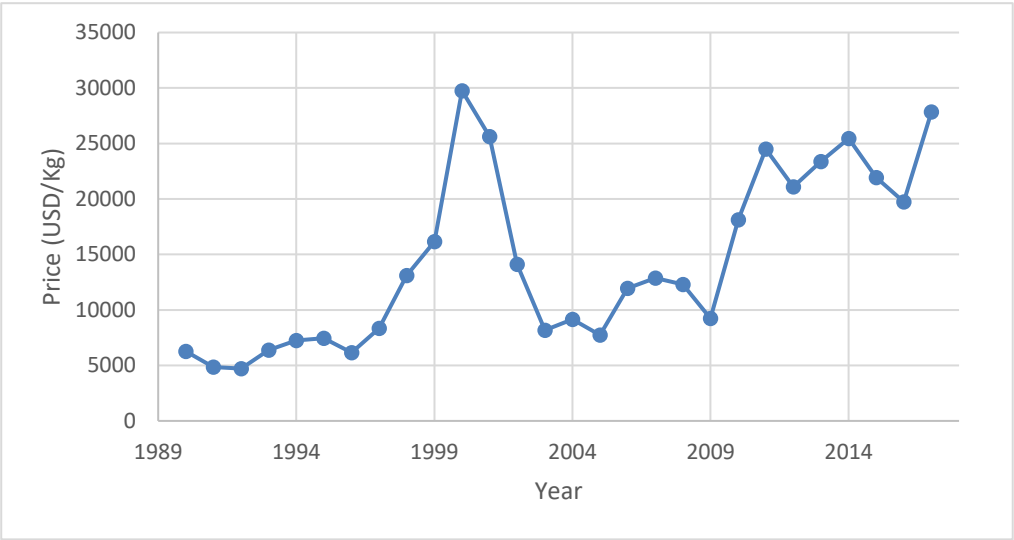

Graphe 1: Evolution of the prices of palladium between 1990 and 2017, in USD/Kg (real price)

Regarding these drawbacks, research in catalysis is now focused on the use of other transition metals, especially first-row transition metal, to adapt the same reactions or to develop new reactivity. Among these metals, a lot of researches are done on the use of iron, cobalt and nickel in coupling reactions to replace their corresponding second-row transition metals. First-row transition metals are indeed more abundant, and therefore less expensive. They also proved to be efficient to catalyze the same type of coupling reactions. Moreover, their capacity to proceed through single electron transfer (radical mechanism) as well as through redox neutral mechanisms allows the development of new reactions and new selectivity.

If iron is the most bio-compatible element of group VIII, and the cheapest, it stands as a metal difficult to use in catalysis.[3] It indeed requires strong reagents, like Grignard reagents, to be activated. On another hand, nickel has a reactivity close to palladium, and can be used as substitution metal in Suzuki-Miyaura cross coupling.[4] But contrary to palladium, it can proceed to radical transfer and single-electron mechanism. However, nickel salts present a high toxicity to the environment, making it an economically better option than palladium, but not a durable option.

Concerning cobalt, it is an element more bio-compatible than nickel, also able to easily proceed through radical or two-electron mechanism. Contrary to rhodium, Co(I) and Co(III) are not very stable, and have to be prepared and stored under controlled conditions, or generated *in situ*. For this reason, cobalt tends to have its proper chemistry, standing more as an element allowing new reactivity or selectivity than an alternative to rhodium. Besides, cobalt salts can also be used to catalyze cross-coupling reactions[5]. If mechanisms are still under investigation by several research groups, cobalt has already be used to catalyzed Kumada cross-coupling,[6] Negishi cross-coupling[7] and recently Suzuki-Miyaura cross-coupling.[8,9] Another type of coupling reactions cobalt is able to catalyzed, as nickel, is the reductive cross-coupling (Figure 1).[10]

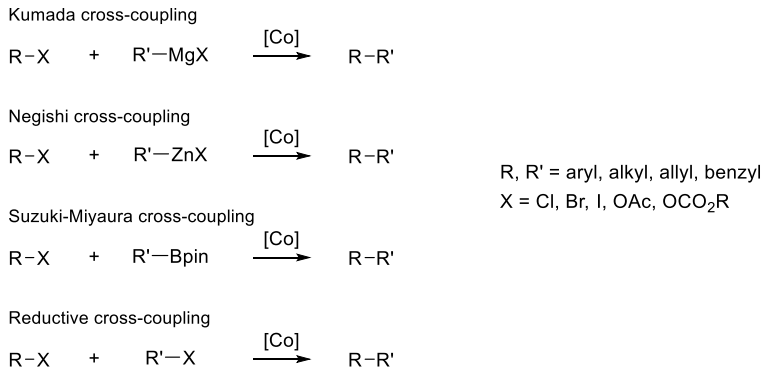

Figure 1: Examples of cobalt-catalyzed cross-coupling reactions

Contrary to the redox neutral cross-coupling, that involves an electrophilic specie and a nucleophilic specie, the reductive cross-coupling involves two electrophilic species and coupled them, under reductive conditions. Generally, the active cobalt specie is a Co(I) complex coming from the *in situ* reduction of a Co(II) complex. In redox neutral coupling reaction, this activation step occurs before the addition of the reagent, in order to have a “classical” catalytic cycle. In the case of a reductive cross-coupling, the presence in the reaction medium of a reductant in excess leads to the continual reduction of the cobalt catalytic specie, in a different catalytic cycle (figure 2).

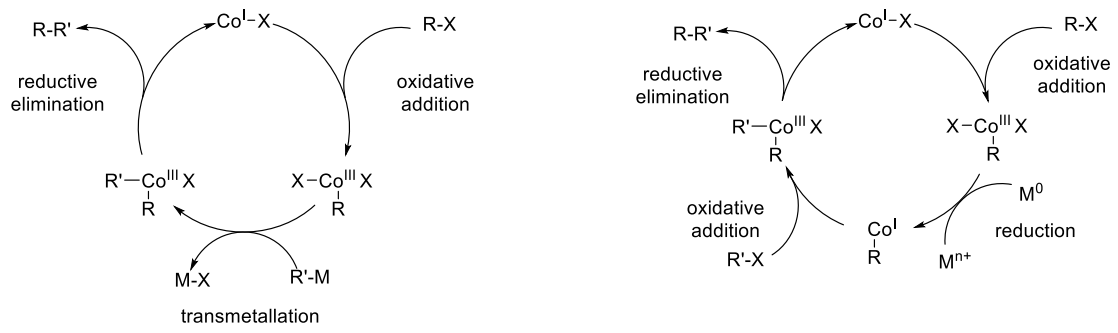

Figure 2: Catalytic cycle for redox-neutral cross-coupling (left) and reductive cross-coupling (right)

This kind of cobalt-catalyzed coupling reaction has been widely studied in our laboratory, and extended to the formation of Csp^2_{aryl}–Csp^2_{aryl},[11] Csp^2_{aryl}–Csp^3_{benzyl},[12] Csp^3_{alkyl}–Csp^3_{alkyl} bond,[13] from two halide, acetate or carbonate electrophilic compounds. Our objectives for this thesis were to continue to extend and explore the reactivity of cobalt catalysts.

In the first part, we describe our research to extend the scope of usable electrophilic coupling partner to amides. In the last years, the development of activated amides allows their use as electrophilic reagent in palladium- and nickel-catalyzed cross-coupling. We thus tried to applied and adapt the conditions of the cobalt-catalyzed reductive coupling to the use of activated amides, in order to develop potential new reactivity.

In the second part, we describe our work to develop a new family of bimetallic cobalt complexes, including a reductant, with a dipyrromethene type ligand. The presence of an regenerable reductant directly linked to these complexes should allow to dispense with the excess of metallic reductant in cobalt-catalyzed coupling reactions.

Bibliography

[1] C. C. C. Johansson Seechurn, M. O. Kitching, T. J. Colacot, V. Snieckus, *Angew. Chem. Int. Ed.* **2012**, *51*, 5062–5085.

[2] Denvergold, "Historical Palladium Prices," can be found under https://www.denvergold.org/precious-metal-prices-chart/historical-palladium-prices/, n.d.

[3] I. Bauer, H.-J. Knölker, *Chem. Rev.* **2015**, *115*, 3170–3387.

[4] F. S. Han, *Chem. Soc. Rev.* **2013**, *42*, 5270–5298.

[5] G. Cahiez, A. Moyeux, *Chem. Rev.* **2010**, *110*, 1435–1462.

[6] G. Cahiez, C. Chaboche, C. Duplais, A. Giulliani, A. Moyeux, *Adv. Synth. Catal.* **2008**, *350*, 1484–1488.

[7] H. Avedissian, L. Bérillon, G. Cahiez, P. Knochel, *Tetrahedron Lett.* **1998**, *39*, 6163–6166.

[8] J. M. Neely, M. J. Bezdek, P. J. Chirik, *ACS Cent. Sci.* **2016**, *2*, 935–942.

[9] S. Asghar, S. B. Tailor, D. Elorriaga, R. B. Bedford, *Angew. Chem. Int. Ed.* **2017**, *56*, 16367–16370.

[10] C. E. I. Knappke, S. Grupe, D. Gärtner, M. Corpet, C. Gosmini, A. Jacobi Von Wangelin, *Chem. Eur. J.* **2014**, *20*, 6828–6842.

[11] C. Gosmini, A. Moncomble, *Isr. J. Chem.* **2010**, *50*, 568–576.

[12] S. Pal, S. Chowdhury, E. Rozwadowski, A. Auffrant, C. Gosmini, *Adv. Synth. Catal.* **2016**, *358*, 2431–2435.

[13] Y. Cai, X. Qian, C. Gosmini, *Adv. Synth. Catal.* **2016**, *358*, 2427–2430.

Part I. Reactivity of cobalt catalyst with non-planar amides

The amide function is a weakly reactive chemical function, very stable and common in nature, mainly as the bond between amino-acids in polypeptidic chains.[1] This strong stability is linked to the planar geometry of amides, due to the conjugation between the π system of the carbonyl and the electronic lone-pair of the nitrogen. This conjugation leads to the formation of equilibrium between 2 resonance structures: neutral and zwitterionic (Figure I-1).

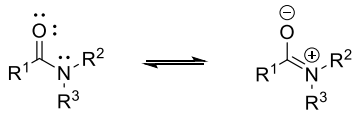

Figure I-1: Classical representation and zwitterionic form of the amide function

Despite its low reactivity, several methods have been developed to allow the transformation of the amide function into other chemical functions. Well known as a formylation method for aromatic cycles, the Vilsmeier-Haack reaction, developed in 1927, allow the formation of a ketone or an aldehyde from a *N*,*N*-disubstituted amide, *via* its "activation" by phosphorus oxychloride.[2]

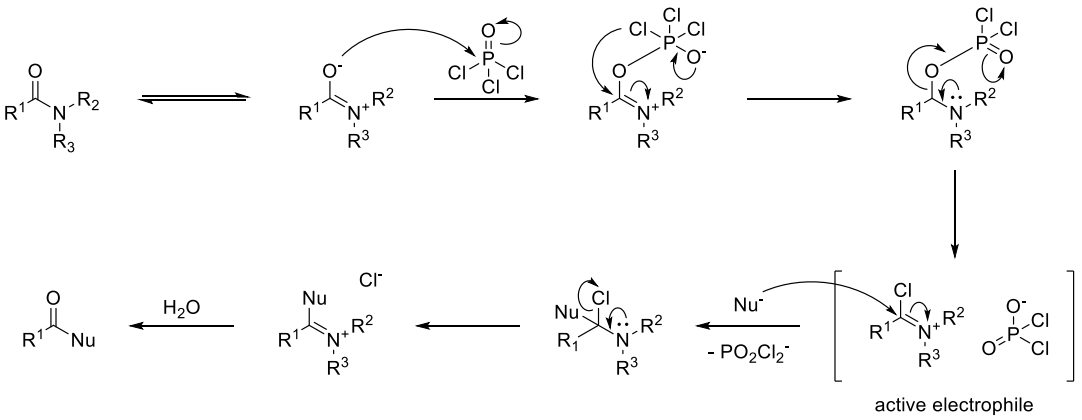

Scheme I-1: Mechanism of the Vilsmeier-Haack reaction

The electrophilic species thus formed can realize an aromatic electrophilic substitution to give the corresponding aroylated compound (Scheme I-1). However, the high reactivity of $POCl_3$ and its halogenating

properties[3] remain major drawbacks, limiting the possibility to use this methodology on highly functionalized substrates.

In 1981, Weinreb published a method to realize controlled nucleophilic mono-addition of organometallic species on amides.[4] Indeed, as other carboxylate derivatives, amides are sensible to strong nucleophiles like organomagnesium or organolithium species. The addition of these reagents on carboxylate derivatives leads to the formation of a tertiary alcohol or a mix between tertiary alcohol and ketone, depending of the used excess of nucleophile: the addition of an organometallic reagent on an amide leads firstly to an intermediate that will rearrange to form a ketone. However, as ketones are more reactive than carboxylate derivatives toward nucleophilic attack, it will undergo a second addition, leading to the formation of a tertiary alcohol. To avoid this second addition, Weinreb developed an amide with a particular nitrogen substitution that stabilizes the first intermediate at low temperature: the *N*-methyl-*N*-methoxy amide. The presence of the methoxy group allows the coordination of a divalent metal between the oxygen of the intermediate hemiaminal and the methoxy, forming a five-membered intermediate preventing the rearrangement leading to ketone. This intermediate is hydrolyzed during the quench of the reaction, producing the corresponding ketone and amine (Scheme I-2).

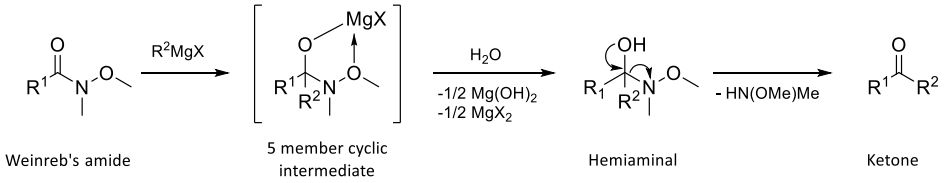

Scheme I-2: Mechanism of the nucleophilic attack on a Weinreb's amide

In 2007, Spletstoser *et al*. used the Schwartz's reagent, known for alkene and alkyne hydrozirconation reaction, to reduce amides into aldehydes. [5] As for Weinreb's amide, the Schwartz's reagent form a four-membered metallacycle intermediate, with zirconium coordinated to the oxygen and the nitrogen of the amides (scheme 4). This reaction is selective of amide and is realized in very mild condition. Regarding the mechanism, it starts with the coordination of the zirconium to the oxygen, allowing the addition of weak nucleophilic hydride to the carbonyl (Scheme I-3).

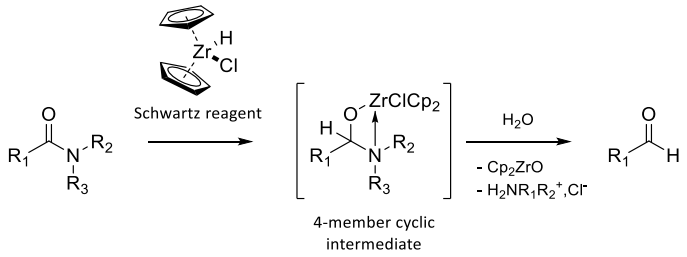

Scheme I-3: Mechanism of the amide reduction by the Schwartz reagent

If these methods allowed a controlled reactivity of amides and their efficient transformation into ketone and aldehyde, they involve the use of highly reactive reagents ($POCl_3$, organomagnesium, organolithium), in stoichiometric amount. Furthermore, they just allow the transformation of amide function into aldehyde or ketone. These reactions appear thus to be weakly chemoselective, limiting the scope of application to weakly functionalized molecules.

From 1997, inspired by the works of several groups, like Ghosez,[6] Grierson and Fowler,[7] and Battaglia,[8] on the activation of the amide function by triflic anhydride, the group of Charette developed several transformations of the amide function into bridged orthoester,[9] thioamides,[10] amidines,[11] and thiazolines (Scheme I-4).[12] They also studied the different intermediates formed during the activation of the amide function.[13] The reaction between a secondary or a tertiary amide and triflic anhydride leads to the *in situ* formation of a highly electrophilic iminium triflate intermediate, able to undergo nucleophilic addition of weak nucleophiles. In 2008, they published the reduction of amides into the corresponding amine with good yield in mild condition, using the Hantzsch ester as hydride source.[14] In 2010, they show that with triethyl silane as reductant, this reaction can conduct to the reduction of the amide function into aldehyde, with a high chemoselectivity, in a metal-free procedure.[15]

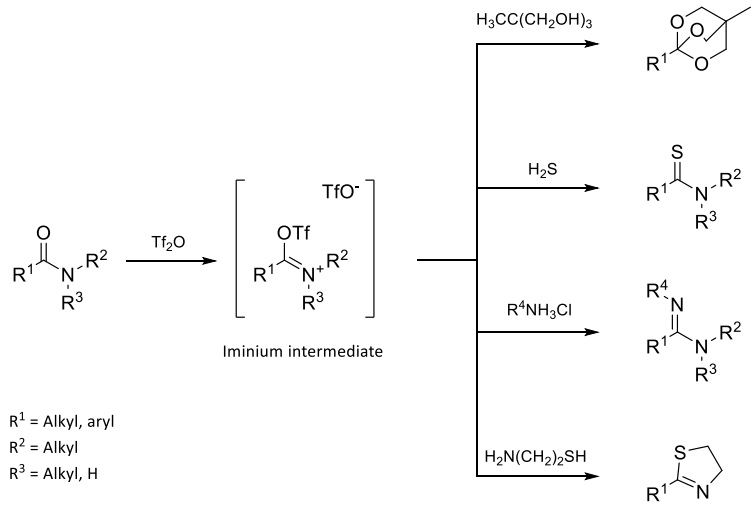

Scheme I-4: Examples of transformation developed by Charette *et coll.* with the activation of the amide function with triflic anhydride

In 2012, using the same activation method with triflic anhydride, Charette *et coll.* involved organometallic reagents as nucleophile to attack the iminium intermediate.[16] They realized with this method the 1,2-addition of organo-magnesium and diorgano-zinc species on thus activated secondary amide to form functionalized ketone products with good to excellent yield. The scope of the reaction includes benzamide derivatives as well as secondary aliphatic amides, bearing sensible functions like aldehydes, ketones, azide, or benzylic halogens. Contrary to the Weinreb's amide, the activation by triflic anhydride is applicable to a large scope of secondary and tertiary amides.

All of the previous described reactions are based on the nucleophilic properties of the oxygen in the amide function. However, another mechanism for metal-assisted activation of the amide function is also possible: the coordination of a transition metal to the nitrogen. Reported in 1970 by Houghtin and Puttner, the coordination of a transition metal to the lone-pair of the nitrogen prevent the conjugation between the nitrogen and the carbonyl, leading to a weakening of the amidic C–N bond and a general destabilization of the amide function.[17] Houghtin and Puttner highlighted this principle by developing the *N*,*N*-di(pyridylmethyl) amide: the presence of 2 coordinating pyridyl groups near the nitrogen part of the amide favors the coordination of transition metal. By adding their amide to a solution of copper (II) chloride in methanol, they observed the transformation of the amide into the corresponding methyl ester. This reaction was studied more deeply in 2004 by Clark, Alsfasser *et coll.*, who isolated and characterized different copper(II) complexes with the amide as ligand, highlighting the mechanism of this amide function activation, and the associated reactivity.[18] Afterward, Bannwarth *et coll.* developed a synthetic method using this type of amide as linker or protective group for carboxylic acids that can be efficiently, smoothly and selectively cleaved *via* copper coordination and treatment in methanol (Scheme I-5).[19]

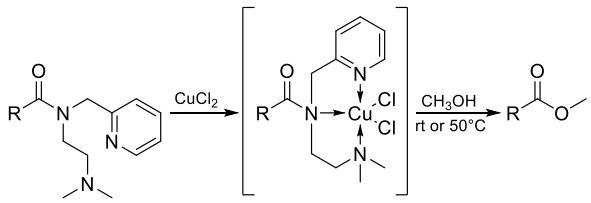

Scheme I-5: Methanolysis of pyramidalized amides by copper complexation

Despite the development of different methodologies allowing the activation of the amide function, there was no versatile reaction allowing an efficient and easy transformation of amides. In 2015, a new reactivity of the amide function has been highlighted: the possible metal insertion into amidic C–N bond and therefore the use of amides as coupling partner in metal-catalyzed cross-coupling reaction.

I.1. State of the art about metal-catalyzed coupling reactions with distorted amides

From this discovery until now, several reactions have been developed. These reactions involve two major common parameters: the choice of the catalytic system, and the choice of the amide. Indeed, any amides do not react with all the conditions that have been developed: the insertion of transition metal into the amidic C–N bond of amide occurs with non-planar amides, and depends on the strength of the catalytic system and the distortion of the amide. Several distorted amides have been thus developed and are now usable in coupling reactions. We can divide them in three groups: the *N*-acyl derivatives activated “amides”, the *N*-aryl activated amides, and the *N*-protected activated amides (Figure I-2).

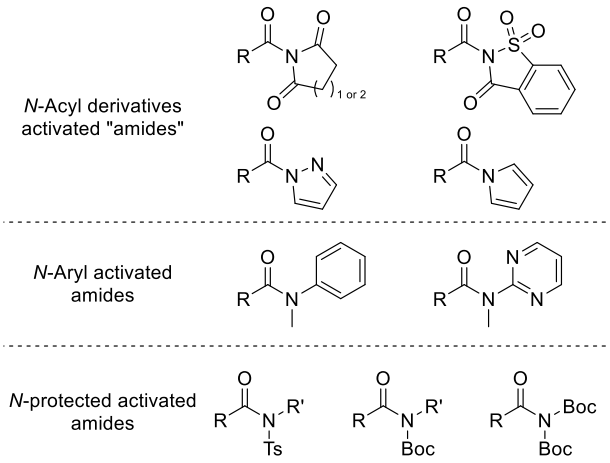

Figure I-2: Non-planar amides involved in cross-coupling reactions

All of these amides derivatives have a different reactivity, due to their different distortion angles. This angle is linked to the nature of the *N*-substituents: their hindrance and their electron-withdrawing capacity. It is then possible to link the reactivity of an amide to the resonance of the nitrogen lone-pair and to the substituents. (Figure I-3) With this scale, the reactivity of distorted amides becomes more predictable, and it is then possible to select a suitable catalytic system for each type of amides.

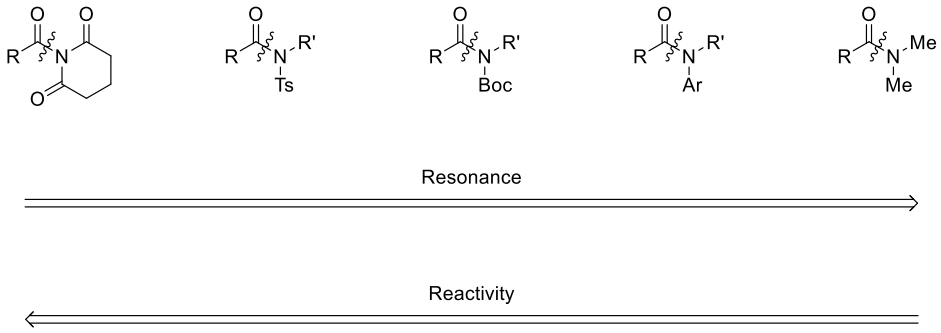

Figure I-3: General reactivity scale of amides in comparison to their resonance

We will focus here on the comparison of the catalytic systems applied in the different developed reactions, as this thesis treat about cobalt catalytic systems and comparison with existing other systems.

I.1.1. Nickel-catalyzed reactions with amides

In 2015, Garg *et coll.* published their work on nickel-catalyzed amide-to-ester conversion.[20] This reaction stands as the first reported insertion of a transition metal into the C–N amidic bond (Scheme I-6). This insertion is realized by a combination between [$Ni^0(COD)_2$] as precursors and SIPr ligand, in toluene, at 80°C, under inert atmosphere. This system appears to be efficiently applicable to benzamides with an electron-withdrawing group on the nitrogen: a weak yield is obtained with a toluenesulfonyl (Ts) group, and very good yields are obtained with *tert*-Butoxycarbonyl (Boc) or phenyl groups. An interesting point is that

the reaction works on the secondary amide *N*-Phenylbenzamide with a fair yield of 55%, proving the importance of this substitution. Besides, good to excellent yields are only obtained with tertiary amides like N-alkyl-N-phenylbenzamide, but the reaction remains limited to benzamides derivatives.

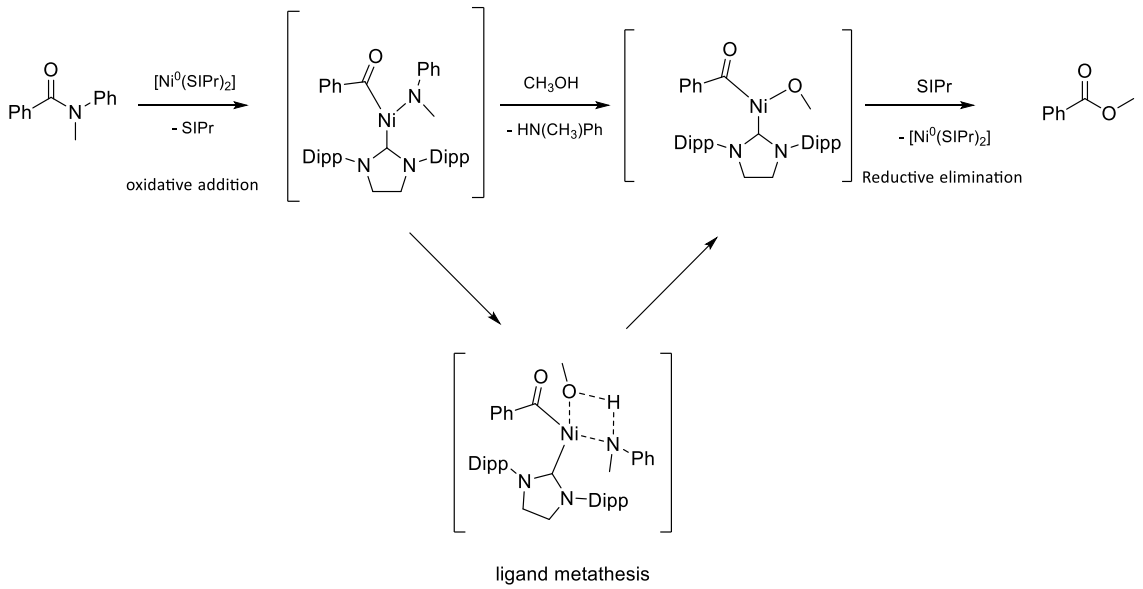

Scheme I-6: Mechanism of the nickel-catalyzed amide-to-ester conversion

About the scope of alcohols, the reaction seems to have no special restrictions on aliphatic alcohols: primary, secondary and tertiary alcohols have been successfully coupled with good yield. The reaction also tolerates other functionalities, like indoles and *N*-protected nitrogen, and works with natural product derivatives (steroid, sugar, fragrances) (Figure I-4).

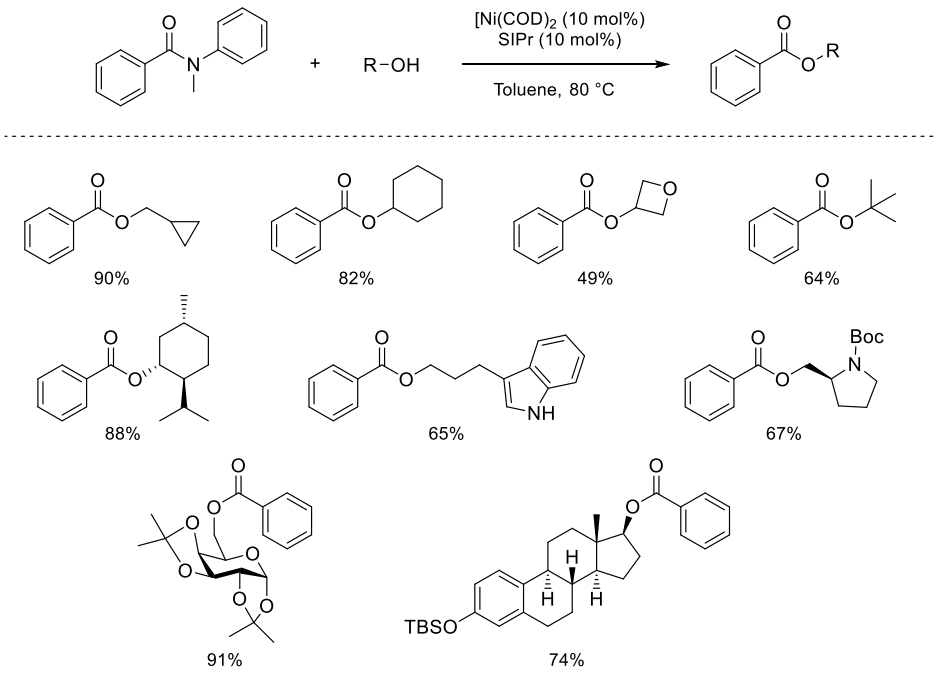

Figure I-4: Scope of alcohols of Garg's amide-to-ester conversion

Concerning the catalytic system in this reaction, [$Ni^0(COD)_2$] has been the only metal precursor that has been tried for this reaction. Besides, two families of ligands have been screened: phosphine and N-Heterocyclic Carbene. With phosphine, only PCy_3 and $PPhCy_2$ allowed the reaction to work but led to very poor yield (respectively 15% and 3%).

This catalytic system [$Ni^0(COD)_2$]/SIPr is as efficient as versatile, allowing several reactions depending on the nucleophilic partner. In 2016, the same group shows that the same reaction conditions allow the transamidation of *N*-Boc-*N*-alkyl, aryl and heteroaryl benzamides.[21] As for the amide-to-ester conversion, the reaction does not work on aliphatic amides, but tolerate a large scope of substituted benzamides and heteroaryl like furane, thiophene and *N*-protected indoles. This catalytic system also allows coupling reactions with organometallic species, like Negishi cross-coupling to proceed to alkylation of benzamides.[22] This reaction allows the formation of aryl alkyl ketones from an *N*-Ts-*N*-methyl benzamide and an alkyl organozinc reagent. By adding K_3PO_4 as base with water to activate boronic esters, Garg shows Suzuki-Miyaura cross-coupling is also possible with this system, in toluene at 50°C, leading to disymmetric diaryl ketone (Scheme I-7).[23]

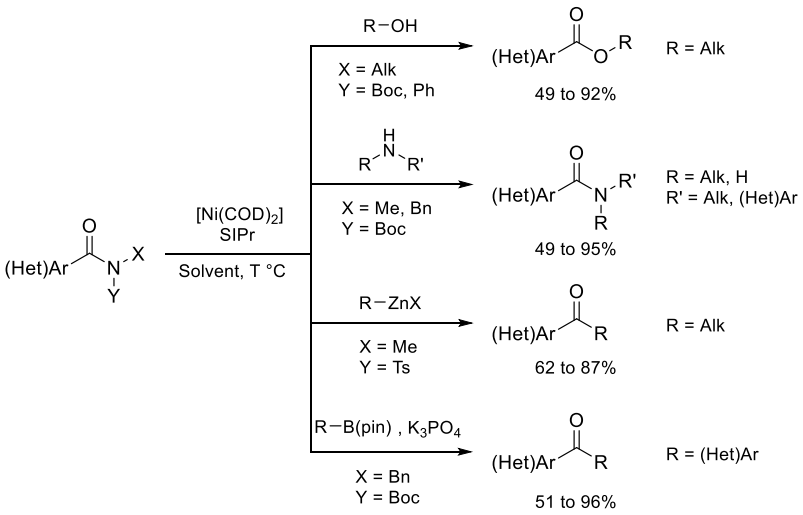

Scheme I-7: Reactions with benzamides enable by the system [Ni(COD)₂]/SIPr

Besides, it is noteworthy that the system [$Ni^0(COD)_2$]/SIPr, allowing the conversion of amides into esters, allows as well the conversion of methyl benzoate derivatives into amides in presence of Al(O*t*-Bu)$_3$.[24]

In spite of its polyvalence and its efficiency, the system [$Ni^0(COD)_2$]/SIPr remains unreactive toward aliphatic amides. To perform the insertion of nickel into the C–N bond of aliphatic amides, the catalytic system needs modifications. Garg's group thereby continued to explore the reactivity of nickel catalyst, and published in 2016 the amide-to-ester conversion of aliphatic amides, replacing the NHC ligand by terpyridine (terpy).[25] Surprisingly, if the terpy ligand allows the conversion of aliphatic amides, it does not allow the conversion of benzamides, which seems then to be a reaction specific to the SIPr ligand. This

difference of reactivity between these two ligands has been explained by Chu and Dang in 2018.[26] They studied by DFT calculations the mechanisms of the catalytic system with aryl and aliphatic amides. They demonstrate that the active species [Ni^0(SIPr)] is able to insert into the C–N bond of aliphatic amide, contrary to [Ni^0(terpy)] that is not nucleophilic enough. However, the steric hindrance brought by the SIPr ligand inhibits the metathesis step between the amine and the alcohol. In the case of [Ni^0(terpy)], the weaker hindrance of the ligand allows the metathesis to occur. In addition to this study, they also proposed another ligand allowing the application of the amide-to-ester conversion on benzamides and aliphatic amides: the *ter*-(4-aminopyridine). Because of the electro-donor amino group, this ligand should allow the nickel to proceed to the oxidative addition step with benzamides, and should also allow the metathesis step with aliphatic amides, according to their calculations.

Another worthwhile particularity of the [$Ni^0(COD)_2$]/terpy system is its specificity for the amide-to-ester conversion reaction. Indeed, no other coupling or conversion reactions seem to work with this ligand. The transamidation of aliphatic amides does not proceed with the terpyridine ligand, whereas the more electron-rich Benz-ICy NHC gives excellent yields.[27] As the oxidative addition is not a problem, according to Chu and Dang, the problem with the terpy ligand should be a ligand metathesis problem between the two amines. This new system [$Ni^0(COD)_2$]/Benz-ICy proved in 2017 its superiority compared to SIPr and ICy in the synthesis of 1-indanone through intramolecular Mizoroki-Heck reaction, in so far others NHC lead to no reaction or poor yield.[28] It is also efficient to realize on aliphatic amides the same reactions than [$Ni^0(COD)_2$]/SIPr on aromatic amides, like the Suzuki-Miyaura cross-coupling with aliphatic amides (Scheme I-8).[29]

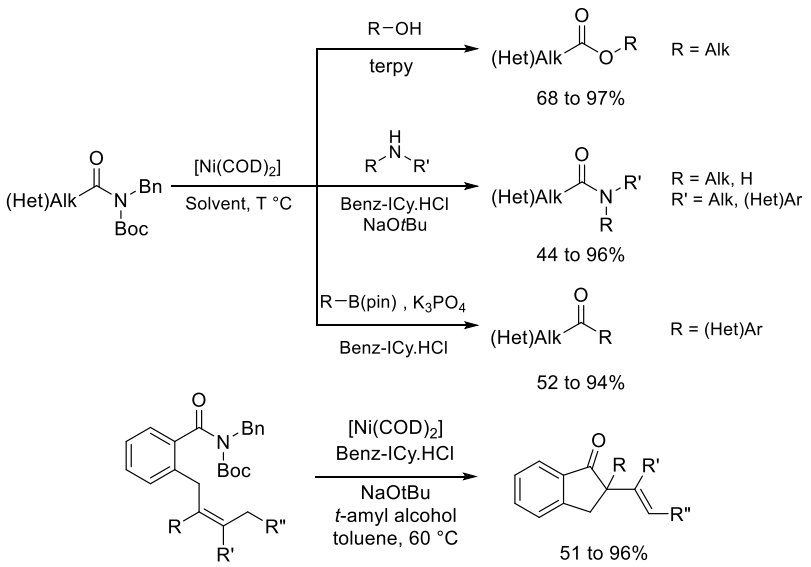

Scheme I-8: Reactions with aliphatic amides enable by terpy or benz-ICy as ligand instead of SIPr

Garg's group was not the only group using a nickel catalytic system to develop coupling reaction with amides. The group of Szostak, that started to study amides reactivity with palladium *(we will discuss about*

these systems later) in the same time than Garg, has developed thereafter several reactions with a more classical catalytic system: $[Ni(PR_3)_2Cl_2]$. They thereby developed between 2016 and 2017 nickel-catalyzed diaryl ketone and biaryl synthesis involving several activated amides into Suzuki-Miyaura[30] and Negishi[31] cross-coupling. This concept is based on the use of amides as arylating or aroylating reagents. Using the N-Acylglutarimide, the Suzuki-Miyaura coupling proceeds with $[Ni(PCy_3)_2Cl_2]$ through the decarbonylation of the amide function after the C–N bond insertion. Then a transmetallation step and a reductive elimination step leads to the biaryl product. The Negishi cross-coupling proceeds with $[Ni(PPh_3)_2Cl_2]$, but no decarbonylative step occurs in the catalytic cycle. For the Negishi coupling, the reaction conditions have been optimized on *N*-acylglutarimide and then successfully applied, with slightly solvent changes, on two other activated amide types: the *N*,*N*-diBoc-amide[32] and the *N*-acylsuccinimide (Scheme I-9).[33]

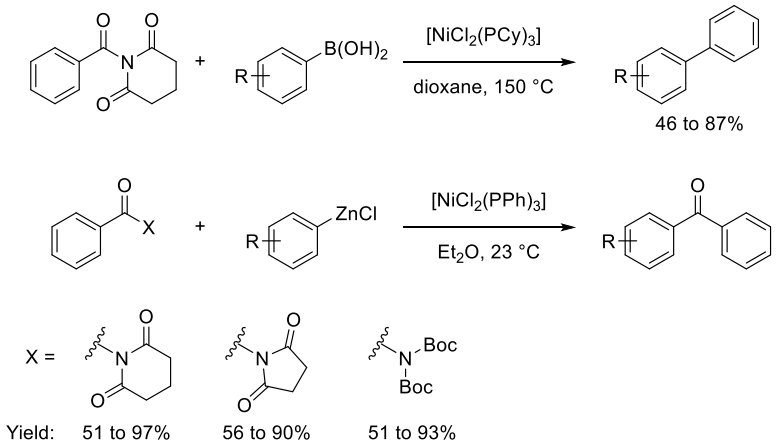

Scheme I-9: Nickel-catalyzed Suzuki and Negishi cross-coupling, with phosphine ligands

The group of Rueping developed in 2017 a series of nickel-catalyzed reactions allowing the replacement of the whole *N*-acyl glutarimide function by a nucleophile (silylation, borylation, amination), using mainly phosphine ligands.[34] We can notice that the borylation of *N*-Boc protected secondary amides was already reported by Shi, in 2016, with a NHC ligand (ICy).[35] By using polymethylhydrosiloxane (PMHS) on *N*-acylglutarimide in presence of $Ni(OAc)_2$ with dcype, they also reported the protodeamidation of the substrates, with good yields.[36] With a primary ketimine as nucleophile, and $[Ni^0(COD)_2]$/dppf as catalytic system, the reaction leads to the corresponding amine product after hydrolysis with good to excellent yield (Scheme I-10a).[37] It is interesting to note that these two reactions are also relevant for phenyl ester. The same catalytic system Ni^0/dcype also allows, associated with CuI, the use of *N*-acylglutarimide as coupling partner for Sonogashira coupling reaction, to lead to the corresponding alkyne, still with a decarbonylative step.[38] Another noteworthy reaction from Rueping's group is the conversion of *N*-substituted 2-pyridinecarboxamide derivatives into the corresponding *N*-substituted 2-aminopyridine, standing as a new synthesis of the amidine function (Scheme I-10b).[39]

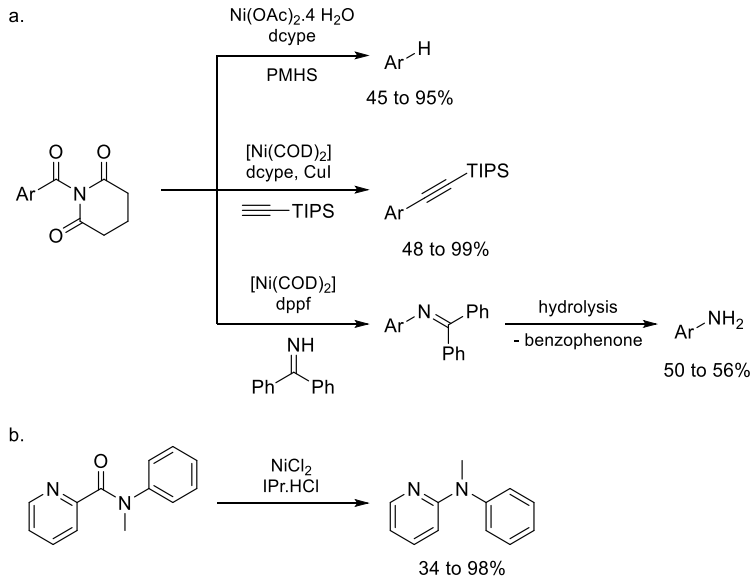

Scheme I-10: Development of Rueping's group about amides reactivity with nickel complexes

I.1.2. Palladium-catalyzed reactions with amides

If several nickel-catalyzed amide cross-coupling reactions have been developed, palladium-catalyzed reaction conditions have also been studied, especially by Szostak's group. As this group is mainly focused on the study of the amide bond and its activation through distortion; they compared the reactivity of different activated amides toward palladium catalytic system

Starting in 2015 with the first palladium-catalyzed Suzuki-Miyaura cross-coupling involving amides, Szostak *et coll.* introduced also the concept of "C–N activation of amides *via* ground-destabilization" with the *N*-acylglutarimide.[40] This amide derivatives is highly activated, due to its twisted geometry, and enables the reaction to give good yields with $Pd(OAc)_2$ and PCy_3•HBF_4 (a bench-stable precursor of PCy_3). This catalyst allows to tolerate several sensitive chemical functions. The ligand PCy_3•HBF_4 has also been used in two other Suzuki coupling reaction involving other amides. One using *N*-mesyl-*N*-phenyl amides as acylating reagents, and Pd_2dba_3 as palladium precursor.[41] In this reaction, the mesyl substituent stands as an atom-economic and efficient way to activate a secondary amide. The other use *N*-acylsaccharine and $Pd(OAc)_2$.[42] For this last one, it has been preferred to replace PCy_3 by PCy_2Ph, which has a weaker donor effect. It is described as having a better range of application among the amide substrates. Surprisingly, $PCyPh_2$ is unsuccessful to perform the same reaction. However, it appears to be the best ligand to realize the decarbonylative cyanation of benzamides.[43] Involving $Zn(CN)_2$ as source of cyanide, the reaction works as a Negishi cross-coupling reaction, beginning with the insertion of the palladium in the amidic C–N bond, followed by a transmetallation of the cyano group from the zinc to the palladium. Then a decarbonylative step occurs, before the reductive elimination giving the final product. This reaction does not work with PCy_3, but gives good yield with PCy_2Ph and excellent yield with $PCyPh_2$ (Scheme I-11).

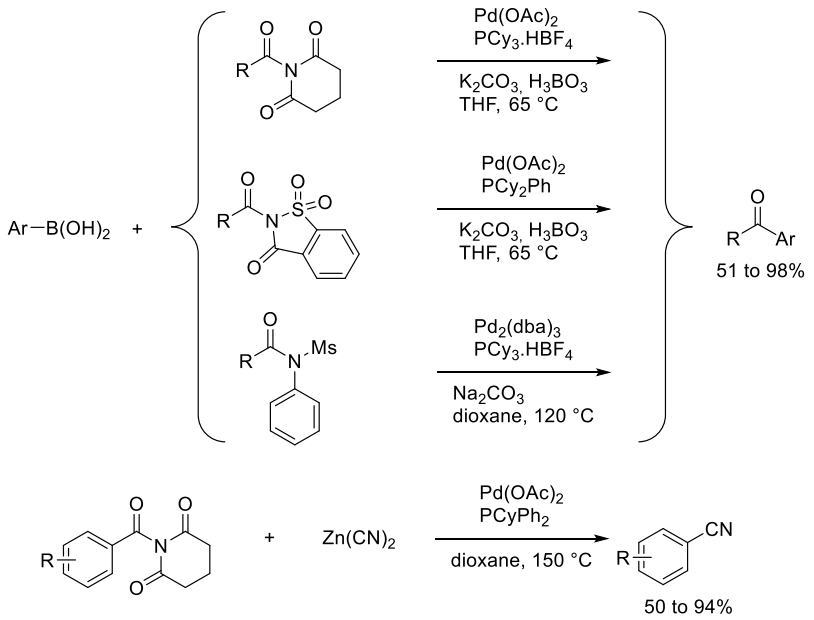

Scheme I-11: Palladium-catalyzed cross-coupling reaction developed by Szostak with phosphine ligands

By continuing in the development of Suzuki cross-coupling with amides, the group of Szostak also explored the influence of NHC ligand on the reactivity of palladium complexes. They started in 2017, with the complex (IPr)Pd(cinnamyl)Cl.[44] As NHC are more donor ligands than phosphine, they facilitate the oxidative addition step, and enlarge the reactivity to less reactive amides. Thus they applied their conditions for Suzuki coupling to the highly reactive *N*-acyl glutarimide, but also to other synthetically more interesting amides, like *N*-tosyl amides and the *N*-Boc benzamides. The reaction works well for every substitution of the benzamides, giving very good to excellent yield with the three amide derivatives. This complex also allows the insertion of palladium into the C–N bond of *N*-acylpyrroles and *N*-acylpyrazoles, considered as planar amides with a weak C–N bond due to the electronic activation of the heteroaromatic ring.[45] Besides, the (IPr)Pd(cinnamyl)Cl is also reactive to *N*-Methylamino Pyrimidyl amides, whereas no reactivity has been observed for other palladium systems with other *N*-alkyl-*N*-aryl amides,[46] highlighting the strength of the Pd-NHC system. When this complex is involved into a Suzuki coupling between a boronic acid and a very reactive amide derivatives, like *N,N*-diBoc amides, the reaction can be proceeded at room temperature, leading to good to excellent yields with a wide panel of substrates. [47] Furthermore, this Pd-NHC system also proved to be able to catalyze efficiently transamidation reactions on *N*-Boc and *N*-tosyl amides (Scheme I-12).[48]

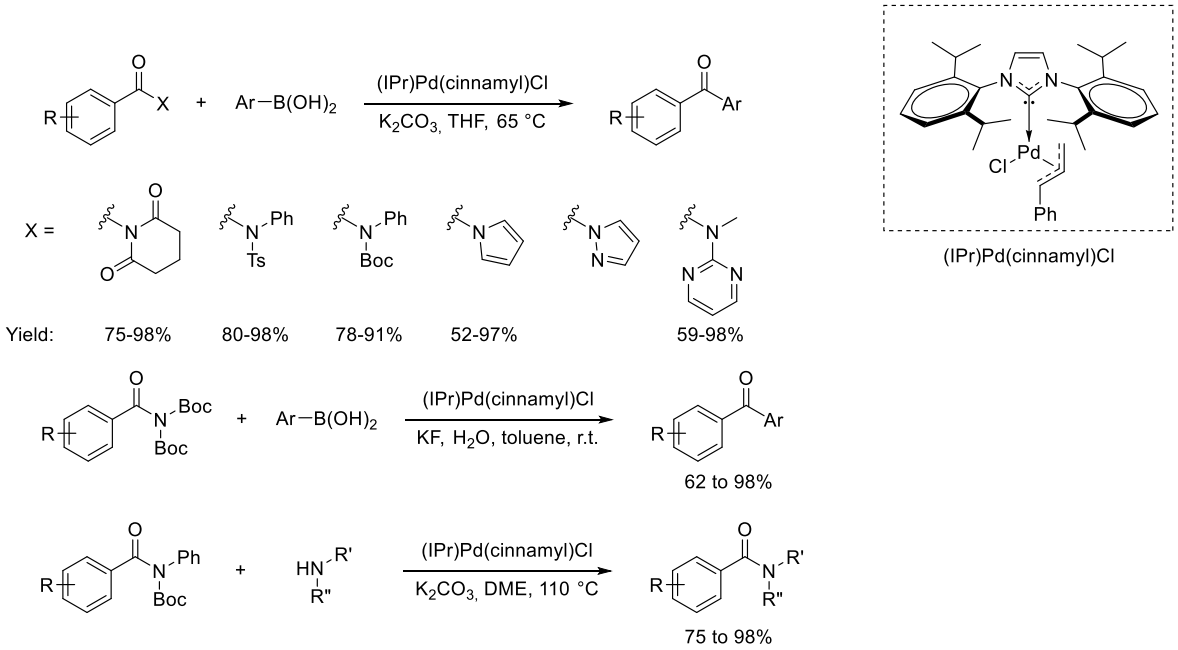

Scheme I-12: Palladium-catalyzed Suzuki cross-coupling with amides, involving (IPr)Pd(cinnamyl)Cl

The complex (IPr)Pd(cinnamyl)Cl was not the only Pd-NHC system to be studied for its reactivity toward amides. The commercial pre-catalyst Pd-PEPPSI has also been involved in Suzuki-Miyaura cross-coupling reactions, providing diaryl ketones with very good yields.[49] This pre-catalyst is as efficient as the (IPr)Pd(cinnamyl)Cl as it can also proceed to transamidation with comparative yields.[50]

Another palladium-catalyzed coupling reactions developed by the group of Szostak with amides is the Heck reaction. Published in 2015 and realized with $PdCl_2$ as catalyst, and LiBr in NMP at 160°C, the mechanism proceeds through insertion of the palladium, followed by a decarbonylative step.[51] Then, the aryl-palladium intermediate realizes the 1,2 addition step on the alkene, and the final substituted alkene is released by a β–H elimination step. This reaction works only with *N*-acylglutarimide as distorted amide and tolerates a wide range of alkene that coupled with good yield. In 2017, the same group shows that the same reaction catalytic system without LiBr work also with *N*-acylsaccharins, to perform the same transformation with comparable yields and regioselectivity for the majority of the substrates.[52]

I.1.3. Rhodium-catalyzed reactions with amides

Nickel and palladium are not the only elements that have been used for amide coupling reactions. Szostak *et coll.* also developed rhodium-catalyzed C–H functionalization reaction with amides as arylating reagents.[53] Using a rhodium(I) catalyst, $[Rh(COD)Cl]_2$, in toluene at 150°C, the reaction is applicable on *N*-acyl glutarimide and succinimide. The mechanism proceeds firstly by the insertion in the amidic C–N bond and the decarbonylation of the benzoyl-metal moiety. Then, the formed rhodium(III) intermediate realize the directed C–H activation of the aromatic coupling partner before releasing the product by reductive

elimination. The reaction tolerates a wide range of substrates and coupling partners, providing the corresponding diaryl compounds with good to very good yields (Scheme I-13).

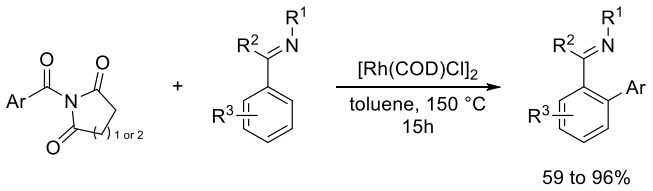

Scheme I-13: Rhodium-catalyzed C–H arylation, using amides as arylating agent

I.1.4. Cooperative catalysis

For all the reactions previously presented, the mechanism was based on a classical catalytic cycle between an electrophile (the amide) and a nucleophile (organozinc, boronic acid, C–H bond to activate), with a first step of insertion/oxidative addition of the metal into the amidic C–N bond. However, with specific substrates, it is possible to explore a different pathway for the activation of the amide bond: the cooperative catalysis.

This pathway has been highlighted by the group of Szostak in 2016, to enlarge the chemistry of the activated amide to primary amides.[54] Primary amides are not active, and have to be activated by Boc-introduction, in order to form the active *N,N*-diBoc amides. To circumvent the use of strong catalytic systems, the concept of the cooperative catalysis is to add to the reaction media a Lewis base that will substitute the amine moiety of the amide to form an acylium species, more reactive and thus making easier the insertion of a transition metal. Applying this principle, they developed a Suzuki-Miyaura cross-coupling reaction involving $Pd(OAc)_2/PCy_3{\bullet}HBF_4$ as pre-catalytic system, and triethylamine as Lewis Base, in THF at 110°C. With a less strong catalytic system than Pd-NHC, the reaction tolerates a broader panel of substitution, as chlorine and nitrile, and gives correct to very good yields (Figure I-5).

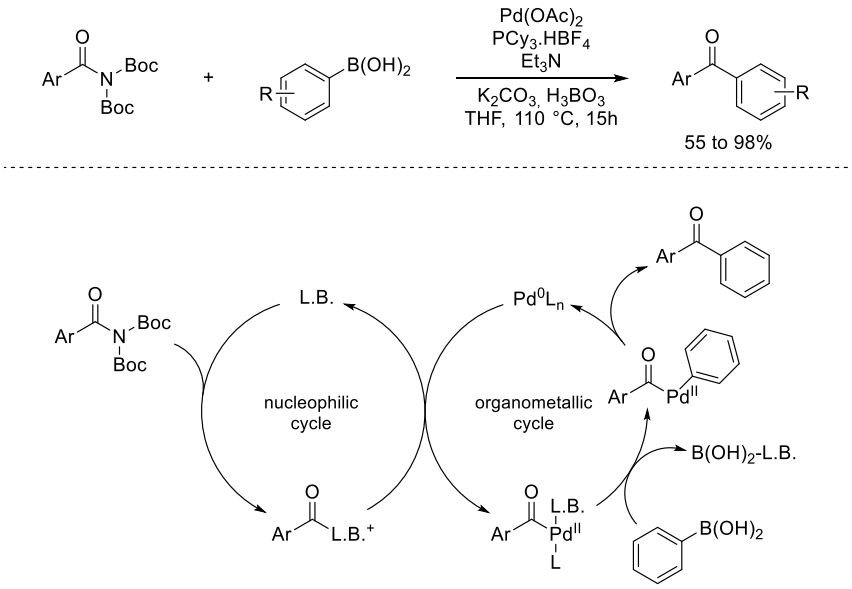

Figure I-5: Mechanism of palladium cooperative catalysis

This methodology has also been applied to the rhodium-catalyzed C–H arylation, by adding tri *n*-butylamine as Lewis base to the reaction conditions presented above, and applying them on *N,N*-diBoc amides (Figure I-6).[55] If yields appear to be better for some substitutions, the cooperative catalytic reaction seems not to tolerate steric hindrance, as *ortho* substituted compounds lead to lower yields.

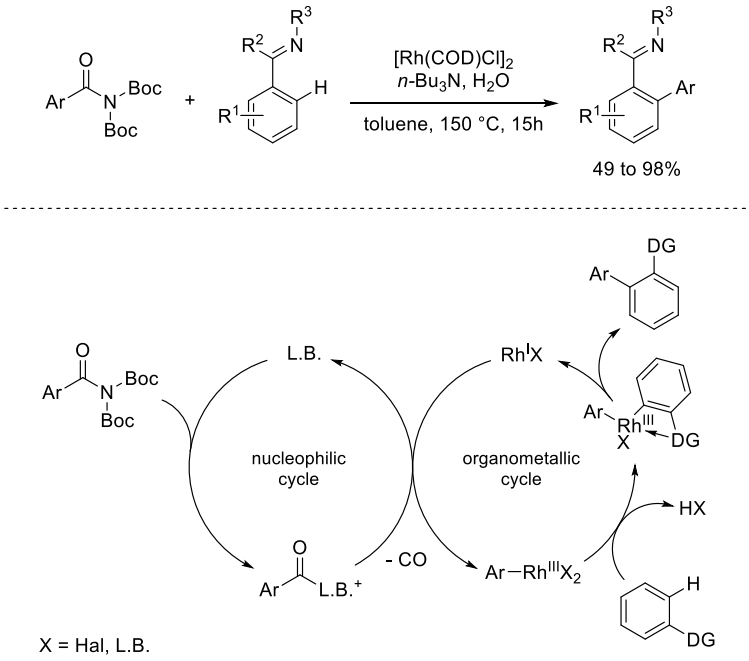

Figure I-6: Mechanism of Rhodium cooperative catalysis

Since 2015, several reactions have been developed, using different catalytic systems and enlarging the scope of usable amides. Despite this fact, the use of a palladium or nickel catalysts limits the presence of functional groups on the substrates, because of their high reactivity. Moreover, some reactions have

been developed on *N*-acyl derivatives amides, which are naturally activated "amides" that can easily react with weak nucleophiles. This drawback has been circumvented by the *N*-protected secondary amides. With this type of amides, the group of Szostak proposed a two-step procedure to realize amidic coupling reactions directly from secondary amides: the first step is the activation of the secondary amide by Boc or Ts moiety, and the second step is the metal-catalyzed coupling reaction, with comparable yield over the 2 steps without isolation of the intermediate amides. In the following of these developments, we decided to work on the development of practical and synthetically interesting methods to realize the activation of the amide function.

I.2. Cobalt reactivity toward non-planar amides

We began our research on amide reactivity during 2016. Only the first works of Garg and Szostak were published, concerning nickel-catalyzed esterification[20] and Suzuki coupling,[23] and palladium-catalyzed Suzuki[40] and Heck[51] couplings. To the best of our knowledge, no metal-catalyzed coupling reactions involving amides have been developed with cobalt. As shown by previous work on cobalt-catalysis with aryl halides,[56] the use of this metal allows to realize several coupling reactions without inert atmosphere, and with undried solvents, like for example the preparation of arylzinc species or the cobalt-catalyzed cross-coupling. Based on these observations, we decided to study the reactivity of cobalt catalytic systems with activated amides, hoping to provide alternative methods to those existing, or even discovering new reactivity and/or selectivity for the amidic coupling chemistry.

I.2.1. The choice of the amide and preliminary studies

Three kind of activated amides were regularly used as coupling partner (Figure I-7):

- The *N*-methyl-*N*-phenyl benzamide **1**, employed by Garg's group to develop the esterification of benzamides, but appeared to be unreactive for other coupling reactions;

- the *N*-Boc-benzamide derivatives, like the *N*-Boc-*N*-phenyl benzamide **2**, employed thereafter by Garg's group to develop amides cross-coupling reactions and study by Szostak;

- the *N*-acyl derivatives amides, like the *N*-benzoylglutarimide **3**, employed by Szostak's group for several palladium- and nickel-catalyzed cross-coupling reaction, as the $C_{benzoyl}$–N bond can easily and selectively be cleaved.

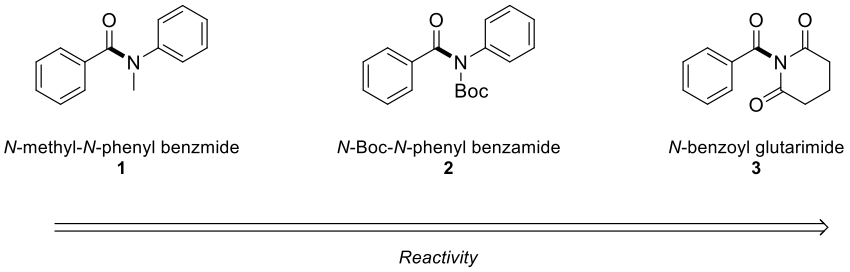

Figure I-7: Scale of reactivity of the amides used for the preliminary study for cobalt reactivity

Without previous work with cobalt and amides to base on our research, we applied the following approach, split in two steps:

1. The first step was the search for hits. With the *N*-benzoylglutarimide **3** as test substrate, we screened several reaction conditions based on the classical cobalt catalytic system developed in the laboratory, in order to experimentally and qualitatively explore the potential reactivity we could develop. As showed previously, the *N*-benzoylglutarimide **3** is highly activated and will easily react even with a lowly efficient catalytic system.
2. The second step was the adaptation and optimization of the interesting preliminary results obtained with **3**. These reaction conditions will be applied on *N*-Boc protected amides and optimized as necessary to obtain an efficient cobalt-catalyzed coupling reaction.

The reason of changing the substrate lies in the high reactivity of *N*-acylglutarimides that, from our point of view, does not suit as an ideal model for an applicable synthetic methodology. The "*N*-acyl derivatives amides" are indeed too reactive, and have reactivity closer to acyl chlorides or activated esters than classical amides, allowing even the substitution of the glutarimide part by an amine to form an amide.[57] From our point of view, the interest of using amides as coupling partner lies in the low reactivity of primary and secondary amides. They can be set on a molecule as a chemoselective functionalization site, only reacting once activated by *N*-Boc protection. After the protection/activation step, they also become highly active,[58] and stand as good model for the development of synthetically interesting reactions.

About the choice of the protecting group, two functions are used for amide coupling reaction: Boc and Ts. By comparing the classical protocols to set each of these protective groups, we chose the Boc, which can be set under milder conditions than the Ts group. The *N*-Boc amide can indeed be obtained by the action of Boc_2O in presence of catalytic amount of DMAP in acetonitrile, at 60°C overnight. In comparison, the *N*-Ts amide is obtained by deprotonation of the secondary amide with a strong base, like NaH, and then addition of toluenesulfonyl chloride.

To begin our screening, we started with classical reaction conditions of cobalt-catalyzed reductive cross-coupling: $CoBr_2$, PPh_3, Mn, DMF/Py. These conditions have been applied on *N*-benzoylglutarimide **3**

with 4-bromoanisole as coupling partner, to evaluate the possibility of involving amides in classical cobalt-catalyzed reductive coupling reactions. Three main products have been observed (Scheme I-14):

- The 4-phenylanisole **4**, from a decarbonylative cross-coupling between the amide and the bromoanisole;
- The 4,4'-dimethoxybiphenyl **5**, product from the reductive homocoupling of the 4-bromoanisole;
- The biphenyl **6**, from a decarbonylative homocoupling of the amide.

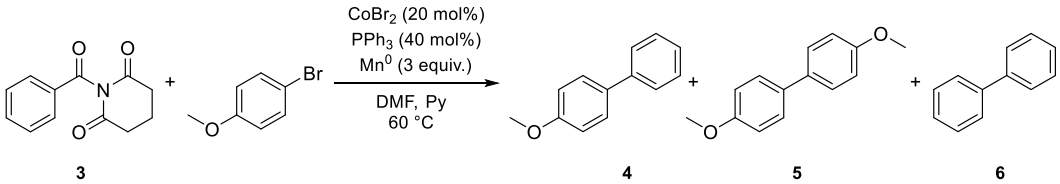

Scheme I-14: Preliminary tests of *N*-acyl derivatives amides with cobalt catalytic system

From these results, we screened different ligands, to see if the ratio between the three biaryl compounds can be increased in favor of the cross-coupling product. It appeared that phosphine-type ligands lead only to the three biaryl compounds, but with poor yields. Monodentate triphenylphosphine-type ligand seemed to be the ligand giving the best ratio in favor of the cross-coupling product. We can notice that best yields were obtained with tris(para-fluorophenyl)phosphine as ligand, with 11% yield of cross-coupling product **4**, 7% yield of dimethoxydiphenyl **5**, and 4% yield of diphenyl **6**. Trialkylphosphine and NHC ligand do not allow any reaction with the amide, as when the reaction is realized without ligand.

Surprisingly, bipyridine and phenanthroline ligands lead mainly to the formation of the benzophenone **7**, from a semi-decarbonylative homocoupling of the amide (Scheme I-15).

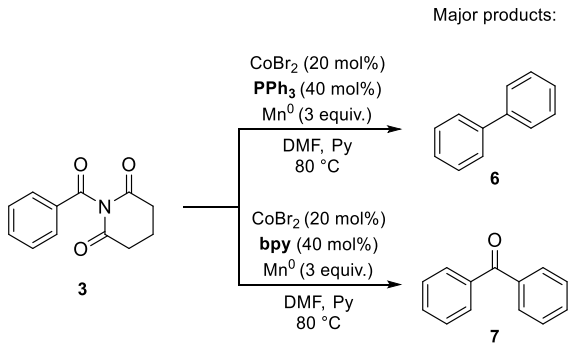

Scheme I-15: Reactivity tests of cobalt catalytic systems with *N*-benzoyl glutarimide

With these hits with the *N*-benzoylglutarimide **3**, we saw that cobalt-based catalytic systems can be used on amides, and allow some particular reactivity, as reductive cross-coupling, but also decarbonylative or semi-decarbonylative homocoupling of amides. We thus continued to the second step of our strategy: the adaptation of these results to the synthetically interesting *N*-Boc-*N*-phenyl benzamide. As main

products, homocoupling of the amide and of the bromo aryl were obtained. We thus removed from the reaction media the bromo aryl coupling partner, in order to focus on this uncommon homocoupling reaction.

By applying the two reaction conditions to the *N*-Boc protected amide **2**, the conditions with triphenylphosphine as ligand surprisingly led to no reaction, whereas the conditions with bipyridine as ligand led to the benzophenone **7**, like with the *N*-benzoylglutarimide **3**, with a yield of 39% after 10 minutes at 80°C. We thus decided to optimize this reaction (Scheme I-16).

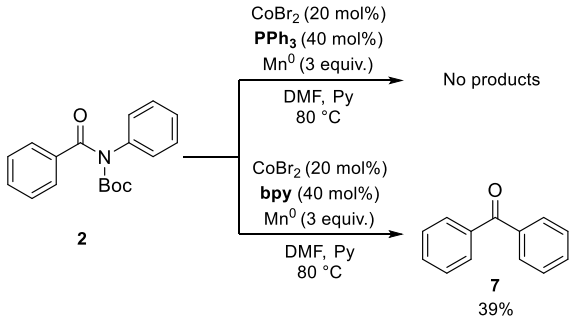

Scheme I-16: Reactivity tests of cobalt catalytic systems with *N*-Boc-*N*-phenyl benzamide

I.2.2. The semi-decarbonylative reductive homocoupling of amides

Firstly, a kinetic study of the formation of benzophenone **7** during the reaction, followed by GC-FID, showed that the reaction stop to progress after 10 minutes at 80°C, giving a yield under 40%. By decreasing the temperature to 60°C, the reaction is slower, but can reach a yield of 45%, after 30 minutes. By continuing to decrease the temperature to 40°C, we still observed a slowdown of the kinetic, but also a plateau around a yield of 45%. At room temperature, the reaction does not go further after 30 minutes, with a maximum yield of 10% (Graph I-1). It is nevertheless important to notice that outside the product, we observed only the starting material and the aniline from the nitrogen part of the amide.

With this study, we determined that the ideal temperature allowing the best yield with these conditions in a reasonable reaction time is 60 °C. Under this temperature, the reaction slows down and reaches a limit, like the 10% yield at room temperature. On the contrary, a higher temperature (80 °C) allows reaching this limit very quickly, but also potentially tends to decrease the yield, or at least lower the limit yield. Besides, the sudden stop of the evolution of the reaction can also be caused by a degradation of the catalytic system due to the temperature, as no side-reactions have been observed.

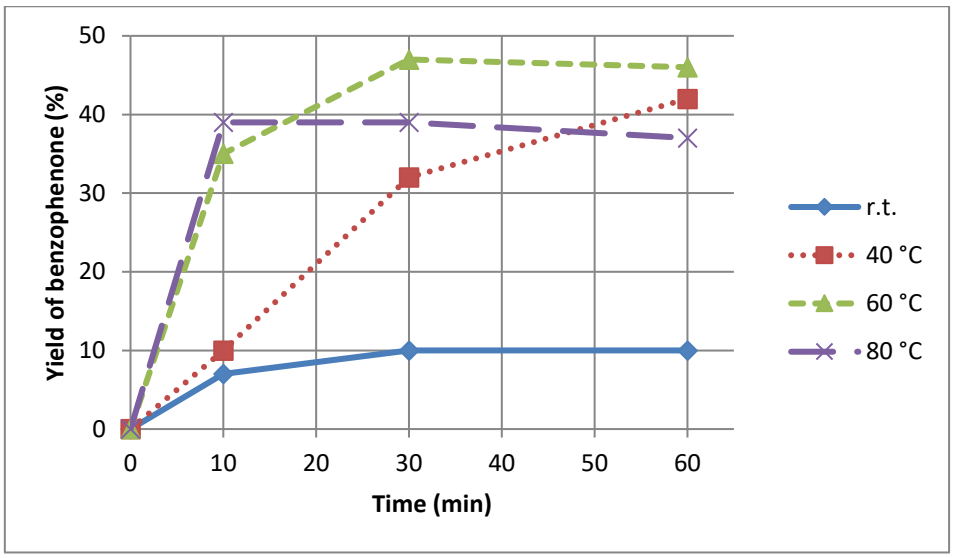

Graph I-1: Kinetic monitoring of benzophenone formation reaction

The screening of solvents showed that DMF remains the best solvent for this kind of catalytic system. Acetonitrile allows a yield of 11%, and no product was obtained in THF. In methanol, no benzophenone was obtained, but the formation of methyl benzoate ester was observed. *We will detail this reaction in a next part.* The use of pyridine as co-solvent is also necessary to increase the yield, as no pyridine decreased it to 34%. However, increasing the quantity of pyridine does not increase the yield.

The reaction, conducted with 0.2 equivalent of cobalt, lead to around 40% yield. We thus realized a test with a bigger quantity of cobalt precursor, to verify if the yield increases proportionally. But with 0.5 equivalent of cobalt, the yield increases to 65%, and with 1 equivalent, it stagnates at 60% (Table I-1).

The optimization of this reaction has been stopped at this point to focus our effort on other reactions more promising.

What we have learned from this optimization is that our catalytic system does not require high temperature. A medium temperature like 60°C allows a quick reaction time with a fair yield near 50%. Moreover, the increase of the cobalt amount does not induce a proportional increase of the yield. As for the temperature, it seems there is an optimal amount to reach the maximum yield. This problem is also the same for the pyridine as co-solvent: there is a minimum quantity of pyridine required by the reaction. Below this quantity, the reaction won't give the best yield possible, but above this quantity, the yield won't be better.

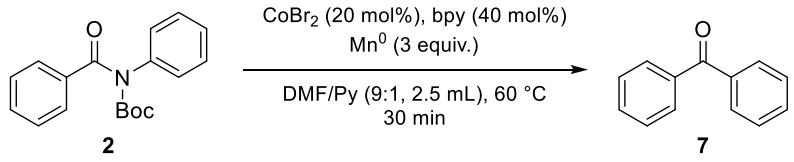

Entry	Deviation from standard conditions	GC Yield (%)
1	none	47
2	No bpy	n.d.
3	No $CoBr_2$	n.d.
4	No TMSCl	n.d.
5	Acetonitrile instead of DMF	11
6	THF instead of DMF	0
7	No pyridine	34
8	2.0 mL of DMF, 0.5 mL of pyridine	45
9	0.5 equivalents of $CoBr_2$	65
10	1 equivalent of $CoBr_2$	60

Table I-1: Optimization of the cobalt-catalyzed semi-decarbonylative reductive homocoupling of amides

In order to propose a mechanism, we hypothesize the insertion of the low-valent cobalt(I) catalytic specie into the C–N amidic bond of **2** (Scheme I-17). From this step, the intermediate cobalt(III) specie is reduced to cobalt(I) and proceed to a second insertion step. The cobalt(III) intermediate undergoes a decarbonylative step, followed by a reductive elimination, which generate the benzophenone product **7**.

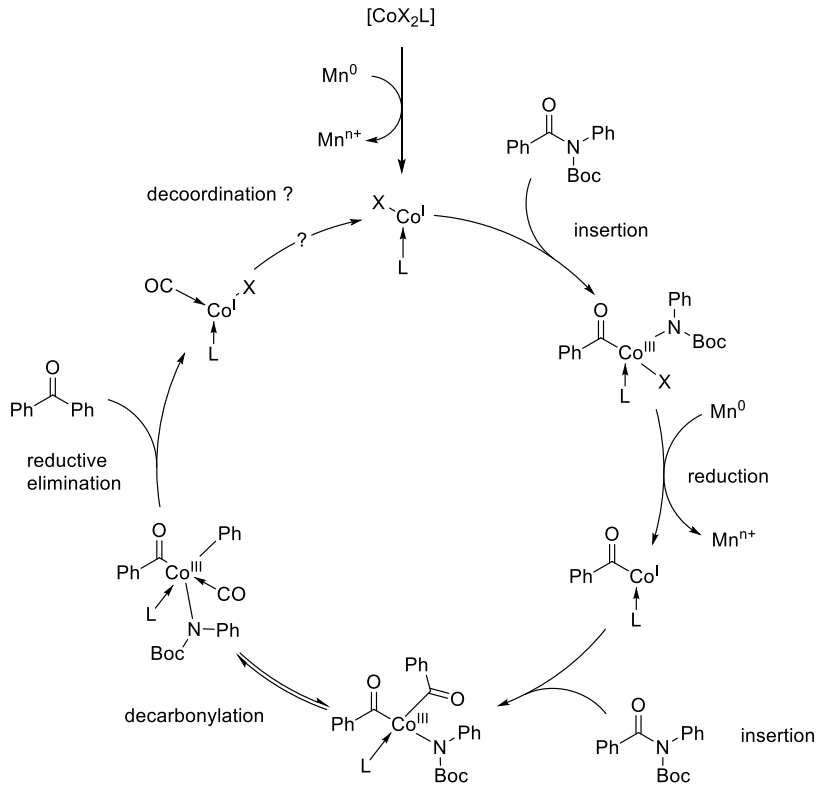

Scheme I-17: proposed mechanism for the cobalt-catalyzed reductive homocoupling of amides

During this reaction, the catalytic cobalt specie get a carbonyl ligand. This type of ligand forms strong interaction with transition metal because of its σ-donor and π-acceptor properties. This strong bonding between the cobalt and the carbonyl let us think that one of the reasons the reaction does not allow a full conversion comes from a poisoning of the catalytic specie during the decarbonylation step. Thereby, the cobalt center adds a carbonyl ligand at each cycle to its coordination sphere, occupying coordination sites and deactivating the catalyst. To circumvent this problem, a solution could be to find another bidentate ligand, more sterically hindered, or with also a σ-donation and a π-backbonding, to compete with the carbonyl and favor its decoordination.

I.2.3. The reductive cross-coupling between amides and aryl halides

With the new considerations obtained during the optimization of the reductive homocoupling, we decided to test again the reductive cross-coupling, with bipyridine as ligand, and a *p*-tolyl halide as coupling partner. It is noteworthy that the pre-catalytic system involved is the pre-formed complex $[CoBr_2(bpy)_2]$. The reaction is performed with the basic reaction conditions, with *p*-chloro-, *p*-bromo- and *p*-iodotoluene. The *p*-chlorotoluene does not lead to the formation of any cross-coupling product, as cobalt does not insert as easily into Csp^2–Cl bond than Csp^2–Br and Csp^2–I bonds. In the case of the bromo- and the iodotoluene, we observed the formation of the 4-methylbenzophenone with 13% yield with the iodotoluene, and 30% yield with the bromotoluene (Scheme I-18). From that point, we started by screened different bipyridine and

similar ligands. 4,4'-alkyl-2,2'-bipyridine, phenanthroline and 4,7-dimethyl-1,10-phenanthroline lead to comparable yield to unsubstituted bipyridine. However, we observed a decrease of the yield to 11% with the 4,4'-dimethoxy-2,2'-bipyridine, highlighting the fact that too electron-rich ligands do not promote the coupling reaction. The effect is the same when phosphine ligands, strongly donor, are involved in the reaction, leading, in the best case with XANTPhos, to 3% yield, and no product with other phosphine ligands or without ligand. However, without ligand, but with pyridine as co-solvent, the reaction works with a yield of 29%.

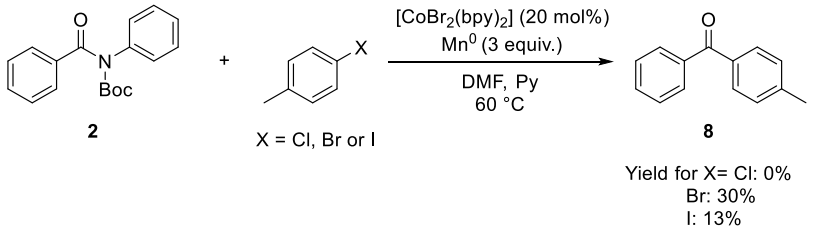

Scheme I-18: Synthesis of asymmetric benzophenone by cobalt-catalyzed amidic cross-coupling

Another ligand effect influencing the yield is the steric hindrance. Indeed the use of 2,9-dimethyl-1,10-phenanthroline as ligand leads to no product, and the bathocuproine to a yield of 5%.

Then, we decided to fix the other parameters of the reaction as the quantity of each coupling partner and the reaction solvent. We decreased thus the amount of bromotoluene to 1.5 equivalents compared to the amide and noticed no change for the yield. An increase to 4 equivalents also gives the same yield of 40%. We decided to stay with 2 equivalent of bromotoluene compared to the amide, as it seems to have no effect. About the solvent, a screening of different classical used solvent showed that the reaction works only in DMF to obtained good yield. Besides, if the presence of pyridine allows to do without ligands, the use of pyridine as co-solvent with bipyridine as ligand do not increase the yield.

After fixing the ratio of the coupling partners and the reaction solvent, we optimized the catalytic system. As seen previously, the reaction works with bipyridine as ligand, and cobalt bromide as cobalt precursor, with 2 equivalents of bipyridine compared to cobalt bromide. We changed this composition to a 1:1 ratio between ligand and cobalt precursor, and obtained a yield of 34%. Surprisingly, the use of pyridine as co-solvent with a 1:1 cobalt/ligand ratio leads to a decrease of the yield to 22%. Keeping this 1:1 ratio, we then tried different cobalt(II) salts as cobalt precursor. All salts give similar yields, between 27% for $Co(acac)_2$ and 41% for CoI_2. For convenient reasons, we continued to use $CoBr_2$.

Despite the optimization of the quantity of the coupling partners, the solvent and the amount of catalyst, the yield stagnates between 35% and 40%. We thus attempted to increase the yield by included salts as additives to the reaction media. As the reaction works better with bromoaryl compounds than with chloro- or iodoaryl, we tried to add bromide sources to the reaction. If the addition of KBr does not lead to

change in the yield, the addition of tetrabutylammonium bromide (TBAB) appears to have an effect on the yield. The addition of 2 equivalents compared to the amide indeed decrease the yield to 32%. Surprisingly, with 1 equivalent, the yield is 38%, and another decrease of the amount of TBAB to 0.5 equivalents finally allows a yield of 50% in cross-coupling product (Table I-2).

Entry	Bromine source	Equivalents	Yield (%)
1	LiBr	2	25
2	$ZnBr_2$	2	23
3	KBr	2	39
4	KBr	1	36
5	TBAB	2	32
6	TBAB	1	38
7	TBAB	0.5	50

Table I-2: Influence of bromide salts on the reaction yield

At this point of the manuscript, the optimization of the reaction has not been completed, and the results presented stand as the last results obtained on this reaction.

I.2.4. The cobalt-catalyzed amide-to-ester conversion[59]

During the screening of the reaction solvent of the reductive homocoupling of amides, we observed the formation of methyl benzoate ester, with a total conversion of the amide, when the reaction is performed in methanol. As previously seen in the literature, the metal-catalyzed amide-to-ester conversion has already been described, by the group of Garg, with a combination [$Ni(COD)_2$]/SIPr as catalytic system. Although effective, this catalytic system suffers from several drawbacks: it is sensible to air and moisture, and thus requires an inert atmosphere; it is an efficient catalytic system, which does not tolerate too sensible chemical functions; the catalyst loading remains important (up to 15%). As our catalytic system proved to be efficient, even under not inert atmosphere, we attempted to optimize this reaction to propose an alternative method to the nickel-catalyzed amide-to-ester conversion.

When the reaction is conducted in methanol, it gives quantitatively the corresponding methyl ester. We thus tried the same conditions in ethanol, but no reaction occurred. We then included ethanol in stoichiometric amount (2 equivalents), in a mixture DMF/pyridine as solvent, and succeeded to obtained the ethyl benzoate ester **10** with a correct yield of 62% after 3h of reaction, without by-products. This reaction has to be compared with the evolution of the homocoupling reaction, which occurs in 30 minutes

to lead to 40% yield of benzophenone **7**. We can thus notice that the presence of an alcohol in the reaction middle inhibit the homocoupling reaction to favor the conversion into ester, which is a slower reaction.

In order to verify the importance of each component of the reaction, we firstly carried out blank experiments. The reaction without any metal did not yield to any ester (Table I-3, entry 2). The reactions in the presence of only $CoBr_2$ and bipyridine without any reductant (Table I-3, entry 3), and in the presence of only activated reductant (Mn^0+TMSCl) (Table I-3, entry 4) were performed and no esters were detected. Only starting material was observed in all control experiments, highlighting the fact that the catalytic species directing the reaction should be low-valent cobalt specie, formed from the reduction of the precatalyst $CoBr_2$/bipyridine by the metallic manganese. About TMSCl, it has no effect on the reaction, except the activation of the manganese. The reaction realized without TMSCl lead to a yield of 24% after 3h, but running the reaction overnight allows having the same yield than with TMSCl in 3h (Table I-3, entry 7 vs. entry 1). We also tried other different cobalt(II) sources, in order to try to optimize the catalytic system, without success. The replacement of bipyridine by phenanthroline does not change the yield, but by triphenylphosphine decrease the yield to 13%, as when the reaction is performed without ligand. Contrary to the reductive cross-coupling, the presence of pyridine as co-solvent, with bipyridine as ligand, is necessary to obtain a good yield, as without pyridine, the yield decreases to 11%.

We then checked the effect of different solvents: it appears that the reaction leads to a poor yield, between 11 and 17%, with almost all the tested solvents (Table I-3, entries 14, 15, 16), except with very polar / aprotic solvents like DMF and NMP (Table I-3, entry 17).

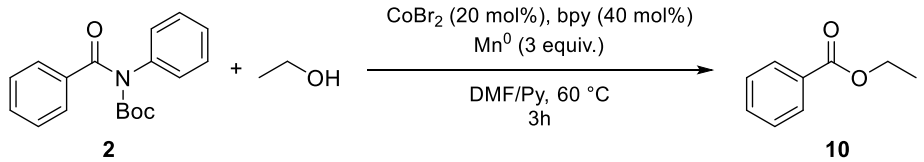

Entry	Deviation from standard conditions	GC yield (%)
1	None	67
2	No CoBr2 / no bpy / no Mn / no TMSCl	n.d.
3	No Mn	n.d.
4	No $CoBr_2$	n.d.
5	No bpy	15
6	No Py	11
7	No TMSCl	65 (20 h)
8	$CoCl_2$ instead of $CoBr_2$	52
9	$Co(OAc)_2$ instead of $CoBr_2$	63
10	PPh_3 instead of bpy	65
11	Phen instead of bpy	13
12	Zn instead of Mn	51
13	In instead of Mn	7
14	Toluene instead of DMF	14
15	THF instead of DMF	17
16	Acetonitrile instead of DMF	11
17	NMP instead of DMF	72
18	10 mol% $CoBr_2$ / 20 mol% bpy	70
19	5 mol% $CoBr_2$ / 10 mol% bpy	80
20	5 mol% $CoBr_2$ / 10 mol% bpy / 1 equiv. Mn / DMF	84
21	5 mol% $CoBr_2$ / 10 mol% bpy / 1 equiv. Mn / NMP	65
22	5 mol% $CoBr_2$ / 10 mol% bpy / 20 mol% Mn / DMF	2

Table I-3: Optimization of the amide-to-ester conversion reaction

As the composition of the reaction was set, we followed the evolution of the formation and the consumption of the starting material, at 40 °C and 60 °C (Graph I-2).

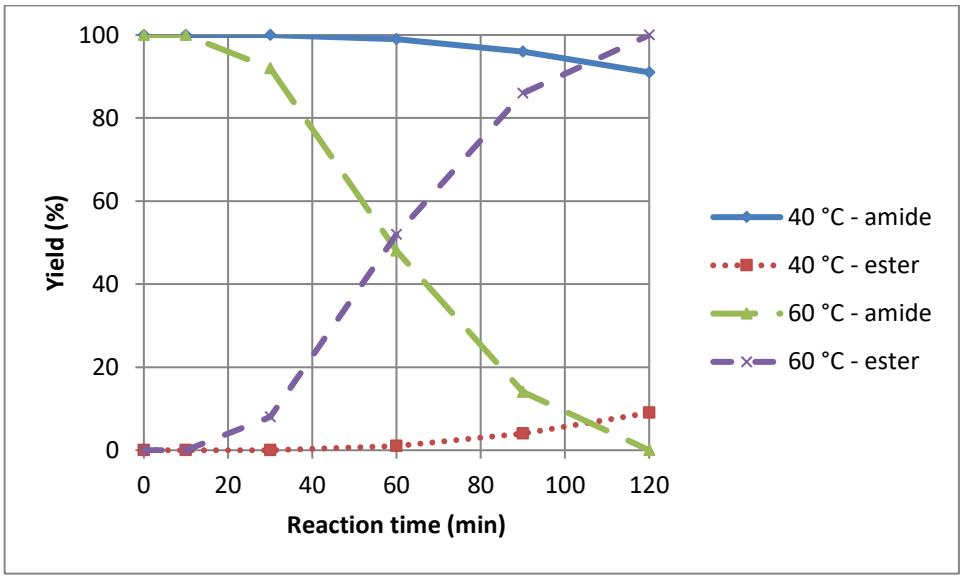

Graph I-2: kinetic monitoring of the amide-to-ester conversion at 40 °C and 60 °C

This study highlights the important influence of the reaction temperature on the reaction kinetic. The higher the temperature is, the faster the reaction occurs. We nevertheless decided to keep 60 °C as reference temperature for the reaction: the kinetic monitoring of the homocoupling tends to show that the catalytic system does not support too high temperatures. However, it seems to be possible to increase the temperature to 80 °C. To keep the smoother reaction conditions, we chose to keep 60 °C as reaction temperature. Thereby, increase the temperature to 80 °C remains an option in the case of substrates difficult to couple.

We then tried to optimize the quantity of the components in the reaction. A decrease of the catalytic loading from 20 to 5 mol% enhanced the reaction yield from 65% to 80% (Table I-3, entry 1 vs. entry 19). As the quantity of cobalt catalyst decreased, the amount of manganese was also reduced to one equivalent, which afforded the ester **10** in 84% yield. A further decrease in the amount of reductant to a catalytic amount (20 mol%) affected the yield, which dropped to 2% (Table I-3, entry 22).

With these optimal reaction conditions fixed, we then explored the scope of *N*,*N*-disubstituted benzamides (Figure I-8). To compare our methodology to the nickel-one existing, we attempted our conditions on the *N*-methyl-*N*-phenylbenzamide **1**. Interestingly, this amide remains unreactive to the cobalt catalytic system, pointing the fact that we should be in presence of a different mechanism that the one calculated by Garg. We also applied our system on the *N*-phenyl-*N*-tosylbenzamide **11** to compare its efficiency with another *N*-protecting/activating group, leading to a yield of 51%, compared to 84% for the boc group. Then, to evaluate to importance of the effect of the carbamate function, we applied our

conditions on the methyl benzoyl(phenyl)carbamate **12**, leading to a yield of 27% and highlighting the importance of the *tert*-butyl carbamate substitution. Thereafter, we also tried our conditions on differently substituted *N*-Boc-benzamide, to check if there is limitation among the *N*-Boc protected secondary amides. The reaction works as well with *N*-phenyl and *N*-benzyl benzamide **2** and **13**, and seems to proceed faster with the *N*-methyl benzamide **14**, as the reaction reach 97% yield in 3h, whereas the *N*-benzyl needs 20h to reach 84% (Figure I-8).

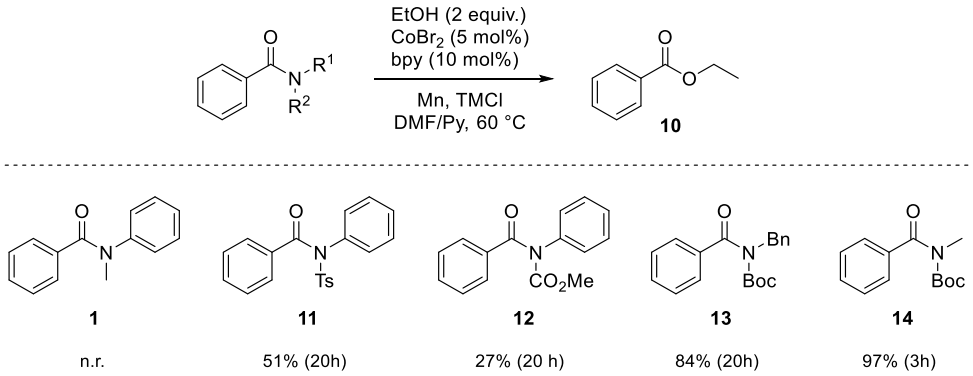

Figure I-8: Scope of *N*,*N*-substituted benzamides. Yield determined by GC yield, using dodecane as internal standard

It is noteworthy that this reaction leads to almost no side products: only the unprotected benzamide and benzophenone were observed by GC as impurity when using *N*-Boc-*N*-phenyl benzamide substrates. The use of *N*-Boc-*N*-methyl benzamide does even not allow the formation of benzophenone, leading to a reaction with very good yield and few side-products. We thus kept the *N*-methyl-*N*-Boc substitution for the benzamides substrates involved for the following scopes.

Starting by the scope of benzamides (Figure I-9), the reaction tolerates a wide variety of functionalities, such as methyl (**15** to **17**), methoxy (**18**), dimethylamino (**19**), ester (**20**), cyano (**21**), and even aldehyde (**22**). With a methyl ester group as *para* substituent of the benzamide, we observed the conversion of the amide function into ester, as the transesterification of the methyl ester function, leading to the diethyl terephthalate (**20**) as product. Another side-reaction occurs in the case of iodo-, bromo- and chlorobenzamides: if the amide function is completely converted into ester, we also observed the protodehalogenation, leading, for the 3 halogenated substrates, to the ethyl benzoate (Scheme I-19). We attempted to follow the evolution of the reaction in this case, but it appeared that side-reactions happen simultaneously with the amide-to-ester conversion. By following the reaction by GC-FID, we could see the formation of three major products: the *N*-Boc-*N*-methylbenzamide **14**, the ethyl benzoate **10** and the ethyl 4-halide-benzoate. These products were formed with comparable reaction speeds. This concomitant evolution indicates that the protodehalogenation reaction is independent of the amide-to-ester conversion.

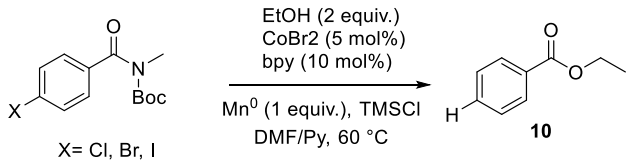

Scheme I-19 Amide-to-ester conversion of halogenobenzamide

Looking for more diversified substrates, we applied the reaction to the *N*-Boc-*N*-methyl cinnamamide and heteraromatic compounds, with success (**23** to **26**). The reaction tolerates indeed pyridyl and thiophenyl moiety, in spite of their coordinating characters. Finally, we also attempted the reaction with aliphatic amides. With our reaction conditions, we are able to convert primary and secondary aliphatic amides into ester with good yield (**27** to **29**). The reaction also worked on amides derived from aminoacid with a correct yield of 53 %, and without epimerization of the chiral α-chiralcenter (**30**). However, neopentylic amides are convert with poor yield and tertiary aliphatic amide are unreactive, probably because of the steric hindrance.

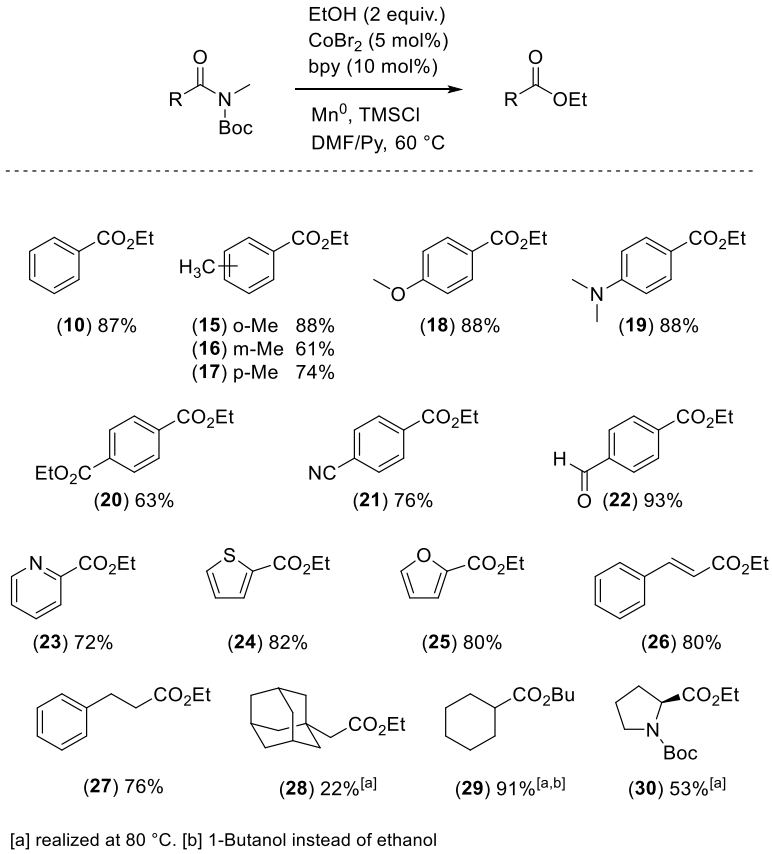

Figure I-9: Scope of *N*-methyl-*N*-Boc-amides. Isolated yields

At last, we examined the scope of alcohol that can be coupled with our conditions (Figure I-10). For this scope, we decreased the amount of alcohol to 1.2 equivalents compared to the amide, except for low-nucleophilic alcohol. In a general way, primary alcohols are coupled with good to very good yield. The

reaction indeed tolerates aliphatic alcohol bearing various chemical functions, such as ether (**35**) and dimethylamino (**36**), that are coupled with excellent yield. However, if the alcohol bears a secondary amine, with an N–H bond, no reaction occurs. As the reaction works with the 2-(*N,N*-dimethylamino)ethanol, the problem does not come from the potential formation of an unreactive complex between the cobalt and the amino-alcohol. Tertiary amines are indeed more nucleophilic and thus more chelating than primary and secondary amines. However, as we noticed previously the important influence of the alcohol on the catalyst to favor of the conversion reaction, we can thus hypothesize that the presence of an amine NH bond inhibits the action of the alcohol on the catalytic system, inhibiting also the whole reactivity.

Concerning other special limitations, allylic and propargylic alcohol are also unreactive, whereas homoallylic, benzylic and heterobenzylic alcohol can be coupled with very good yield (**38**, **39**, **40**, **49**). It is also noteworthy that the 4-chlorobenzylic alcohol is coupled with very good yield (**39**), without product of protodehalogenation. Interestingly, the 2-chloroethanol can also be coupled with a fair yield of 53 % (**37**), as cobalt does not easily insert into Csp^3–Cl bonds. Nevertheless, we observed the protodehalogenated product as side-product, with a ratio chlorinated/dechlorinated product of 83:17.

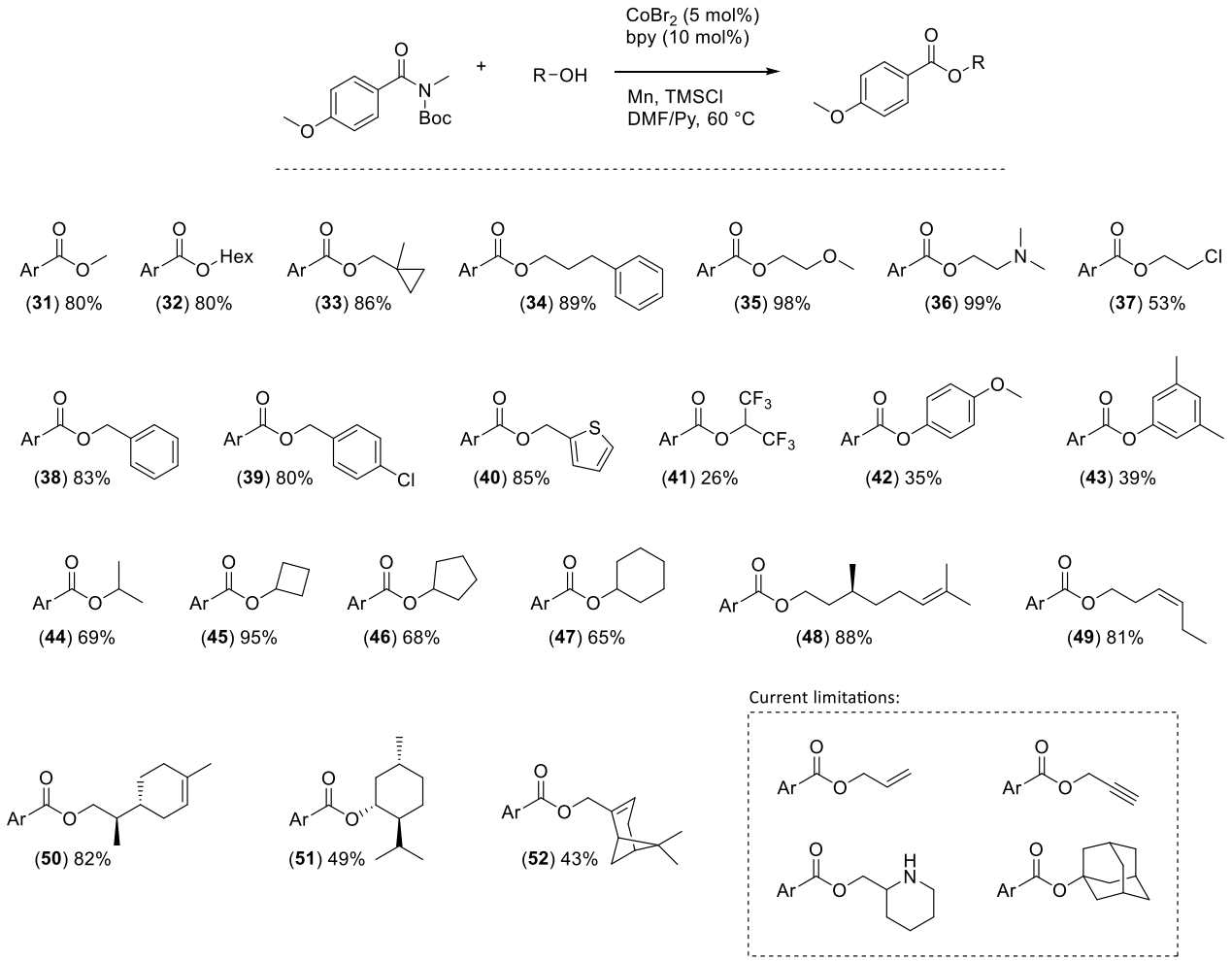

Figure I-10: Scope of alcohols involved in the cobalt-catalyzed amide-to-ester conversion reaction

As the reaction seems sensible to the steric hindrance, secondary alcohol can also be coupled, but in order to obtain correct to very good yield, the reaction has been conducted at 80 °C (**44** to **47**). For example, the cyclobutanol gives a very good yield of 95 % because of the ring strain that decrease the hindrance around the hydroxyl group. The ring strain of cyclopentanol and cyclohexanol being less important, they give their corresponding esters with respectively a yield of 68 % and 65 %. In the case of menthol, despite its cyclohexanol core, the presence of alkyl substituents, and especially the bulky isopropyl group in position 2, leads to a weaker –but still correct– yield than the unsubstituted cyclohexane (**47** vs. **51**). Because of this influence of the steric hindrance on the reactivity, tertiary alcohol cannot be coupled with our conditions, even at 80°C.

However, if our catalytic system cannot react with bulky alcohol, it is surprisingly reactive to weakly nucleophilic alcohol, like phenols and hexafluoroisopropanol (**41** to **43**). They can be converted with poor to fair yield into ester, but in smooth conditions, with selective reagents. It is interesting also to notice that these coupling are not possible with a nickel-catalyzed method: nickel catalyst reacts indeed with phenyl ester, allowing their involvement in coupling reaction, as amides.

To close this scope, we involved natural product as alcohol coupling partners, like citronellol (**48**), menthol isomers (**50** and **51**) and myrtenol (**52**). As expected, *L*-citronnellol and (+)-*p*-menth-1-en-9-ol lead to the right esters with very good yields and without modification of chiral centers, as they are primary alcohol. Surprisingly, (-)-myrtenol, with an allylic alcohol, successfully coupled with a correct yield of 43 %. We hypothesized that the strain of the bridged cycle decreased the allylic character of the hydroxyl group, allowing the coupling reaction to proceed as if it were a hindered alcohol. Compared to the scope of alcohols the Garg's amide-to-ester conversion reaction tolerates, we have similar results with primary alcohols. However, the nickel-catalyzed reaction tolerates hindered alcohol, as tertiary alcohols. But the use of a cobalt catalyst allows the coupling reaction with phenol derivatives, without further reactions on the phenyl ester formed. Moreover, our conditions allow also converting aliphatic amides into esters. We can thus consider these two methods as complementary methods or alternative conditions, depending on the substrates or the alcohol to couple.

The scopes of amides and alcohols gave us several informations allowing us to have an insight about the mechanism of the reaction. Concerning the catalytic system, we have no precise idea on the active species, except that it is a low-valent cobalt specie. As the presence of an alcohol favors specifically the conversion than the homocoupling, we can hypothesize an influence of the alcohol on the catalytic system, by coordination of the alcohol on the cobalt. This can explain the absence of reactivity with hindered alcohol: the presence of bulky groups does not allow the coordination of the alcohol or prevent the approach of other molecules because of their steric hindrance. With a not-hindered alcohol, the cobalt catalyst proceed to the insertion into the C–N bond of the amide. For the next step, we hypothesized a

ligand metathesis, like Garg's proposed for its reaction. Then, a reductive elimination step allows the formation of the ester and the regeneration of the catalyst (Figure I-11).

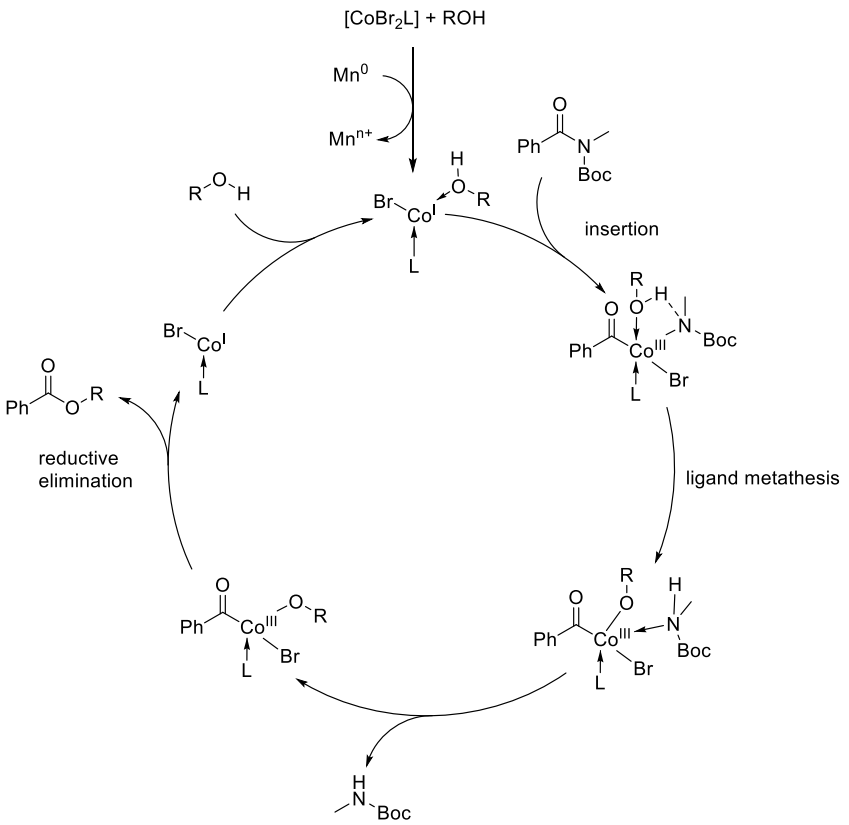

Figure I-11: Proposed mechanism for the cobalt-catalyzed amide-to-ester conversion reaction

To finish with the study of this reaction, we evaluated the scalability of the reaction (Scheme I-20). Aiming for a scale up, we take this opportunity to decrease the amount of catalyst from 5 mol% to 1 mol%, as we stopped at 5 mol% during the optimization for practical reasons. This scale up is also the opportunity to increase the concentration of the reaction media. The reaction has thus been realized on a 10 mmol scale, between the *N*-Boc-*N*-methyl 4-methoxybenzamide and the *L*-citronellol, in 10 mL of a mixture DMF/pyridine (ratio 23:2). After 20 hours of reaction at 60°C and purification, the reaction led to the expected product **48**, with a yield of 76%. Compared to the yield of 88% obtained on the 1 mmol scale, this result shows that these conditions can be applied to gram-scaled reactions with a smaller amount of metal catalyst and with a weak loss of yield.

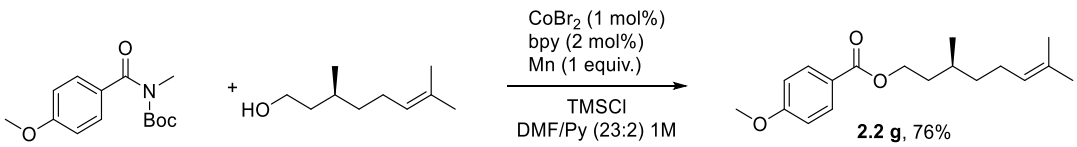

Scheme I-20: Gram-scale synthesis of the L-citronellyl 4-methoxybenzoate by cobalt-catalyzed amide-to-ester conversion

Finally, to support the use of the *N*-Boc protective group as good synthetic option for the activation of amides, we developed a one-pot procedure to convert secondary unprotected amide into ester, *via* the Boc-protection and the cobalt-catalyzed coupling (Scheme I-21). The main interrogation is if the coupling reaction works in presence of the remaining compounds after the protection step: DMAP, Boc_2O, and *tert*-butanol. DMAP is a substituted pyridine, and should have the same action than the pyridine, and the reaction does not proceed with tertiary alcohol. With these considerations, we can envisage they should not interfere. Only Boc_2O could be a problem with the alcohol or the catalyst.

To develop this two-step methodology, we searched for reaction conditions that would allow us to not change the solvent. For the Boc protection of amides, it is generally done in THF or acetonitrile to get an excellent yield. However, to avoid a step of evaporation, we tried to protect the amide with a slight excess of Boc_2O, with catalytic amount of DMAP, in the reaction mixture of solvent (DMF:pyridine). The alcohol is not added at this step because it can also react with Boc_2O to form a carbonate. In these conditions, the amide is protected with success: after 5 hours at 60°C, the protection of the amide seems lead to quantitative conversion on TLC. Fortunately, after the addition of the pre-catalytic system, manganese and the alcohol, we obtained the corresponding ester with a GC yield of 84%. None of the remaining compounds led to side-reactions. This yield has to be compared to the yields of both the protection and the coupling: generally, the Boc-protection step works with an average yield above 90%; the cobalt-catalyzed amide-to-ester conversion with a GC yield of 97%. It corresponds to a global yield of at least 87% over two steps. Compared to this value, the GC yield of the one-pot two-step procedure is similar. It is thus possible to directly convert into ester a secondary amide without isolate the pure *N*-Boc protected intermediate, and to obtain a similar yield in a one-pot procedure, compared to the yield in two separated steps.

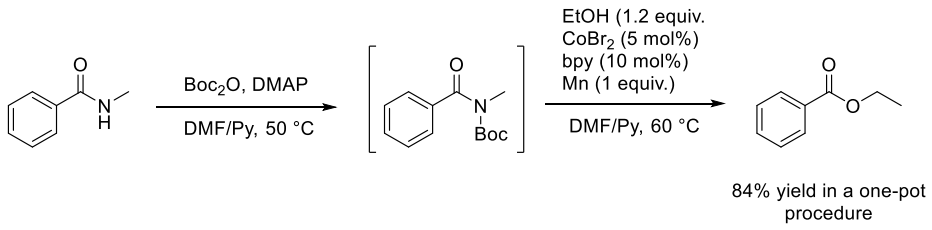

Scheme I-21: One-pot procedure for the amide-to-ester conversion, starting from secondary amide

I.3. Application of the amide-to-ester conversion: toward new synthetic strategy

The transformation of amides into esters, and *a fortiori* all the metal-catalyzed coupling reactions involving amides, remained a challenging reaction for a long time. But since these reactions are no longer impossible and can be applied on a broad range of amides, we can wonder about the potential synthetic applications arising from the amidic C–N bond activation. *As we developed the cobalt-catalyzed amide-to-*

ester conversion, we will propose applications for this reaction, but the proposed strategies could be used with other metal-catalyzed C–N activation.

To validate a potential use of this method for synthetic strategy, we applied it with success on two specific secondary amides: *N*-(8-aminoquinolyl) benzamide (**53**) and *N*-methoxy benzamide (**54**) (Figure I-12). These two *N*-substitutions are well known and very used as efficient C–H directing groups.[60–63] However, the high stability of these amides appears to be a problem to remove or transform them, making them difficult to apply in total synthesis. A lot of researches are ongoing to find easy way to hydrolyze or to develop traceless alternative directing group to circumvent this major drawback.

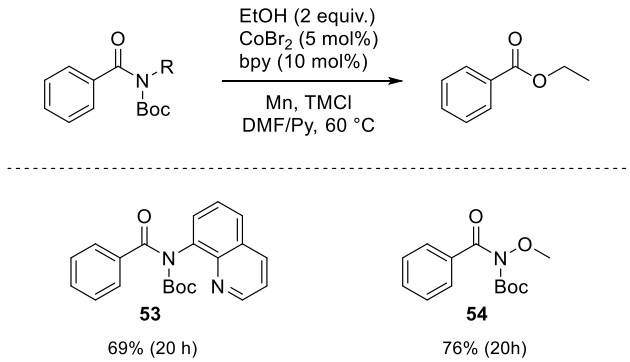

Figure I-12: Cobalt-catalyzed conversion of *N*-Boc protected C–H activation directing group

In this context, the metal-catalyzed activation of the amidic C–N bond stands as a practical and strategic solution for the use and the post-functionalization of amide directing groups. Based on this observation, it is now possible to imagine multi-step synthesis that would involve a C–H activation step followed by a metal-catalyzed coupling reaction with the amide directing group.

To highlight this principle, we tried to propose the synthesis of molecules of interest including an ester function. As the most common C–H activation reactions allow the *ortho* functionalization of aromatic rings, we thus looked for structures derived from *ortho*-functionalized benzoic acid. Three interesting families of compounds match with our structural restrictions: the resorcylic macrolactones, the isocoumarins and dihydroisocoumarins, and the salicylic esters (Figure I-13).

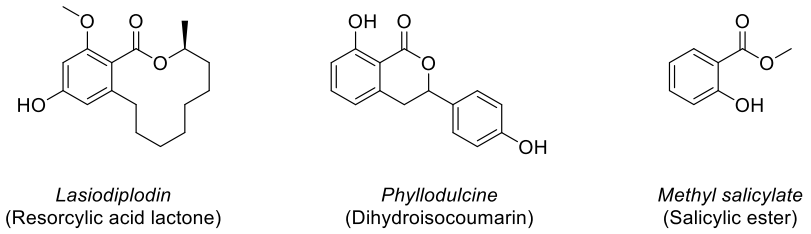

Figure I-13: Examples of resorcylic acid lactones, dihydroisocoumarins and salicylic esters

We decided to focus our prospective work on resorcylic acid lactone, representing a synthetically more interesting family of diversified compounds.

I.3.1. The Resorcylic Acid Lactones[64]

The resorcylic acid lactones are a family of benzannulated macrolactones including the motif β-resorcylic acid. This family includes several macrocyclic compounds of 10-, 12- or 14-member. These compounds are naturally produced by fungi and present different biological activities, from estrogenic to antileukemic effects. Because of their properties, the total synthesis of resorcylic acid lactones is the center of an important interest, and especially the Zearalenone, the Lasiodiplodin and their derivatives, which had been synthesized with different approaches. (Figure I-14)

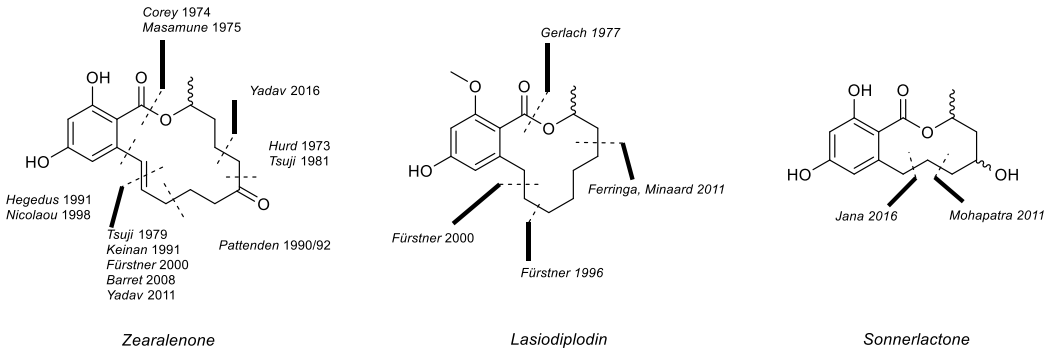

Figure I-14: Disconnections in previous published syntheses of resorcylic acid lactones

The Zearalenone has been one of the most synthesized compounds of this family. Concerning the strategies applied, we can notice that one of the most exploited disconnections recently is the double bond, which can be easily and efficiently made by ring closing metathesis, as Fürstner,[65] Yadav[66] and Feringa[67] did. Yadav published thereafter another synthesis of zearalenone with a succession RCM/selective reduction as ring-closing step. The method RCM/hydrogenation has often been used for the synthesis of different resorcylic macrolactones, like Zearalenone, Lasiodiplodin, or Sonnerlactone.

For older syntheses of resorcylic acid, we can find disconnections of the ester functions. These syntheses based the ring closure step on a macrolactonisation reaction, like the syntheses of Zearalenone by Corey in 1974,[68] and the synthesis of Lasiodiplodin by Gerach in 1977.[69]

Despite all these syntheses, , we can notice that even for close structures, like the different lasiodiplodin derivatives, the key steps and disconnections are different (Figure I-15). No general synthetic pathway has been proposed for this family of compounds. With the development made by the metal-catalyzed C–N amide bond activation, we wanted to propose a strategy that could be applicable to the synthesis of the majority of the resorcylic acid lactones.

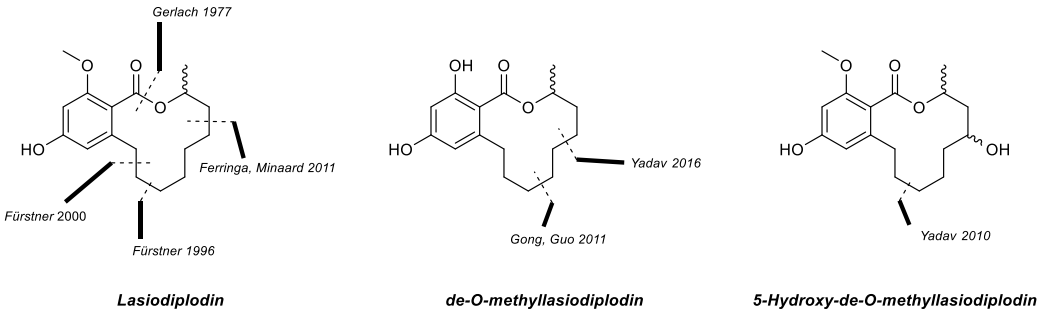

Figure I-15: Main disconnections in syntheses of Lasiodiplodin derivatives

We will apply our concept on the case of the resorcylic macrolactones to show the synthetic potential of the metal-catalyzed C–N bond activation. As our work does not concern the C–H activation step, methods that are described in the literature will be proposed for this step. This part consists in the conceptualization of a synthetic strategy using the cobalt-catalyzed amide-to-ester conversion. No experiences have been realized for now to validate or invalidate this idea.

I.3.2. The C–H functionalization / Amide-to-ester conversion strategy

The resorcylic macrolactones can be divided in two parts: the resorcylic acid part and a 2-hydroxyalkyl part. The principle of this strategy is to connect these two parts by efficient and mostly versatile reactions. Another part of the strategy is to use easy-to-access and weakly functionalized starting materials, like the 2,4-dihydroxybenzoic acid (Figure I-16).

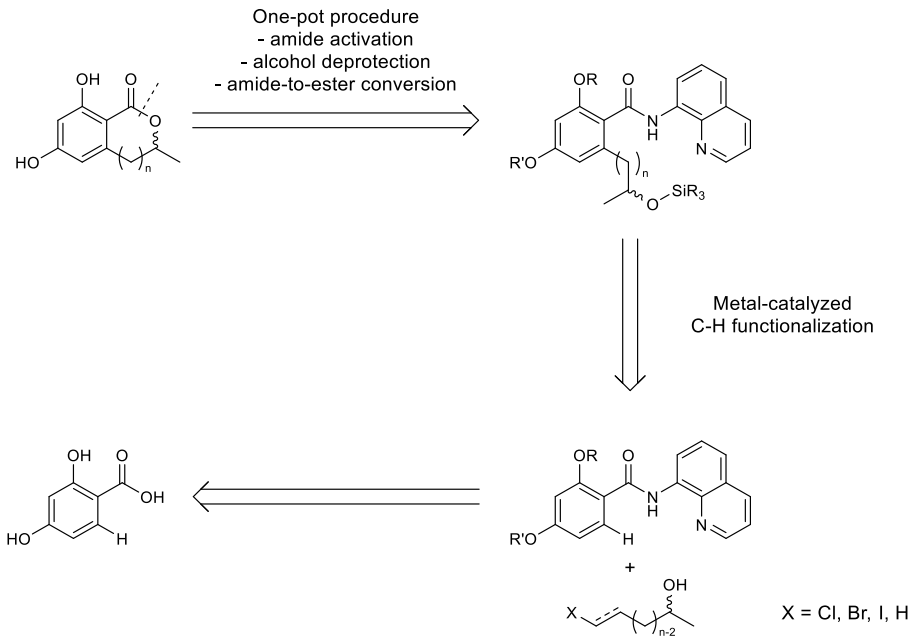

Figure I-16: Retrosynthesis of resorcylic acid lactones with the C-H functionalization/amide-to-ester conversion strategy

The alkyl part has to be synthesized apart, with on one extremity the 2-hydroxyethyl- pattern, present in each member of the resorcylic acid lactone family, and on the other extremity a chemical function allowing a coupling reaction. The main idea is to not use expensive or very toxic transition metals, like ruthenium for metathesis reactions or palladium for cross-coupling reactions, or to avoid organometallic intermediate. The best option would be to connect the alkyl part to the resorcylic acid part *via* C–H functionalization. A C–H functionalization step would allow indeed creating a Csp^2–C bond directly between the resorcylic acid amide derivative and an alkyl part functionalized with a halogen or a double bond, depending on the reaction used. Besides, the current researches on C–H activation reactions are mainly focused on the use of first-raw metals, like nickel and cobalt.

Once the alkyl part is connected to the *ortho* position of the resorcylic acid part, the ring can be closed by a one-pot procedure amide boc-protection/amide-to-ester conversion. However, for the macrolactonisation step, a major point is to take in account: the hydroxyl group have to be protected beforehand. *It could also be protected before the CH functionalization step, depending if the conditions of this step tolerate or not a free hydroxyl group.*

Indeed, in the previously described one-pot procedure, the reaction was between two distinct coupling partners; the alcohol was added in the reaction middle after the protection. For a lactonization, the hydroxyl group is a part of the molecule, as the amide, and both of these functions can react with Boc_2O. It is thus necessary to find a selective alcohol protective group.

As in our case, we are planning to have a convenient one-pot lactonization procedure; this protective group has to be easily removable and has to remain unreactive to the amide-to-ester conversion. The method of deprotection has also to be chosen carefully, as the Boc protective group must not be removed and the deprotecting reagent has to be also “innocent” toward the cobalt catalytic system. This restriction excludes every protective groups that require acidic conditions and strong nucleophiles. We thus decided to choose silyl ether as protective group for the hydroxyl group: the protection method is smooth and selective, as the deprotection process; as we already use TMSCl as activating agent without problem, it should not cause problems to use an excess or another silyl chloride; and the deprotection process can be done with TBAF, which is an organic salt, relatively inert to the majority of chemical functions. After the deprotection, the silyl fluoride by-product should also be unreactive, the Si–F bond being one of the most stable chemical bond.

To summarize this strategy, it consists in a general pathway for the formation of the macrocycle of resorcylic acid lactone. The idea is to start from the resorcylic acid amide derivatives, prepared from commercially available resorcylic acid, and from the synthetized 2-hydroxyl alkyl chain corresponding to the wanted resorcylic acid lactone. These two part are bonded together by a C–H functionalization step, avoiding other function insertion steps or classical coupling reaction step. Then, the macrolactone ring is

closed in a one-pot four-step procedure involving the silylation of the alcohol, the Boc-protection of the amide, the deprotection of the alcohol and the cobalt-catalyzed amide-to-ester conversion.

However, some unknown points remain to study before to apply this strategy in total synthesis:

- The C–H functionalization step has also to be tried before its application in a total synthesis. If several reactions are described in the literature to form Csp2–Csp3 bonds, they cannot be suitable to our case.
- We did not study the lactonization *via* our amide-to-ester conversion reaction. As seen before, different restrictions have to be taken in account, and this step has to be independently studied, with its own optimization process: dilution, catalytic system, temperature…
- It has been reported by Madsen *et coll.* that the desilylation of the *N*-Boc-pyroglutaminol leads to the migration of the Boc group from the nitrogen to the alcohol.[70] This potential side-reaction has to be watched out, because if it occurs, the hydroxyl protective will have to be changed.
- Also, Zeng *et coll.* developed recently the metal-free amide-to-ester conversion, using CsF on *N*-Boc-*N*-Phenyl benzamide.[71] Their reaction seems to work in DMF, with TBAF, and at 80°C. This reaction is not a proper problem for the strategy, as it allows the formation of the ester from the amide. However, this reaction has to be compared to the cobalt-catalyzed esterification in the case of a macrolactonization.

I.4. Conclusions and perspectives

In conclusion, we started to develop the cobalt-activation of the amide function, using $CoBr_2$ / bpy as catalytic system, and manganese as reductant, in DMF. Three reactions are under investigation:

- The semi-decarbonylative homocoupling of amide, allowing the preparation of symmetric benzophenone from activated *N*-Boc-*N*-phenyl benzamide. The development of this reaction is not complete, the maximum yield obtained being 65% with 0.5 equivalents of catalyst. An optimization of the ligand can be realized, maybe with a more electron-rich ligand or a NHC-ligand, to favor a complete decarbonylation step or the decoordination of the CO ligand.
- The reductive cross-coupling between amide and aryl bromide, allowing the preparation of asymmetric benzophenone. The kinetic of the reaction has to be more studied, in order to determined which step is the more problematic, and which insertion occurs first between the aryl bromide and the amide.
- The amide-to-ester conversion, allowing the transformation of *N*-Boc-amide into alkyl or aryl esters. This reaction has been fully optimized, but some improvements can still be done, like the

possibility to involve tertiary alcohols. Besides, this reaction will be also under development to proceed to lactonizations and macrolactonizations.

The final goal would be to successfully applied one of these reactions as a key step in the synthesis of a molecule of interest, to highlight the synthetical advantages of this new amide chemistry.

Bibliography of part I

[1] L. Pauling, R. B. Corey, H. R. Branson, *Proc. Natl. Acad. Sci.* **1951**, *37*, 205–211.

[2] A. Vilsmeier, A. Haack, *Berichte der Dtsch. Chem. Gesellschaft* **1927**, *60*, 119–122.

[3] M. S. Meier, S. M. Ruder, in *Encycl. Reagents Org. Synth.*, John Wiley & Sons, Ltd, Chichester, **2001**, pp. 1–6.

[4] S. Nahm, S. M. Weinreb, *Tetrahedron Lett.* **1981**, *22*, 3815–3818.

[5] J. T. Spletstoser, J. M. White, A. R. Tunoori, G. I. Georg, *J. Am. Chem. Soc.* **2007**, *129*, 3408–3419.

[6] J.-B. Falmagne, J. Escudero, S. Taleb-Sahraoui, L. Ghosez, *Angew. Chemie Int. Ed. English* **1981**, *20*, 879–880.

[7] N. J. Sisti, E. Zeller, D. S. Grierson, F. W. Fowler, *J. Org. Chem.* **1997**, *62*, 2093–2097.

[8] G. Barbaro, A. Battaglia, C. Bruno, P. Giorgianni, A. Guerrini, *J. Org. Chem.* **1996**, *61*, 8480–8488.

[9] A. B. Charette, P. Chua, *Tetrahedron Lett.* **1997**, *38*, 8499–8502.

[10] A. Charette, P. Chua, *Tetrahedron Lett.* **1998**, *39*, 245–248.

[11] A. B. Charette, M. Grenon, *Tetrahedron Lett.* **2000**, *41*, 1677–1680.

[12] A. B. Charette, P. Chua, *J. Org. Chem.* **1998**, *63*, 908–909.

[13] A. B. Charette, M. Grenon, *Can. J. Chem.* **2001**, *79*, 1694–1703.

[14] G. Barbe, A. B. Charette, *J. Am. Chem. Soc.* **2008**, *130*, 18–19.

[15] G. Pelletier, W. S. Bechara, A. B. Charette, *J. Am. Chem. Soc.* **2010**, *132*, 12817–12819.

[16] W. S. Bechara, G. Pelletier, A. B. Charette, *Nat. Chem.* **2012**, *4*, 228–234.

[17] R. P. Houghton, R. R. Puttner, *J. Chem. Soc. D Chem. Commun.* **1970**, 1270.

[18] N. Niklas, F. W. Heinemann, F. Hampel, T. Clark, R. Alsfasser, *Inorg. Chem.* **2004**, *43*, 4663–4673.

[19] S. Mundinger, U. Jakob, P. Bichovski, W. Bannwarth, *J. Org. Chem.* **2012**, *77*, 8968–8979.

[20] L. Hie, N. F. Fine Nathel, T. K. Shah, E. L. Baker, X. Hong, Y. F. Yang, P. Liu, K. N. Houk, N. K. Garg, *Nature* **2015**, *524*, 79–83.

[21] E. L. Baker, M. M. Yamano, Y. Zhou, S. M. Anthony, N. K. Garg, *Nat. Commun.* **2016**, *7*, 1–5.

[22] B. J. Simmons, N. A. Weires, J. E. Dander, N. K. Garg, *ACS Catal.* **2016**, *6*, 3176–3179.

[23] N. A. Weires, E. L. Baker, N. K. Garg, *Nat. Chem.* **2016**, *8*, 75–79.

[24] L. Hie, N. F. Fine Nathel, X. Hong, Y.-F. Yang, K. N. Houk, N. K. Garg, *Angew. Chem. Int. Ed.* **2016**, *55*, 2810–2814.

[25] L. Hie, E. L. Baker, S. M. Anthony, J.-N. Desrosiers, C. Senanayake, N. K. Garg, *Angew. Chem. Int. Ed.* **2016**, *55*, 15129–15132.

[26] C. Chu, L. Dang, *J. Org. Chem.* **2018**, *83*, 5009–5018.

[27] J. E. Dander, E. L. Baker, N. K. Garg, *Chem. Sci.* **2017**, *8*, 6433–6438.

[28] J. M. Medina, J. Moreno, S. Racine, S. Du, N. K. Garg, *Angew. Chem. Int. Ed.* **2017**, *56*, 6567–6571.

[29] T. B. Boit, N. A. Weires, J. Kim, N. K. Garg, *ACS Catal.* **2018**, *8*, 1003–1008.

[30] S. Shi, G. Meng, M. Szostak, *Angew. Chem. Int. Ed.* **2016**, *55*, 6959–6963.

[31] S. Shi, M. Szostak, *Chem. Eur. J.* **2016**, *22*, 10420–10424.

[32] S. Shi, M. Szostak, *Org. Lett.* **2016**, *18*, 5872–5875.

[33] S. Shi, M. Szostak, *Synth.* **2017**, *49*, 3602–3608.

[34] S. C. Lee, L. Guo, H. Yue, H. H. Liao, M. Rueping, *Synlett* **2017**, *28*, 2594–2598.

[35] J. Hu, Y. Zhao, J. Liu, Y. Zhang, Z. Shi, *Angew. Chemie* **2016**, *55*, 8718–8722.

[36] H. Yue, L. Guo, S.-C. Lee, X. Liu, M. Rueping, *Angew. Chem. Int. Ed.* **2017**, *56*, 3972–3976.

[37] H. Yue, L. Guo, H.-H. Liao, Y. Cai, C. Zhu, M. Rueping, *Angew. Chem. Int. Ed.* **2017**, *56*, 4282–4285.

[38] W. Srimontree, A. Chatupheeraphat, H. H. Liao, M. Rueping, *Org. Lett.* **2017**, *19*, 3091–3094.

[39] X. Liu, H. Yue, J. Jia, L. Guo, M. Rueping, *Chem. Eur. J.* **2017**, *23*, 11771–11775.

[40] G. Meng, M. Szostak, *Org. Lett.* **2015**, *17*, 4364–4367.

[41] C. Liu, Y. Liu, R. Liu, R. Lalancette, R. Szostak, M. Szostak, *Org. Lett.* **2017**, *19*, 1434–1437.

[42] C. Liu, G. Meng, Y. Liu, R. Liu, R. Lalancette, R. Szostak, M. Szostak, *Org. Lett.* **2016**, *18*, 4194–4197.

[43] S. Shi, M. Szostak, *Org. Lett.* **2017**, *19*, 3095–3098.

[44] P. Lei, G. Meng, M. Szostak, *ACS Catal.* **2017**, *7*, 1960–1965.

[45] G. Meng, R. Szostak, M. Szostak, *Org. Lett.* **2017**, *19*, 3596–3599.

[46] G. Meng, R. Lalancette, R. Szostak, M. Szostak, *Org. Lett.* **2017**, *19*, 4656–4659.

[47] P. Lei, G. Meng, Y. Ling, J. An, S. P. Nolan, M. Szostak, *Org. Lett.* **2017**, *19*, 6510–6513.

[48] G. Meng, P. Lei, M. Szostak, *Org. Lett.* **2017**, *19*, 2158–2161.

[49] P. Lei, G. Meng, Y. Ling, J. An, M. Szostak, *J. Org. Chem.* **2017**, *82*, 6638–6646.

[50] S. Shi, M. Szostak, *Chem. Commun.* **2017**, *53 VN-r*, 10584–10587.

[51] G. Meng, M. Szostak, *Angew. Chem. Int. Ed.* **2015**, *54*, 14518–14522.

[52] C. Liu, G. Meng, M. Szostak, *J. Org. Chem.* **2016**, *81*, 12023–12030.

[53] G. Meng, M. Szostak, *Org. Lett.* **2016**, *18*, 796–799.

[54] G. Meng, S. Shi, M. Szostak, *ACS Catal.* **2016**, *6*, 7335–7339.

[55] G. Meng, M. Szostak, *ACS Catal.* **2017**, *7*, 7251–7256.

[56] C. Gosmini, A. Moncomble, *Isr. J. Chem.* **2010**, *50*, 568–576.

[57] Y. Liu, M. Achtenhagen, R. Liu, M. Szostak, *Org. Biomol. Chem.* **2018**, 1322–1329.

[58] Y. Liu, S. Shi, M. Achtenhagen, R. Liu, M. Szostak, *Org. Lett.* **2017**, *19*, 1614–1617.

[59] Y. Bourne-Branchu, C. Gosmini, G. Danoun, *Chem. Eur. J.* **2017**, *23*, 10043–10047.

[60] R. Y. Zhu, M. E. Farmer, Y. Q. Chen, J. Q. Yu, *Angew. Chem. Int. Ed.* **2016**, *55*, 10578–10599.

[61] G. Rouquet, N. Chatani, *Angew. Chem. Int. Ed.* **2013**, *52*, 11726–11743.

[62] O. Daugulis, J. Roane, L. D. Tran, *Acc. Chem. Res.* **2015**, *48*, 1053–1064.

[63] X. Yang, G. Shan, L. Wang, Y. Rao, *Tetrahedron Lett.* **2016**, *57*, 819–836.

[64] S. Bräse, F. Gläser, C. Kramer, S. Lindner, A. M. Linsenmeier, K.-S. Masters, A. C. Meister, B. M. Ruff, S. Zhong, *The Chemistry of Mycotoxins*, Springer Vienna, Vienna, **2013**.

[65] A. Furstner, O. R. Thiel, N. Kindler, B. Bartkowska, *J. Org. Chem.* **2000**, *65*, 7990–7995.

[66] J. S. Yadav, P. V. Murthy, *Synthesis (Stuttg).* **2011**, 2117–2124.

[67] M. P. Baggelaar, Y. Huang, B. L. Feringa, F. J. Dekker, A. J. Minnaard, *Bioorganic Med. Chem.* **2013**, *21*, 5271–5274.

[68] E. J. Corey, K. C. Nicolaou, *J. Am. Chem. Soc.* **1974**, *96*, 5614–5616.

[69] H. Gerlach, A. Thalmann, *Helv. Chim. Acta* **1977**, *60*, 2866–2871.

[70] L. Bunch, P. O. Norrby, K. Frydenvang, P. Krogsgaard-Larsen, U. Madsen, *Org. Lett.* **2001**, *3*, 433–435.

[71] H. Wu, W. Guo, S. Daniel, Y. Li, C. Liu, Z. Zeng, *Chem. Eur. J.* **2018**, *24*, 3444–3447.

Part II. Development of new cobalt catalysts with dipyrromethene ligands

Cobalt can react in many ways, and perform different and unusual reactions. This versatility depends on the composition of the reaction medium and principally the ligands on which the cobalt is associated. Indeed, as seen with previously developed reactions, the presence or not of an additive or a co-solvent can easily improve or alter the yield of a reaction. However, another parameter with a high influence on the cobalt reactivity is the choice of the ligand. The preliminary results concerning cobalt reactivity toward amides show that cobalt has potential unknown reactivity, and this reactivity could be unlocked by a thoughtful choice of ligands. To support this principle, we look for other cobalt complexes described in the literature and our attention was caught by the work of three research groups: Patrick Holland's group, Paul Chirik's group and Theodore Betley's group.

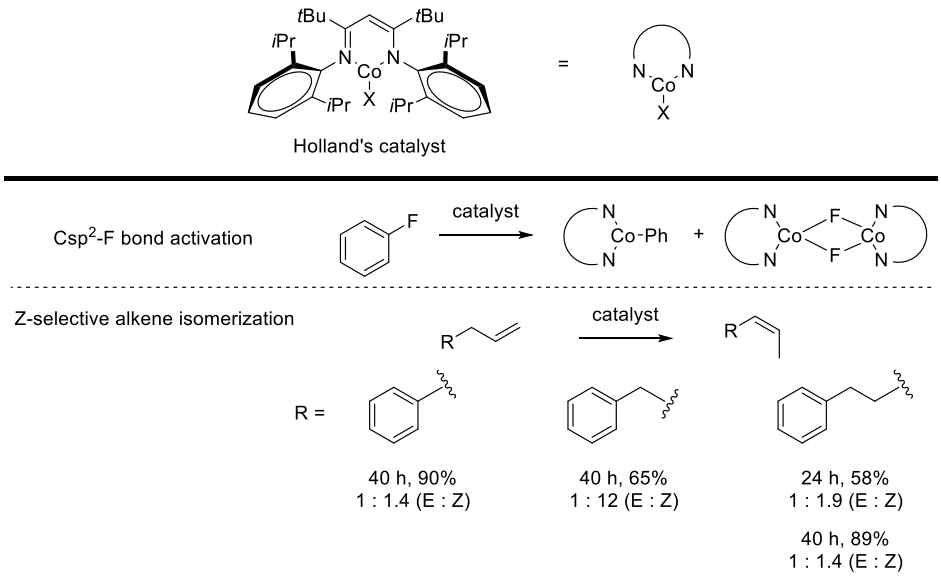

Figure II-1: Structure of Holland's catalyst and examples of reactions

Holland's group is mainly focused on iron and cobalt complexes based on β-diketiminitate ligands, and their associated reactivity. β-diketiminitate ligands, also called nacnac, are LX type bidentate ligands widely used in catalysis.[1,2] Structurally, nacnac are the nitrogenous equivalent of acetylacetonate (or acac), but the presence of nitrogens allows the introduction of functionalizations around the coordination site.[3] This possibility of adding functions allows the tuning of the steric hindrance and the electronic properties of

the complex, and thus an accurate tuning of the complex reactivity. By studying the effect of the ligand on the metal center, and selecting carefully the substitution of their nacnac ligand, they developed highly reactive three-coordinated cobalt complexes, which allow them to perform unusual reactions, like the insertion of a cobalt complex into a Csp^2–F bond[4] or the cobalt-catalyzed selective isomerization of alkenes (Figure II-1).[5]

On its side, Chirik's group works on nickel, cobalt and iron complexes with tridentate pincer ligands. The tridentate ligands they use can be divided in three main family: *bis*(diarylphosphinomethyl)pyridines (PNP), terpyridines (NNN) and diiminopyidines (NNN). The association of cobalt with these types of ligand allows Chirik's group to develop different kind of reactions, like Suzuki-Miyaura cross-coupling (PNP ligand),[6] Csp^2–H borylation (PNP ligand)[7,8] and hydrosilylation (NNN ligand) (Figure II-2).[9]

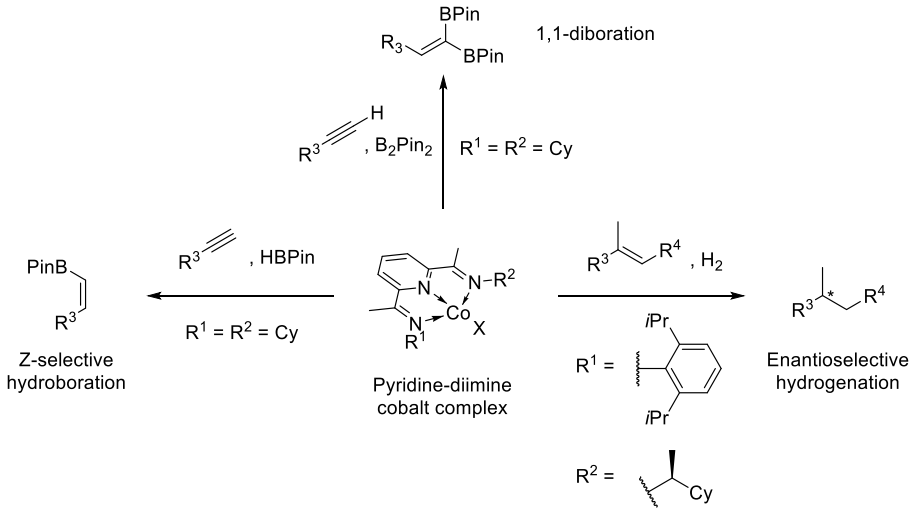

Figure II-2: Examples of cobalt-catalyzed reactions developed by Chirik's group, using a pyridine-diimine tridentate ligand[10–12]

Betley's group works on two main subjects: the study of polynuclear complexes for small molecule activation and the C–H bond functionalization to build molecules with heteroatoms. For this part, we got interested by this last subject on C–H functionalization. For this subject, they developed iron and cobalt complexes with a dipyrromethene ligand and study their electronic properties and their reactivity.[13,14] These studies led to the development of complexes able to realize amination *via N*-group transfer,[15] and to prepare substituted pyrrolidine (Figure II-3).[16]

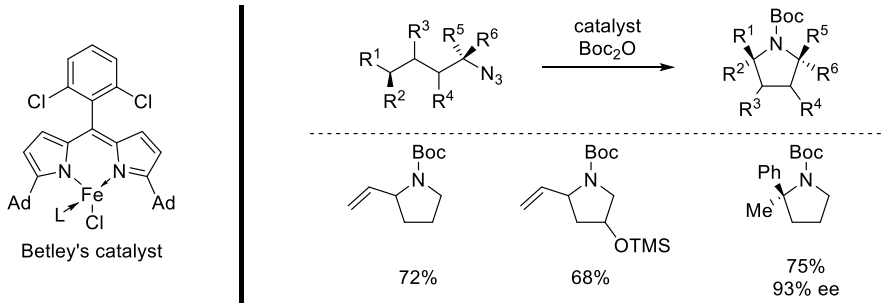

Figure II-3: Reaction developed by Betley's group. Selected examples with isolated yields given

Inspired by the work of these groups, we decided to develop a new family of cobalt complexes, based on a ligand that could give access to a new reactivity for cobalt-catalyzed cross-coupling reactions. The main interest to develop this kind of elaborated complexes is to have a well-defined and characterized catalyst or pre-catalyst, in order to have a better idea of mechanisms. But as we exposed before, the choice of the complex, and *a fortiori* the choice of the ligand, has to be carefully done. To this end, we have to list the conditions and restrictions dictated by cobalt-catalyzed coupling reactions, beginning by thinking about the active species. Generally, in cobalt catalysis, for reaction outside a glovebox, the cobalt complex introduced in the reaction medium is not the active species. The pre-catalyst is usually a bench-stable cobalt(II) complex, that will be reduced into a low-valent cobalt complex to perform the coupling reaction.

In reductive cross-coupling, the cobalt species is generally reduced by a large excess of metallic powder to obtain undefined low-valent cobalt (0) or (I). Besides, the presence of metallic powder also becomes a drawback to analyze the reaction medium and follow the reaction by NMR. To simplify the reaction conditions, we searched for a solution to reduce the cobalt without the presence of a heterogeneous reductant. To avoid the addition of a strong reductant, that can induce side-reactions, we thought about electron-transferring compounds that could allow a smooth activation of the pre-catalyst. We decided to look for organometallic compounds with reducing properties: organometallic compounds can be chelated to another coordination site on the ligand, and thereby combine to the cobalt complex.

We would thus aim at a bimetallic complex with three distinct parts to consider: a reactive part including a cobalt complex to perform reactions, a reductant part including an organometallic moiety able to transfer electron in order to reduce the cobalt reactive part; and a bridging ligand between these two metals allowing the electron-transfer from the reductant part to the reactive part (Figure II-4).

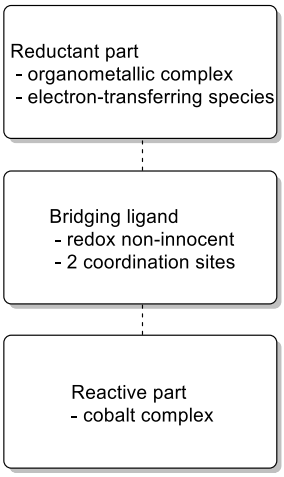

Figure II-4: Concept of our bimetallic complex

To reach this aim, we have to choose a redox non-innocent ligand, able to be reduced, to store and transfer electrons, and to participate to the global oxidation degree of the complex.[17,18] This ligand also needs to include two separated coordination sites. The coordination site of the cobalt would be bidentate or tridentate, to ensure a strong coordination of the metal to the ligand. Insofar as different possibilities are available for the reducing part, we imposed no structural restrictions to the other coordination site, except that it would include only L coordination mode. About the reductant part, we investigated two type of electron-transferring species: divalent organolanthanides and photosensitive polypyridyl ruthenium(II). *The choice of these species will be discussed thereafter.*

Another point in the choice of the ligand was that the two coordination sites have to be conjugated, but also clearly separated through space to avoid potential troubling interaction between the two metal centers. To finally decrease the number of potential ligands that fit with these restrictions, we also limit our choice to ligands that can be prepared in a reasonable number of simple steps.

With these conditions, we could envisage using, like Chirik, a terpyridine derivative or another pincer ligand, but this kind of ligand have already been widely studied.[19] They are also difficult to synthesize in few steps in satisfying yield and do not allow a large possibility of functionalization outside commercial starting materials.[20] Besides, they do not include the transition metal center into their conjugation. Compared to tridentate pincer ligands, bidentate nacnac ligands get the metal more involve in the conjugation of the coordination site, because of the LX coordination mode and the mesomeric form of the ligand.

However, nacnac ligands have also already been widely studied in catalysis.[21] We thus searched for similar LX bidentate ligands from the β-diketiminate family, and, motivated by the results of Betley's group in catalysis with their iron complexes,[22] we finally decided to choose a ditopic dipyrromethene ligand, with

a pyridyl substituent. This ligand is reachable in two steps and allows several functionalizations on the dipyrrin part and the pyridyl part (Figure II-5).

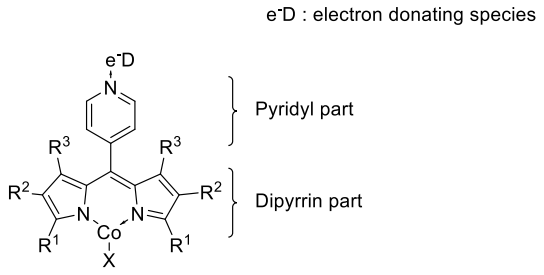

Figure II-5: general concept of the new family of bimetallic complexes

An important and interesting point concerning the structure of dipyrromethene ligands, for our case, is the fact that the dipyrrin part and the pyridyl part are not conjugated at the ground state: there is a dihedral angle, generally between 50° and 60°, between the aryl part and the dipyrrin part in 5-aryl dipyrromethenes. However, it has been shown with the case of BODIPY that this angle can decrease by an energetic contribution to the complex, if no steric restrictions prevent the rotation.[23,24] Indeed, BODIPY have two pathways to expend energy: they fluoresce or stretch and rotate their bonds. Without restrictions, the angle between the two parts can decrease and gets closed to 0°. The two parts would be then conjugated, allowing an energy transfer, generally from the dipyrrin part to the aryl part. In our case, the concept is to transfer an electron to the pyridyl part in order to destabilize the complex and observe if the rotation occurs. If the rotation, and thus the conjugation of the two parts, can be forced by this way, the question will be: will the electron be transferred to the dipyrrin part, and then to the catalyst metal center? (Figure II-6)[25]

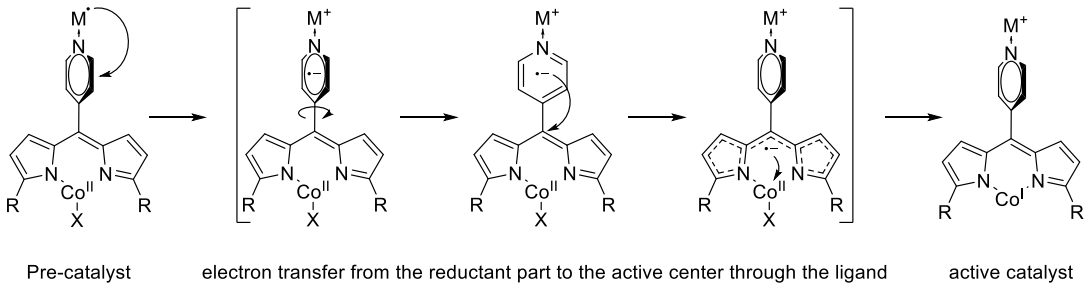

Figure II-6: Concept of the use of dipyrromethene ligand for this project

II.1. State of the art about dipyrromethene metallocomplexes

Dipyrromethenes are a family of compounds with a structure corresponding to a half-porphyrin. They are composed by a pyrrole unit linked to an azafulvene unit by its methine carbon (*meso* position). The

conjugation between these two units results in an interexchange between them, and thus an equivalence between position 1 and 9, 2 and 8 and 3 and 7 (Figure II-7).

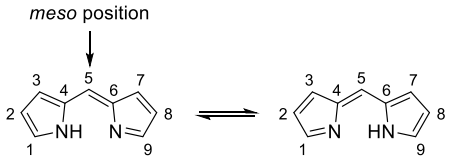

Figure II-7: Numbering of the position on dipyrromethenes

The chemistry of dipyrromethenes (also called dipyrrins) belongs for a long time to porphyrin chemistry, as building blocks for the synthesis of asymmetric porphyrins. They first appeared as side-product in the porphyrin synthesis proposed by Rothemund in 1935,[26,27] as zinc complexes. Since, several dipyrrin complexes have been reported with a large diversity of transition metals,[28] as the formation of homoleptic dipyrrin metallocomplexes is generally easy. Indeed, the coordination of a transition metal can be realized by mixing the dipyrrin ligand with a metal salt (acetate most of the time).[29] The formation of heteroleptic metallocomplexes including dipyrrin ligand is more difficult and depends on the lability of the ligands of the salt precursor. For example, Telfer *et coll.* reported in 2008 the synthesis of two different heteroleptic dipyrrin/bipyridine ruthenium complexes (Scheme II-1): one with two bipyridine ligands for one dipyrrin, and another with two dipyrrin ligand for one bipyridine.[30] Each complex has been prepared from a different precursor:

- With the precursor $[Ru(bpy)_2Cl_2]$, bipyridine ligands are not labile and have a strong coordination bonding with ruthenium. In that case, the dipyrrin ligand substitutes only the chloride ligands, to give the cationic complex $[Ru(bpy)_2(dpm)]^+$, Cl^-.
- With the precursor $[Ru(dmso)_4Cl_2]$, dmso ligands are more labile:[31] The dipyrrin ligand can replace the two chloride X ligands, as two dmso L ligands to give in a first time $[Ru(dpm)_2(dmso)_2]$. The two dmso ligands can then be substituted by a bipyridine ligand, to obtain $[Ru(dpm)_2(bpy)]$.

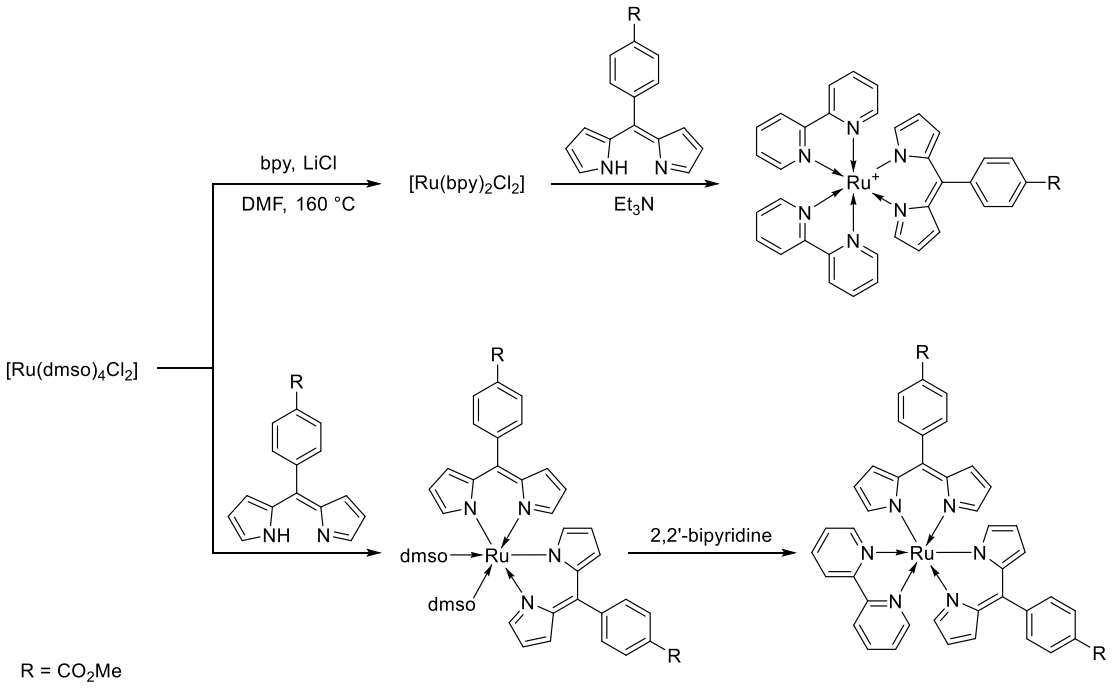

Scheme II-1: Synthesis of different heteroleptic dipyrrin/bipyridine ruthenium complexes

Generally, heteroleptic acac/dipyrrin complexes are also easily accessible, by mixing the metal-acac salt with the dipyrrin ligand.[32] The use of other salts (acetate, halides) leads to the homoleptic complex, replacing all the X type ligands. We can notice that in the case of some transition metals with stable high oxidation degree (iron, cobalt, manganese) associated with dipyrrin ligand tend to be oxidized by air and form the *tris*(dipyrrin) complex, or the *bis*(dipyrrin)(acac) complex (Scheme II-2).

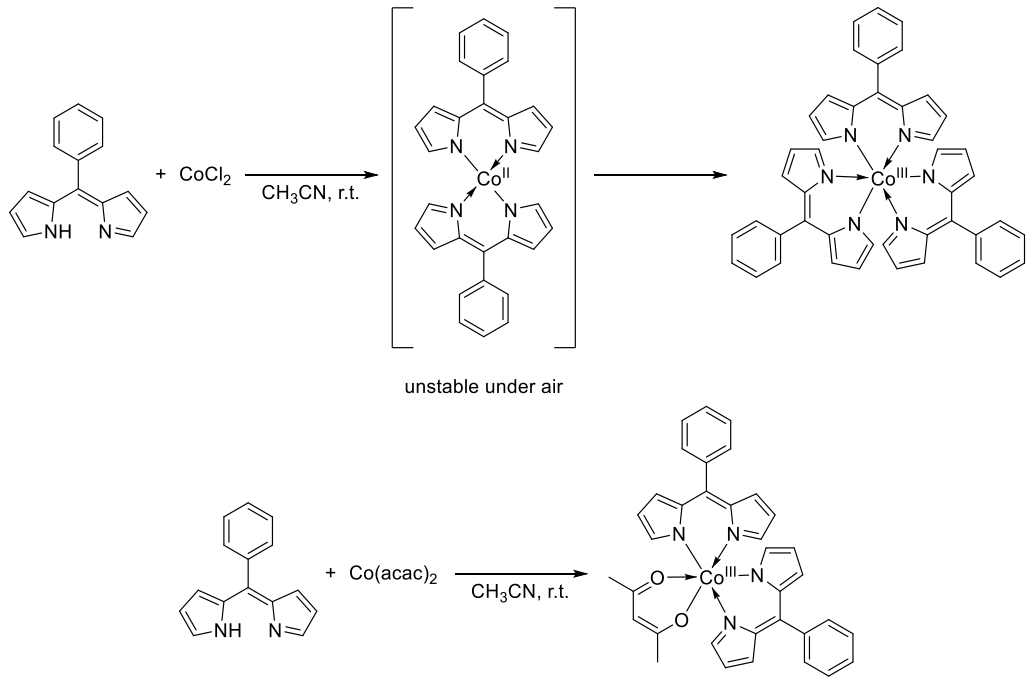

Scheme II-2: Examples of cobalt coordination with unsubstituted dipyrromethene ligands

Another method to obtain heteroleptic dipyrrin/dipyrrin complexes, or simple *mono*(dipyrrin) complexes, is to have bulky group at positions 1 and 9 of the dipyrrin ligand. By using two dipyrromethenes with different substitutions, Sakamoto *et coll.* succeeded to obtain heteroleptic dipyrrin/dipyrrin complexes of copper and nickel.[33]

About the use of dipyrromethene metallocomplexes, several applications have been developed, taking advantages of their properties, beginning by their luminescent properties.

Dipyrromethenes have been well-studied especially for their use for the preparation of BOron DIPYrrin compounds (BODIPY), which are compounds known for their high fluorescence.[34] However, dipyrrin metallocomplexes also present luminescent properties. In 1979, Falk *et coll.* reported a fluorescent zinc-dipyrrin complex, [(1,2,3,7,8,9-hexamethyldipyrrin)zinc(II)], with a weak quantum yield of 7.10^{-3}. By comparison, the nickel dipyrrin complex has no fluorescence, but the BODIPY with the same dipyrrin lead to a quantum yield of 0.82.[35] Thereafter, several studies have been realized by Lindsey *et coll.* to control the fluorescence of $Zn(dpm)_2$ complexes, in order to use them as linking unit between photoactive macrostructure.[36] Sakamoto *et coll.* also developed highly luminescent heteroleptc dipyrrin/dipyrrin zinc[37] and indium complexes.[38] Besides these developments, Cohen and Magde reported two fluorescent *tris*(dipyrrin) complexes, based on gallium and indium.[39]

Cohen's group also studied the possibility to form metal-organic frameworks (MOFs) or coordination polymers with dipyrrin metallocomplexes. They published in 2004 the synthesis of a coordination polymer, using copper(II) acetylacetonate and a dipyrrin ligand.[40] By using a dipyrromethene with a pyridyl part at the *meso* position, they formed the complex [Cu^{II}(4-Pydpm)(acac)], and this complex appears to form coordination polymers, by chelating the copper with the pyridyl part of another complex, bridging the Cu(acac) unit with the 4-pyridyl-dipyrrin ligand (Figure II-8a.). In early 2005, using the same ligand, they report the synthesis of MOFs with *tris*(dipyrrin) metal complexes. They formed the corresponding *tris*(dipyrrin) cobalt(III) complex, and then bound these structures together with silver atoms, which coordinate to the pyridyl parts of dipyrrins (Figure II-8b.).[41] At the end of 2005, they published a new MOF, still combining cobalt(III) and silver(I) species, but with the 5-(4-cyanophenyl)dipyrrin as ligand.[42] By changing the ligand, they also changed the size and the shape of the MOF, compared to the previous one.

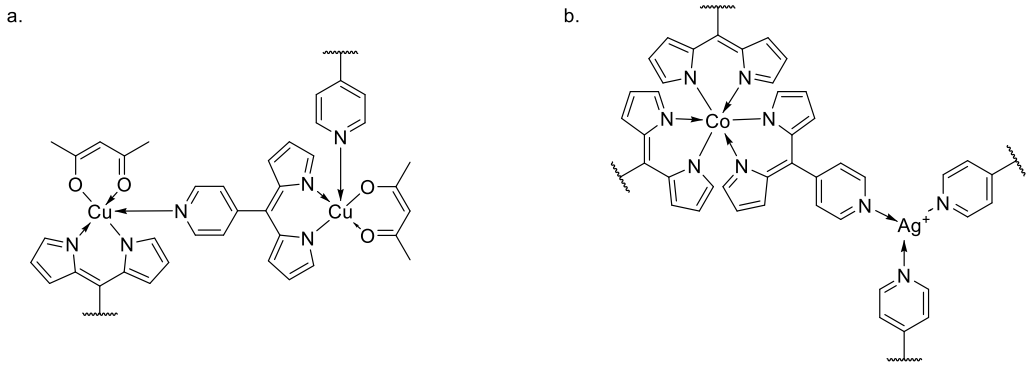

Figure II-8: Applications of Cohen's metallocomplexes to form coordination polymers (a.) and MOFs (b.)

Another application of dipyrrin metallocomplexes is their use in homogenous catalysis. Lastly, Betley *et coll.*, who motivated our choice of ligand, developed an hindered iron *mono*-dipyrrin complex for catalysis. The study of the interaction of this complex with azide compounds led to the development of an iron-catalyzed synthesis of substituted *N*-Boc-pyrrolidine from aliphatic chain substituted by an azide.[22] This example highlights the potential of the use of dipyrrin as ligand homogenous catalysis.

The following part details our works and the molecules and complexes we have synthesized. For more clarity about the numbering, a figure with all the ligands and complexes is available on page 93 (Figure II-23).

II.2. Synthesis and optimization of dipyrromethenes

The most common synthesis for a symmetric dipyrromethene is a two steps process from α-unsubstituted pyrrole and an aldehyde (Scheme II-3).[28] The first step is the condensation of the pyrrole on the aldehyde, catalyzed by a Lewis acid.[43] This condensation involves one equivalent of aldehyde for two equivalents of pyrrole which react together in dichloromethane at room temperature. It proceeds by a first nucleophilic attack of a pyrrole on the aldehyde, forming a secondary alcohol. This intermediate appears to be highly reactive and the hydroxyl group is quickly substituted by another pyrrole to give the dipyrromethane. The presence of a catalytic Lewis acid allows the completion of this reaction in less than one hour.

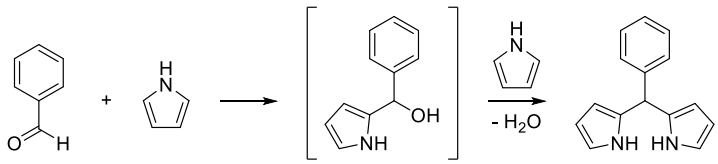

Scheme II-3: Mechanism of the dipyrromethane formation

The second step consists in the oxidation of the dipyrromethane into dipyrromethene. The main oxidants used in the literature are DDQ and *p*-chloranil. As for the condensation, the reaction is performed

in a mixture dichloromethane/benzene or chloroform/toluene at room temperature. The dipyrromethene is thus obtained in very good yield according to the literature. Moreover, as these reactions can proceed in the same type of solvent without side-products, the condensation and the oxidation can be realized applying a one-pot two-steps procedure.

Another method to obtain symmetric dipyrromethene directly in a one-step procedure consists in using an acyl chloride, more electrophilic than of an aldehyde (Scheme II-4).[29]

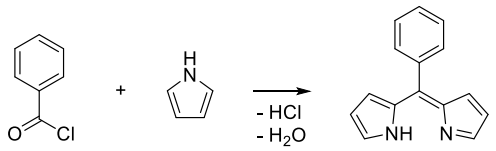

Scheme II-4: Synthesis of dipyrromethene from an acyl chloride

This kind of condensation can also be done between a 2-formylpyrrole and a pyrrole, in acid-catalyzed conditions. In that case, the product obtained is the 5-unsubstituted dipyrrin (Scheme II-5). This method especially allows obtaining asymmetric and *meso*-unsubstituted dipyrromethenes.[29]

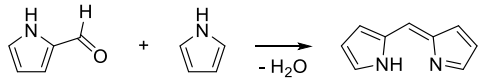

Scheme II-5: Synthesis of dipyrromethene by condensation between 2-formylpyrrole and pyrrole

II.2.1. State of the art about 5-(4-pyridyl)dipyrromethenes

After studying the literature, we chose the 5-(4-pyridyl)dipyrromethene as ligand for our project. The work of Cohen's group with this ligand demonstrates its potential use as ligand for bimetallic complex, and the work of Betley demonstrates the possibility to obtain a *mono*(dipyrrin) cobalt(II) complex and to use it as catalyst.

The synthesis of 5-(4-pyridyl)dipyrromethene, as described in the literature, is different than the synthesis of other dipyrromethenes: the condensation cannot be done with a 2:1 ratio between the pyrrole and the pyridine carboxaldehyde in dichloromethane. In the same way, the oxidation is also described as giving a lower yield. For the preparation of the 5-(4-pyridyl)dipyrromethane, the first method, described by Ashley *et coll.* in 1974, involved pyrrole and 4-pyridine-carbaldehyde in methanol, with gaseous HCl, leading to a yield of 60%.[44] Thereafter, in 2000, Lindsey proposed a new method allowing the condensation under neat conditions at 90 °C for several hours, with a large excess of the pyrrole (12 to 15 equivalents).[45] The corresponding dipyrromethane is obtained with 58% yield, without acidic conditions. However, the oxidation by DDQ or *p*-chloranil is not efficient, and only lead to low yield (Scheme II-6).[46]

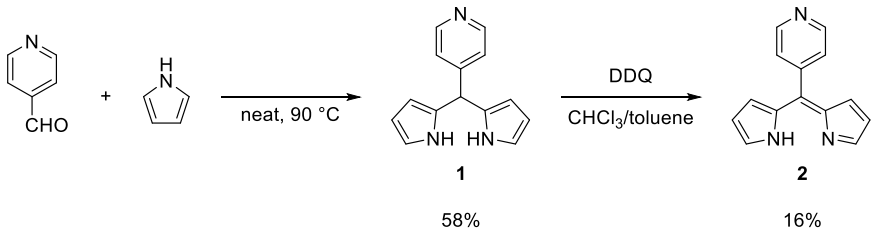

Scheme II-6: Synthesis of 5-(4-pyridyl)dipyrromethene 1, as reported in the literature

The pyridyl part and the dipyrrin part of our ligand can be independently modified before being coupled. The modification or the addition of functional groups on the pyridyl part could interfere with the coordination or the properties of an electron-transferring species. We decided thus to keep the 4-pyridinecarboxaldehyde without modifications for the beginning of the project. However, we chose several substitutions for the dipyrrin part to study the influence of the steric effect around the catalytically active metal (Figure II-9). To introduce these substitutions on our ligand, it is necessary to prepare the corresponding functionalized pyrroles.

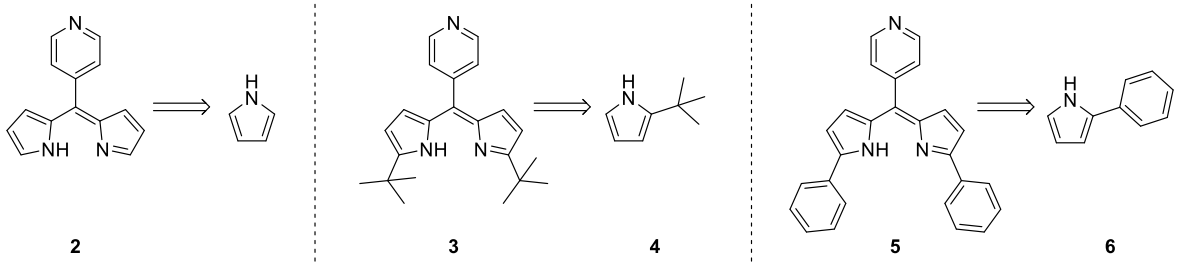

Figure II-9: The selected ligands for this study and their corresponding pyrroles

II.2.2. The synthesis of pyrroles

We decided to begin our study with three ligands: the 5-(4-pyridyl)dipyrromethene **2**, without substitutions, the 1,9-*tert*-butyl-5-(4-pyridyl)dipyrromethene **3** and the 1,9-diphenyl-5-(4-pyridyl)dipyrromethene **5**. The interest of these substitutions is the difference of steric hindrance they bring. To prepare these ligands, we managed to prepare the 2-*tert*-butylpyrrole **4** and the 2-phenylpyrrole **6**.

Following the procedure of Harman *et al.*,[47] we synthesized **4** in two steps with very good yield from the ethyl pyrrole-2-carboxylate. The first step is the formation of the intermediate ethyl 5-*tert*-butyl-pyrrole-2-carboxylate **7**, obtained by Friedel-Craft alkylation. If pyrroles are good substrates for this type of reactions, they also present an important problem of regioselectivity between position 2 (or α) and position 3 (or β). To control the regioselectivity of aromatic electrophilic substitution on a pyrrole, it is necessary to have bulky or an electrophilic aromatic directing group, hence the use of ethyl pyrrole-2-caroxylate. Once **7** obtained, it undergoes a decarboxylation reaction to give the 2-*tert*-butylpyrrole **4** with 60% yield over two steps without chromatography (Scheme II-7).

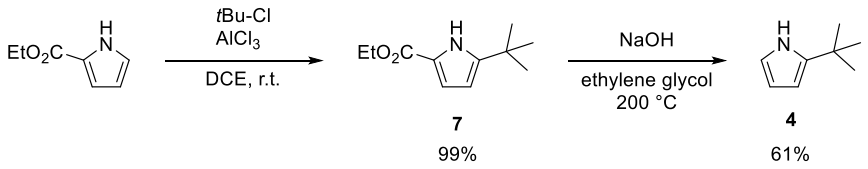

Scheme II-7: Synthesis of 2-*tert*-butylpyrrole 4

The synthesis of the 2-phenylpyrrole **6** needed more research, as the main methods described for this compound and its derivatives involved Negishi coupling reaction[48] or Trofimov reaction.[49] However, using a metal-catalyzed reaction during a ligand synthesis is a potential risk to contaminate the ligand, and thus the final complex, by another catalytically active metal. We attempted nevertheless a derivatives of the Trofimov reaction, replacing the gaseous acetylene by 1,2-dichloroethane.[50] However, the reaction did not lead to a satisfying yield. To circumvent the drawbacks of the use of metal-catalyzed coupling reaction, Zhang and Yu developed a method allowing the selective α-arylation of pyrrole with diaryliodonium (Scheme II-8).[51] This reaction uses pyrrole as solvent, and gives **6** with a yield of 67%, calculated from the diphenyliodonium **8**. The excess of pyrrole can be recovered by evaporation and the residue of the reaction extracted and purified by chromatography.

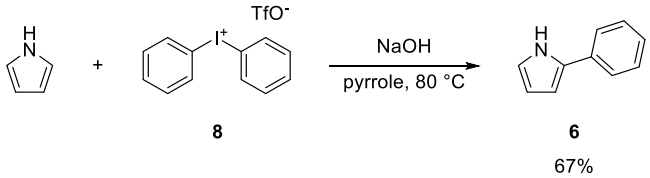

Scheme II-8: Synthesis of 2-Phenylpyrrole 6

II.2.3. Study of the condensation step: synthesis of dipyrromethane

Once we established how to prepare the pyrroles we needed, we firstly began a study of the condensation reaction, to determine if the use of an excess of pyrrole is a necessity. Indeed, the classic method of condensation is not a problem to obtain the unsubstituted 5-(4-pyridyl)dipyrromethene, because of the commercial availability of the pyrrole, but it is one for 2-*tert*-butylpyrrole and 2-phenylpyrrole. As these pyrroles have to be synthesized, it is difficult to have them in a consistent amount to be used in a large excess.

If we examine the reaction conditions, the condensation proceeds by heating a mixture of the 4-pyridinecarboxaldehyde in a large excess of pyrrole, at 90 °C overnight. The excess of pyrrole is then evaporated and the raw product purified by chromatography on alumina. Except for the fact that the conditions are harsher than for other dipyrromethenes, the setup is not difficult, and the yield is correct for this step, described in the literature up to 58%.[45]

We continued to study the evolution of the reaction, and applied some variation of parameters. We first decreased the quantity of pyrrole to two equivalents. By heating the mixture at 90 °C, a white solid quickly appears, stopping the stirring. Analyzes of this solid reveal that this was not the dipyrromethane **1**, but the (4-pyridyl)-(1*H*-pyrrol-2-yl) ketone **9** that is mainly formed in these conditions (Scheme II-9). We assume that when the pyrrole is not in excess, the second addition is too slow, and the intermediate alcohol oxidizes faster. Surprisingly, the same result is obtained when the reaction is carried out under nitrogen atmosphere. We thus increased the amount of pyrrole to five equivalents, and observed the formation of the dipyrromethane **1**, as well as the formation of the ketone side-product **9**.

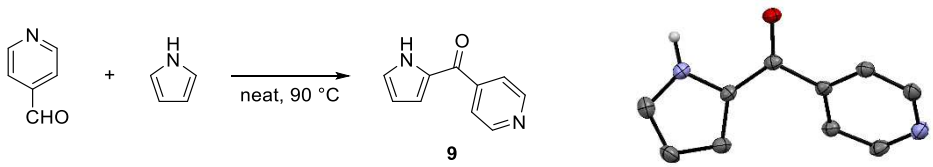

Scheme II-9: Formation of the (4-pyridyl)(1H-pyrrol-2-yl)ketone 9 (left) and ORTEP structure

We then followed the reaction with 6, 12 and 24 equivalents of pyrrole over 24 hours. If the reaction cannot reach a better yield than 48% with 6 equivalents, the reaction with 12 equivalents of pyrrole gives an NMR yield of 61%. The reaction carried out with 24 equivalents did not give a significant better yield. (Table II-1) therefore, for practical reasons, we kept an amount of pyrrole of 12 equivalents.

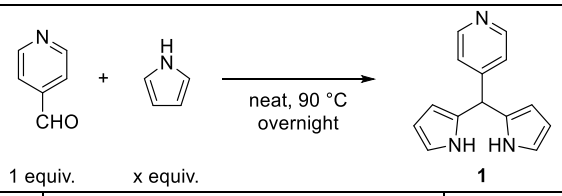

Entry	Equivalents of pyrrole	^{1}H NMR Yield (%)
1	6	48
2	12	61
3	24	65

Table II-1: Yield of dipyrromethene isolated , depending of the excess of pyrrole engaged in the reaction

We also defined a correct eluent for the chromatography. As pyrrole is an apolar compounds, whereas the dipyrromethene is a more polar compounds, the column is first eluted with petroleum ether, to drag selectively the pyrrole along, and then with ethyl acetate, to get the dipyrromethene remaining on the alumina.

We attempted the condensation with the 2-*tert*-butylpyrrole **4** (Scheme II-10). It is a solid with a melting point around 40 °C,[52,53] which is inferior to the reaction temperature. We thus performed the

reaction with 14 equivalents of **4** and 1 equivalent of 4-pyridinecarboxaldehyde and obtained the corresponding dipyrromethane **10** with 58% yield.

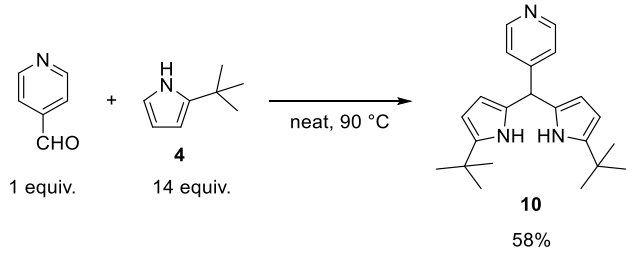

Scheme II-10: Synthesis of the 1,9-di-*tert*-butyl 5-(4-pyridyl) dipyrromethane 8

However, the melting point of the 2-phenylpyrrole is 135 °C. As we estimated that it was an excessive temperature, we decided to look for another method.

II.2.4. The case of the 2-phenylpyrrole condensation

As **6** is a solid compound with a high melting point, we managed to try a condensation with a minimum amount of solvent. As the reaction medium has to be heated for the condensation to occur, this solvent needs a high boiling point. The reaction also has to be very concentrated, to keep a high probability of meeting between the aldehyde and the pyrrole, and **6** must be very soluble in it. 2-phenylpyrrole is a non-polar compound, we thus chose toluene as non-polar, aprotic solvent, with a boiling point of 110 °C.

As the phenyl group is a weakly mesomeric electron-donating group,[54] we considered it has an activating influence on the pyrrolic cycle, and favors the nucleophilic attack on the aldehyde. We thus decided to decrease the amount of 2-phenylpyrrole to five equivalents. We began by solubilizing **6** (2 g, 5.0 equivalent) in 2 mL of toluene heated at 110 °C, and then adding the pyridine-4-carboxaldehyde (0.26 mL, 1.0 equivalent). The reaction ran overnight at 110 °C, and was then directly chromatographed on alumina. By this method, we succeeded to form the 1,9-diphenyl-5-(4-pyridyl) dipyrromethane **11** with a yield of 90%. However, when we attempted the reaction in a more diluted mixture, the condensation was unsuccessful. We thus fixed the quantity of solvent at five equivalents of toluene, for five equivalents of **6** and one equivalent of pyridine-4-carbaldehyde (Scheme II-11).

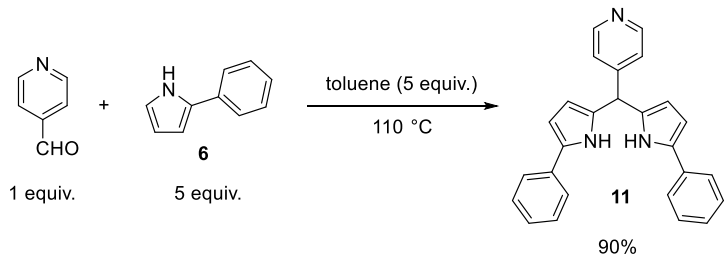

Scheme II-11: Optimized synthesis of 9

II.2.5. Optimization of the oxidation step

After optimizing the reaction conditions and the purification process of the condensation step, we worked on the optimization of the oxidation step. By following the oxidation of **1** into **2** by ^{1}H NMR, we noticed that the reaction quickly stops its progression to give a low yield with 1 equivalent of DDQ. However, by increasing the amount of DDQ, the yield does not significantly increase.

We hypothesized that DDQ proceeds to an over-oxidation of the unsubstituted 5-pyridyldipyrromethane: Csp^2–Csp^2 bond formation between two pyrrole units is a known reaction, used for the formation of the corrole cycle. The synthesis of corroles passes upon the condensation of three pyrrole units with two aldehydes.[55] The resulting intermediate is transformed into corrole under the action of the DDQ, which aromatizes the dipyrromethane units and close the cycle by creating a Csp^2–Csp^2 bond between the two "ending" pyrroles (Figure II-10).

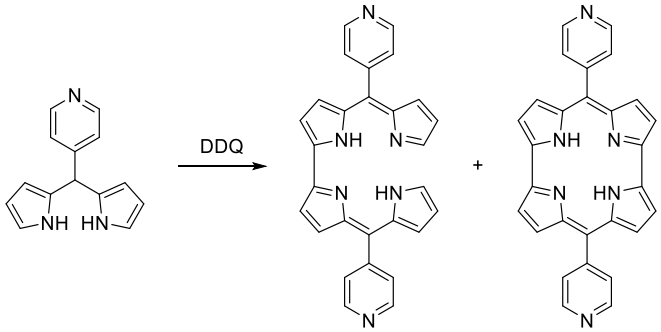

Figure II-10: Hypothetical poly-pyrrolic by- products formed during the oxidation step of 1 with DDQ

Considering this reactivity of DDQ with dipyrromethene derivatives, we can envisage the possibility that, in the case of 5-pyridyldipyrromethane **1**, the aromatization of the dipyrromethane is concomitant to the formation of polydipyrrin system. *This hypothesis has not been verified, however, the oxidation realized on 2,8-disubstituted-5-pyridyldipyrromethane with DDQ tends to give better yields than on the unsubstituted dipyrromethane. Moreover, the presence at the end of the oxidation step of a deep purple insoluble product makes us think about a poly-pyrrolic compound.*

Lastly, Gonçalves *et coll.* reported that selenium dioxide is able to replace DDQ for the oxidation of porphyrinogens into porphyrins.[56] We tried this method to oxidize our dipyrromethane, but no oxidation occurred. However, this publication highlights that DDQ or *p*-chloranil are not the only oxidants that can be used for this aromatization step. As DDQ seemed not to be a suitable oxidant for our aromatization, we thus decided to look for another oxidant that could lead to a better yield. Following the success of selenium oxide for porphyrins, we firstly focused our research on inorganic oxidants with a similar mechanism than quinone derivatives, meaning mild oxidants able of hydrogen abstraction. Inspiring from mild oxidants able to oxidize alcohols into aldehydes, we tried manganese dioxide MnO_2, which is also known for

dehydrogenation and aromatization reactions,[57] and has also been studied by Pineiro *et coll.* as selective oxidant for tetrapyrrolic macrocycles, with poor yield to obtain porphyrin to good yield to obtain bacteriochlorins and chlorins.[58]

If SeO_2 led to no reaction in our case, MnO_2 tended to realize a complete oxidation of the dipyrromethane into dipyrromethene after 24 hours at room temperature. We thus worked to optimize this reaction (Figure II-11).

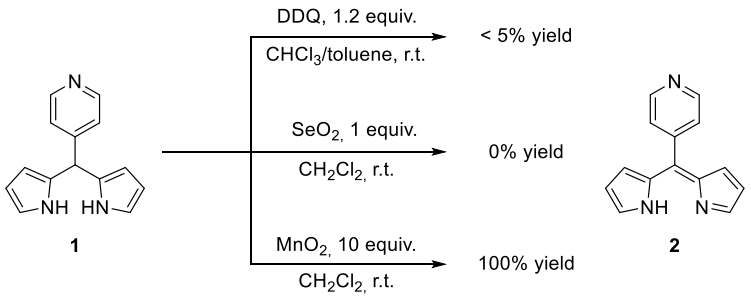

Figure II-11: Test of different oxidant for the formation of dipyrromethene 2

The first tried the conditions used for the oxidation of allylic primary alcohol into aldehyde, with 10 equivalents of MnO_2 in dichloromethane, at room temperature, after 24 hours. The reaction medium was thereafter filtered and evaporated to get the raw product. The ^{1}H NMR spectrum of the raw product presents only peaks corresponding to **2**. We then decreased the amount of oxidant to 5 equivalents, and monitored the reaction progression by ^{1}H NMR to determine the conversion of dipyrromethane in dipyrromethene. The decrease of the amount of MnO_2 to 5 equivalents leads to a conversion of 67% after 24 hours. We then heated the reaction mixture to 40 °C and obtained a conversion of 96% after 24 hours. Finally, we tried to continue to decrease the amount of oxidant to 3 equivalents, but we obtained a conversion of 66%. We thus decided to keep the following conditions: MnO_2 (5 equivalents), in dichloromethane, at 40 °C for 24 hours (Scheme II-12).

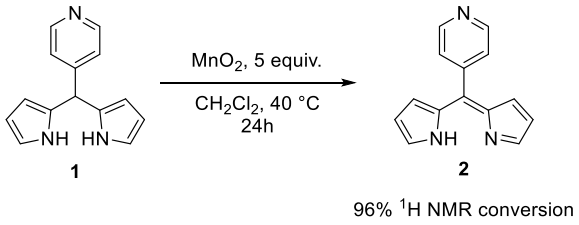

Scheme II-12: Optimized conditions for the oxidation of dipyrromethane 1 in dipyrromethene 2

Concerning the isolation of the final product, the raw product obtained after filtration and evaporation of the reaction medium appears to be pure when analyzed by ^{1}H NMR. However, it is possible to purify it by silica chromatography column, by elution with petroleum ether and ethyl acetate.

With the different syntheses we have developed, we managed to get crystal structures of **2** (Figure II-12), **3** (Figure II-13) and **5** (Figure II-14), allowing us to compare them and determined if the substitution on position 1 and 9 bring an important difference on the bond lengths and the dihedral angles.

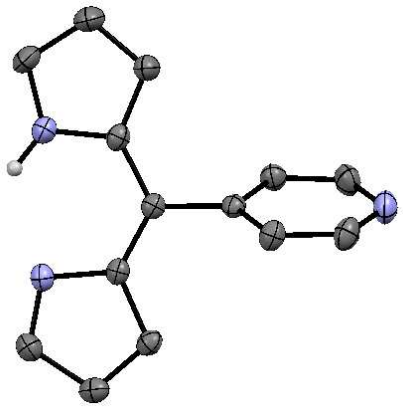

Figure II-12:ORTEP of the X-Ray structure of 2 Thermal ellipsoids are represented at 50% level. Hydrogens and other same molecules in the cell were removed for clarity.

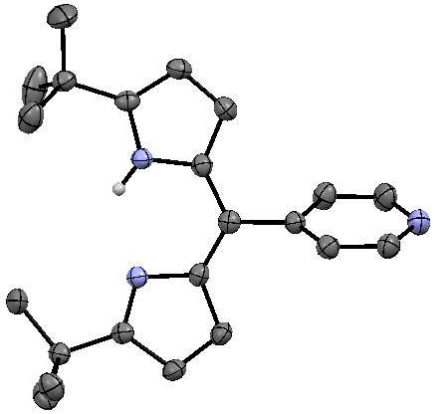

Figure II-13: ORTEP of the X-Ray structure of 3 Thermal ellipsoids are represented at 50% level. Hydrogens and disorder on the pyridyl part were removed for clarity.

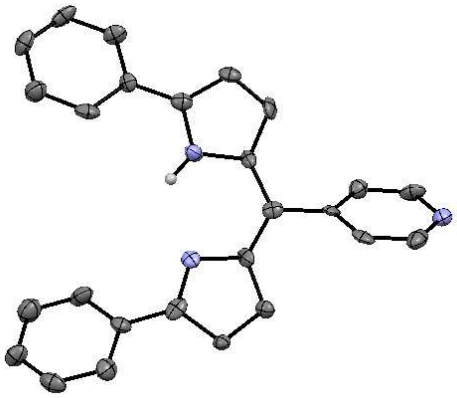

Figure II-14: ORTEP of the X-Ray structure of 5 Thermal ellipsoids are represented at 50% level. Hydrogens and other same molecules in the cell were removed for clarity.

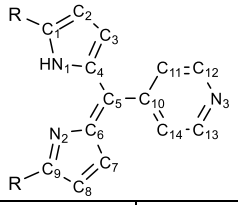

Ligand	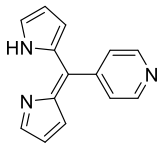 **2**	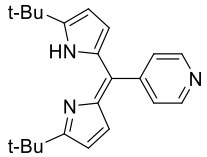 **3**	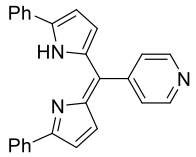 **5**
Dihedral angle py/dpm	62.11°	62.50°	48.95°
Distance N_1-C_1 (Å)	1.351	1.352	1.332
C_1-C_2	1.381	1.391	1.382
C_2-C_3	1.400	1.394	1.356
C_3-C_4	1.393	1.400	1.438
C_4-N_1	1.379	1.381	1.394
C_4-C_5	1.432	1.425	1.403
C_5-C_6	1.378	1.382	1.381
C_6-N_2	1.408	1.407	1.401
C_6-C_7	1.444	1.442	1.437
C_7-C_8	1.348	1.353	1.379
C_8-C_9	1.447	1.451	1.418
C_9-N_2	1.315	1.314	1.326
C_5-C_{10}	1.493	1.490	1.493
C_{10}-C_{11}	1.391	1.387	1.381
C_{11}-C_{12}	1.377	1.376	1.383
C_{12}-N_3	1.340	1.320	1.359
N_3-C_{13}	1.333	1.378	1.343
C_{13}-C_{14}	1.388	1.382	1.373
C_{14}-C_{10}	1.394	1.380	1.395

Table II-2: Measured values from the X-ray structures of the bond length of the pyridyl and the dipyrrin part in ligand 2, 3 and 5

By comparing dipyrromethenes **2**, **3** and **5** with each other, we can see an influence of the dipyrrin substitution on the global structure (Table II-2). The first point to notice is the non-equivalence between the bond lengths at the solid state. For example, for each dipyrrin, C_1-C_2 (Table II-2, 1.381 Å) has a complete different length than C_8-C_9 (Table II-2, 1.447 Å), while they should be equivalent due to the global conjugation of the dipyrrin part. Moreover, the bond lengths of the dipyrrin part of **2** and **3** appear to be similar, whereas **5** has dipyrrin bond lengths significantly different. Another observation can be done on the

dihedral angle: this angle is the same in the cases of **2** and **3**. However, for the diphenyl compounds, this angle is lower. By examination of the X-ray structure, it can be caused by the steric hindrance of the phenyl, which induces a slightly twist between the pyrrole units of the dipyrrin part.

II.3. Preliminary tests of cobalt complexation

With the optimized synthesis of different 5-(4-pyridyl)dipyrromethenes in hand, we then got interested in the coordination of cobalt salts to these ligands. The main characteristic we have to keep in mind is the presence of two coordination sites: the dipyrrin part and the pyridyl part. These two sites imply to determine an order for the coordination of the two metals we want to coordinate on. This order will depend on the metal precursor used and the reaction conditions for the coordination of each metal precursor. As our goal is to coordinate the cobalt in the dipyrrin part, we first studied the coordination of different cobalt salts on the synthesized ligands.

II.3.1. Coordination with 5-(4-pyridyl) dipyrromethene

The first combination we tried was the coordination of cobalt chloride with **2**. Cobalt chloride was solubilized under stirring in methanol with **2** at room temperature, and a red solid precipitated (Scheme II-13). After filtration of this precipitate and several washes with diethyl ether, the solid was characterized by ^{1}H NMR and mass spectrometry, since no crystals have been obtained. The ^{1}H NMR presents diamagnetic signals and mass spectrometry indicates the mass of complex **12**. The mass spectrum presents also the fragmentations of **12**, with a mass of *m/z* = 499, corresponding to the mass of **12** minus one ligand, and a mass of *m/z* = 279, corresponding to the mass of **12** minus two ligands. We concluded to the formation of the *tris*(5-(4-pyridyl)dipyrromethene)cobalt(III), which is coherent with the literature.[59]

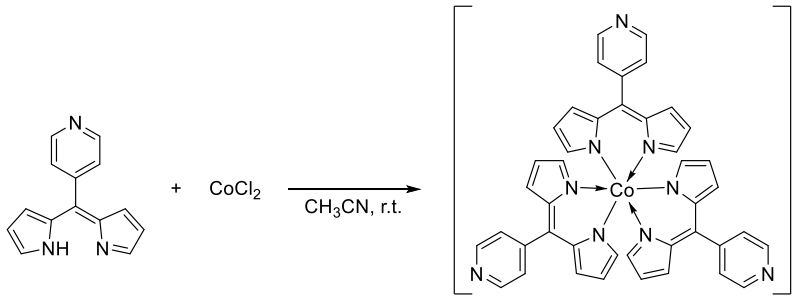

Scheme II-13: Synthesis of 12

As all the coordination sites of this metal center are occupied, it should not present interesting properties for coupling reactions. Moreover, the presence of three dipyrromethenes implies, for our

bimetallic purpose, the presence of three reducing agents on the complex, which could favor an over-reduction of the cobalt center and the ligand decoordination. Besides, *tris*(dipyrrin) cobalt(III) structure has already been used as ligand supporting a rhodium catalyst, highlighting its high stability and its non-reactivity (Scheme II-14).[60]

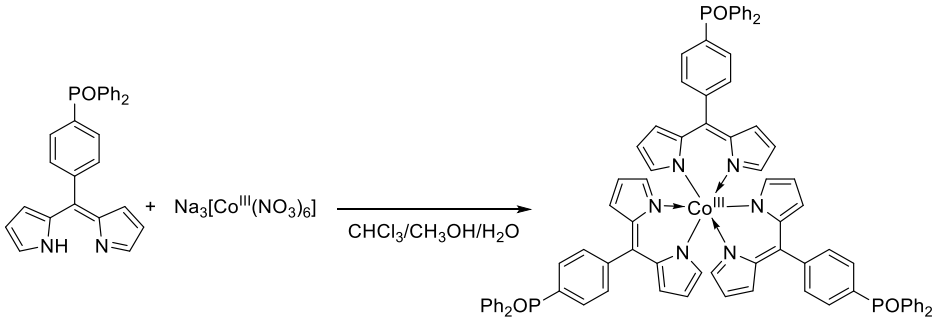

Scheme II-14: Synthesis of a *tris*(dipyrrin) cobalt(II) complex as supporting ligand[60]

For a use in catalysis, the final complex has to keep a dispensable X or LX ligand, that will be decoordinated during the activation/reduction of the complex. As the dipyrromethene is the ligand of interest, the dispensable ligand has to come from the cobalt precursor. The first experience and the literature showed cobalt halides, as cobalt acetate, do not match with this criterion when associated with **2**.

According to the literature, when associated to unsubstituted dipyrromethenes, $Co(acac)_2$ is described as leading to bis(dipyrromethene)cobalt(III)acetylacetonate complexes, the ligand acetylacetonate being the dispensable ligand.[32] However, the presence of two dipyrromethene ligands remains a problem for the control of cobalt center reduction.

Finally, we decided to use a cobalt precursor with a leaving X ligand for the dipyrromethene chelation, and a hindered ligand, to avoid a multiple coordination of dipyrromethene. We thus attempted to use $[Cp^*CoCl]_2$, in spite of the strong basicity of the Cp* ligand compared to the chloride ligand. As this precursor is moisture- and air-sensitive, the reaction was carried out in a glovebox. The precursor and the ligand are solubilized in acetonitrile, and stirred at room temperature (Scheme II-15). After storage in the fridge, we obtained red crystals, allowing us to get a crystalline structure of the resulting complex (Figure II-15). As expected, the precursor kept the Cp* ligand and release the chloride to coordinate one ligand **2** to the cobalt center by the dipyrrin part. We thus succeeded to obtain the complex **13** with a global yield of 58% after successive crystallization from the reaction medium.

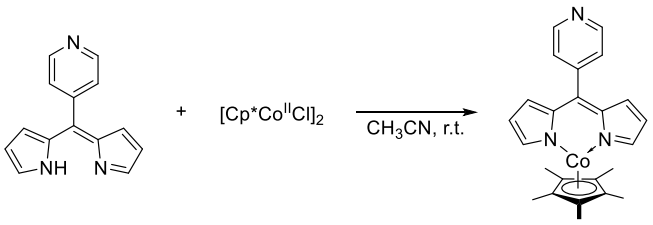

2 **13**

Scheme II-15: Synthesis of complex 13

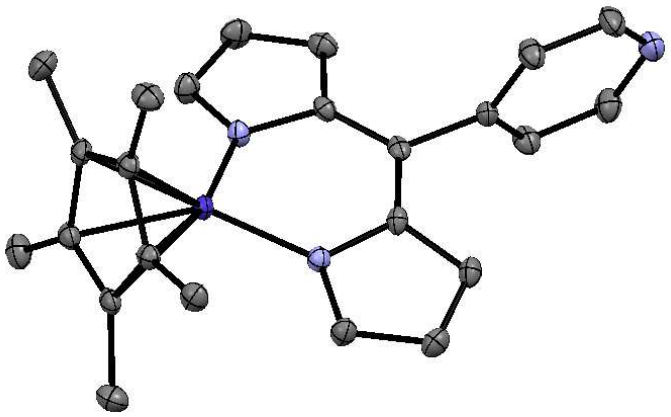

Figure II-15: ORTEP of the X-Ray structure of 13. Thermal ellipsoids are represented at 50% level and hydrogens were removed for clarity.

By comparing the measurements of complex **13** to the measurements of the free ligand **2**, we can see that the cobalt has an influence on the structure of the ligand (Table II-3). First of all, the dihedral angle between the dipyrrin part and the pyridyl part has increased from 60° to 84°. There is no change in the length of the bond between the two part. However, by measuring the length of each bond of the dipyrrin moiety, we can see that the two pyrrole units became equivalent when coordinated to the cobalt, reinforcing the idea that the cobalt participate to the conjugation of the whole dipyrrin part. It is noteworthy that the cobalt is not in the same plane as the dipyrrin. It forms a plane with the two nitrogens, with an angle of 19.08°. The distance between the cobalt and the Cp* ligand is 1.711 Å. As comparison point, we can take the distance Co–Cp* in the complex [Co(Cp*)$_2$], which is 1.714 Å.[61] As these distances are equivalent, it seems there is no influence of the presence of the dipyrrin on the coordination of the Cp* ligand.

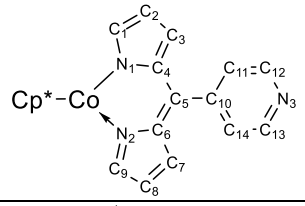		
	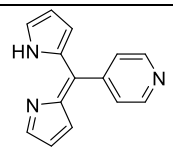 **2**	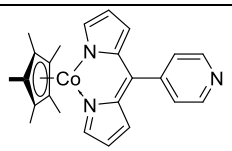 **13**
Dihedral angle py/dpm	62.11°	84.1°
Distance N_1-C_1 (Å)	1.351	1.343
C_1-C_2	1.381	1.405
C_2-C_3	1.400	1.375
C_3-C_4	1.393	1.428
C_4-N_1	1.379	1.407
C_4-C_5	1.432	1.394
C_5-C_6	1.378	1.397
C_6-N_2	1.408	1.396
C_6-C_7	1.444	1.425
C_7-C_8	1.348	1.376
C_8-C_9	1.447	1.402
C_9-N_2	1.315	1.347
C_5-C_{10}	1.493	1.497
Co-Cp*	/	1.711
Co-N_1	/	1.919
Co-N_2	/	1.924

Table II-3: Comparison of dihedral angle and bond length between the ligand 2 and the complex 13

These complexation tests with ligand **2** showed that this ligand was not good to lead to cobalt complexes matching to our catalysis purposes. However, combine with $[Cp^*CoCl]_2$ as cobalt precursor, it allows the formation of a cobalt complex without any available heteroatom except the nitrogen of the pyridyl part. This complex is thus the ideal one in the case of a bimetallic cobalt-lanthanide complex. Otherwise, for a potential catalytic complex in coupling reaction, we need to envisage another ligand.

II.3.2. Coordination with 1,9-*tert*-butyl-5-(4-pyridyl) dipyrromethene

Since the unsubstituted pyridyl dipyrromethene **2** was not suitable to our catalytic purpose, we continued the coordination tests with the 1,9-*tert*-butyl-5-(4-pyridyl) dipyrromethene **3** as ligand. The

presence of the two *tert*-butyl (*t*-Bu) groups on the dipyrrin part should bring enough hindrance to prevent the coordination of the cobalt to a second ligand. Besides, as seen on the crystal structure, the *t*-Bu forms a cavity around the dipyrrin part, potentially forcing the cobalt to get a specific conformation, and thus restraining its reactivity.

We thus attempted the simplest complexation (as for **2**) by mixing the ligand and $CoCl_2$ in acetonitrile, at room temperature (Scheme II-16). A green precipitate forms quickly, with beginning of crystals. The reaction medium was then stored into the fridge to help crystals growing and the latter have been analyzed by X-Ray diffraction (Figure II-16).

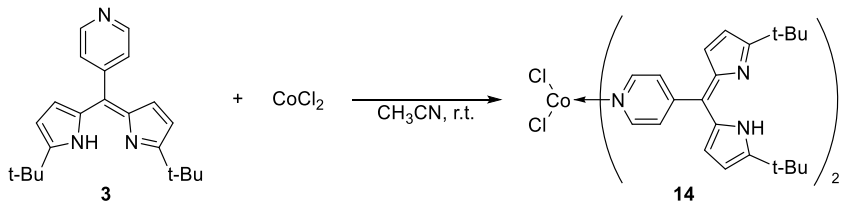

Scheme II-16: Synthesis of complex 14

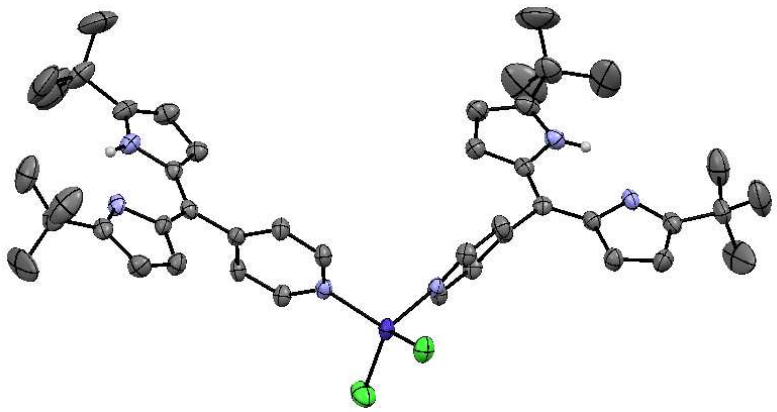

Figure II-16: ORTEP of the X-Ray structure of 14. Thermal ellipsoids are represented at 50% level. hydrogens were removed for clarity.

Surprisingly, the obtained XR structure attests of the coordination of the cobalt to the pyridyl parts of two ligands, in a tetrahedral geometry.

The green precipitate has been recovered and solubilized in acetonitrile, and the solution was slowly evaporated, leading to the formation of red crystals (Scheme II-17). The XRD analysis revealed that these crystals correspond to the complex with a cobalt chloride coordinated to four ligands by the pyridyl part, in an octahedral geometry (Figure II-17).

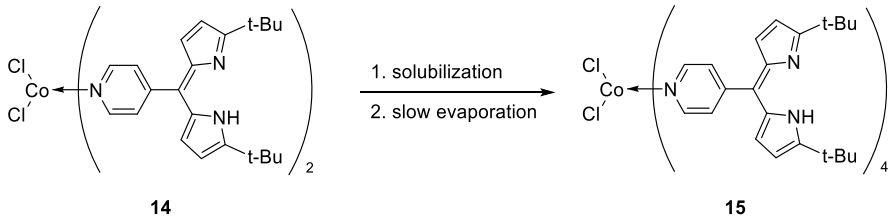

Scheme II-17: Obtention of 15 from 14 by solubilization and evaporation

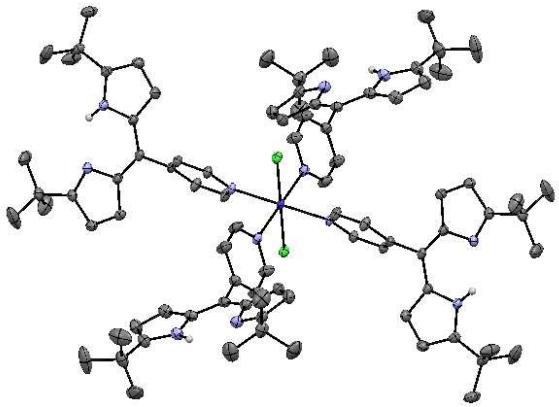

Figure II-17: ORTEP of the X-Ray structure of 15 Thermal ellipsoids are represented at 50% level and hydrogens and acetonitrile solvent were removed for clarity.

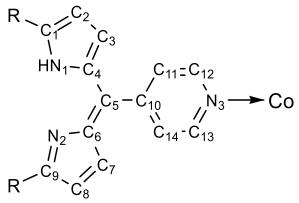

	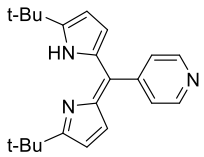 **3**	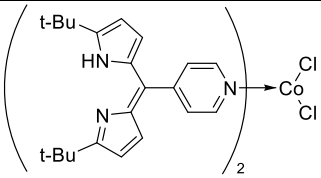 **14**	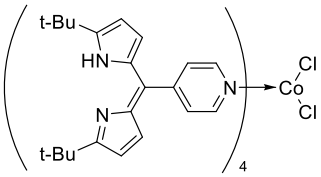 **15**
Dihedral angle py/dpm	62.50°	74.85°	81.40° 58.83°
C_{10}-C_{11}	1.387	1.377	1.386 1.393
C_{11}-C_{12}	1.376	1.329	1.387 1.386
C_{12}-N_3	1.320	1.325	1.335 1.341
N_3-C_{13}	1.378	1.329	1.337 1.345
C_{13}-C_{14}	1.382	1.387	1.388 1.387
C_{14}-C_{10}	1.380	1.392	1.382 1.391
Co-N_3	/	2.034	2.206 2.223

Table II-4: Comparison of dihedral angle and bond lengths between ligand 3, complex 14 and the complex 15

If we compare the bond lengths between the ligand and the two complexes obtained, we can observe the influence of the presence of the cobalt coordinated on the pyridyl part (Table II-4). The first influence, and most important, is on the pyridyl moiety. For **14**, we can notice that the bonds of the pyridyl moiety have not the same length than for the free-ligand **3**. However, if the C_1-C_2 bond is longer, there is no change concerning the bonds of the dipyrrin part. In the case of **15**, surprisingly, each of the ligand does not have the same interaction with the cobalt: two ligands are closer than the two others. This leads to different deformations of the pyridyl moiety. However, no deformation of the dipyrrin part is notable.

II.3.3. Coordination with 1,9-diphenyl-5-(4-pyridyl) dipyrromethene

With the cobalt complexes obtained using ligand **3**, we assume that this ligand has a too hindered dipyrrin part, creating a competition of coordination between the pyridyl part and the dipyrrin part. To circumvent this problem, we set apart **3** to continue the coordination tests with the 1,9-diphenyl-5-(4-pyridyl) dipyrromethene **5**. With two phenyl groups instead of *tert*-butyl, the hindrance around the dipyrrin coordination site should decrease compared to **3**, and reverse the coordination competition in favor of the dipyrrin part. However, the possibility to have a coordination of the cobalt to two dipyrrin parts will increase. Indeed, by extended the literature of dipyrromethene complexes to other transition metals, complexes of copper(II) with two 1,9-diphenyl dipyrromethenes as ligand coordinated to the metal can be found.[62]

So, we began with the $Co(acac)_2$ precursor. Previous experiments and literature with this kind of derivatives of transition metals report the fact that a ligand acetylacetonate always remains in the final complex. Considering the steric hindrance of the diphenyl ligand and the property, we expected to finally obtain the complex (1,9-diphenyl-5-(4-pyridyl)dipyrromethene)cobalt(II)(acac) (Figure II-18).

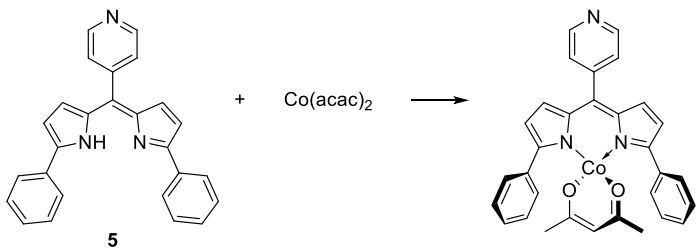

Figure II-18: Expected complex, by reacting 5 with $Co(acac)_2$

However, while trying the complexation, we surprisingly obtained the unexpected *bis*(1,9-diphenyl-5-(4-pyridyl)dipyrromethene)cobalt(II)$(acac)_2$ **16**, for which the cobalt is coordinated to the pyridyl part of the ligand (Scheme II-18). The structure has been verified by XRD, indicating an octahedral cobalt(II) specie, in a *trans* configuration, with the two pyridyldipyrromethene ligands on axial coordination sites (Figure II-19).

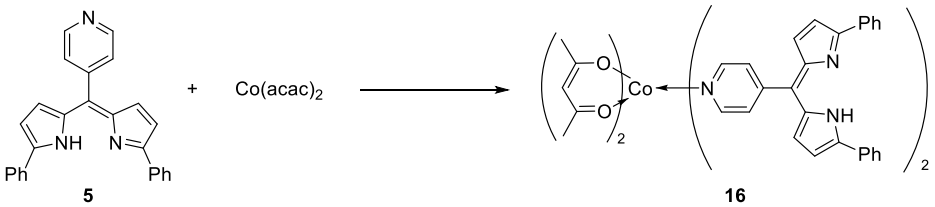

Scheme II-18: Synthesis of complex 16

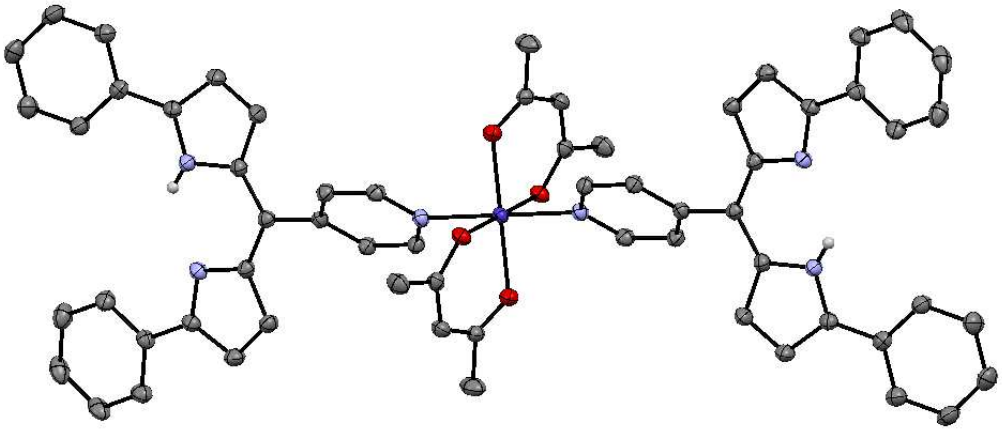

Figure II-19 ORTEP of the X-Ray structure of 16. Thermal ellipsoids are represented at 50% level. THF solvent and hydrogens were removed for clarity.

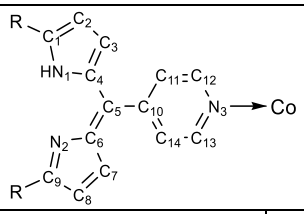

	5	16
	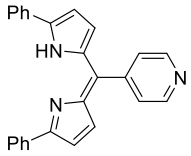	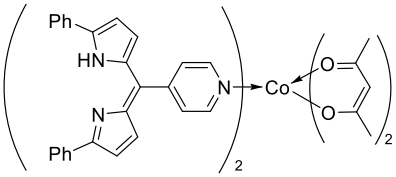
Dihedral angle py/dpm	48.95°	45.12°
Distance C_5-C_{10} (Å)	1.493	1.488
C_{10}-C_{11}	1.381	1.396
C_{11}-C_{12}	1.383	1.385
C_{12}-N_3	1.359	1.338
N_3-C_{13}	1.343	1.339
C_{13}-C_{14}	1.373	1.389
C_{14}-C_{10}	1.395	1.399
Co-N_3	/	2.176

Table II-5: Comparison of dihedral angle and bond length between ligand 5 and the complex 16

For **16**, the dihedral angle between the pyridyl moiety and the dipyrrin is similar to the angle of the free ligand **5** (Table II-5). As for the other complexes, the coordination of the cobalt on the pyridine leads to a homogenization of the bond lengths. However, we can notice the rotation of the phenyl groups in the same plane as the dipyrrin for **16**. But it would be difficult to determine if it is due to the influence of the cobalt on the dipyrrin part, or if it is the natural rotation of these groups that allows them to position themselves.

With these results in hand, we decided to use another cobalt precursor: the complex bis(pyridine) cobalt(II) chloride **17** (Scheme II-19 a.). We expected two actions from pyridine ligands: the prevention of the chelation by the pyridyl part of the ligand, and assistance for the coordination to the dipyrrin part *via* abstraction of the N–H proton. We thus attempted the coordination between **5** and **17** (Scheme II-19 b.), but it also led to the coordination of the cobalt on the pyridyl part, forming the (1,9-diphenyl-5-(4-pyridyl)dipyrromethene)(pyridine)cobalt(II)chloride **18** (Figure II-20).

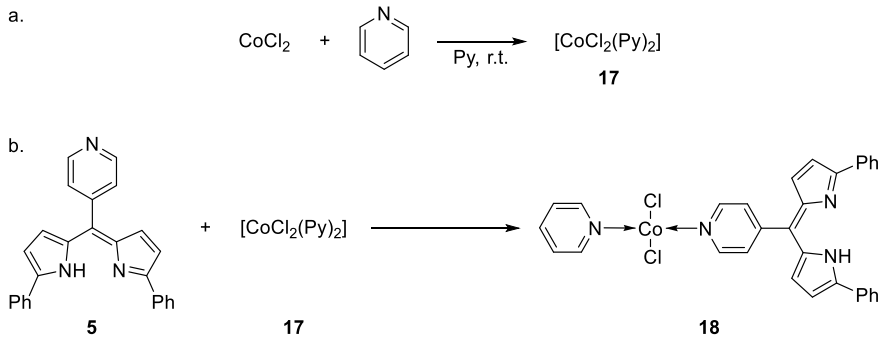

Scheme II-19: Synthesis of complexes 17 and 18

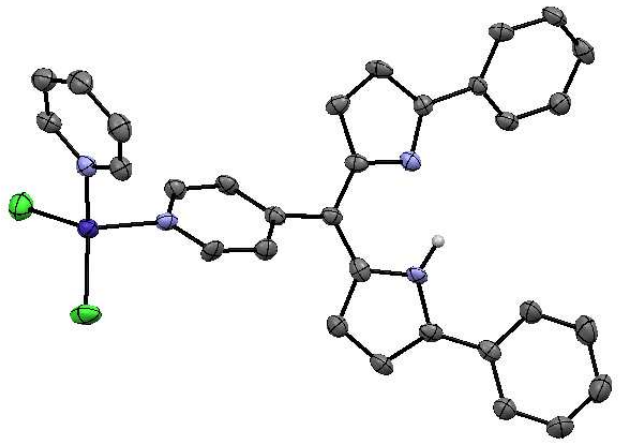

Figure II-20 ORTEP of the X-Ray structure of 18. Thermal ellipsoids are represented at 50% level. THF solvent and hydrogens were removed for clarity.

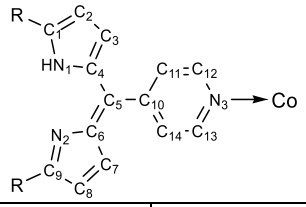			
	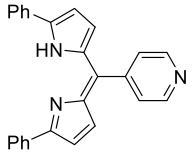 **5**	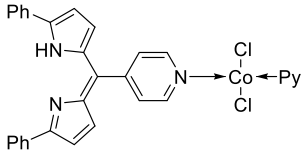 **18**	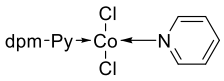 **18**
Dihedral angle py/dpm	48.95°	43.96	/
Distance C_5-C_{10} (Å)	1.493	1.473	/
C_{10}-C_{11}	1.381	1.395	1.390
C_{11}-C_{12}	1.383	1.364	1.367
C_{12}-N_3	1.359	1.352	1.345
N_3-C_{13}	1.343	1.344	1.340
C_{13}-C_{14}	1.373	1.370	1.365
C_{14}-C_{10}	1.395	1.415	1.394
Co-N_3	/	2.035	2.031

Table II-6: Comparison of dihedral angle and bond lengths between ligand 9 and the complex 18

The dihedral angle of **18** between the dipyrrin and the pyridyl parts is similar to the free ligand **5** (Table II-6). We can also notice a slight deformation of the pyridyl with the coordination of the cobalt. However, the bond lengths of the pyridyl part are comparable to the bond lengths of the pyridine chelated to the cobalt. Besides, the distance between the cobalt and the nitrogen of the pyridyl part is also similar to the distance to the pyridine. We can thus notice that the interaction of the cobalt with the ligand pyridyl part is similar to the interaction of the cobalt with an unsubstituted pyridine.

However, the most interesting point is the comparison of **14** and **18**: they are indeed both dipyrromethene with a tetrahedral cobalt(II) coordinated on their pyridyl parts (Table II-7). If the distance Co–N is similar for both complexes, the interaction of the cobalt on each of the pyridyl part seems to be different. First, we observed an increase of the dihedral angle for **14**, compared to the free ligand **3**, whereas this angle slightly decreases in the case of **18**, compared to **5**. In both case, the pyridyl part undergoes a deformation. As we determined that the chelation of cobalt on the pyridyl part of 5-(4-pyridyl)dipyrromethenes is equivalent to the chelation on a pyridine, we assume that these differences between **14** and **18** are linked to the difference between **3** and **5**, and that the substitution of the dipyrrin part can have an influence on the pyridyl part, despite the absence of conjugation.

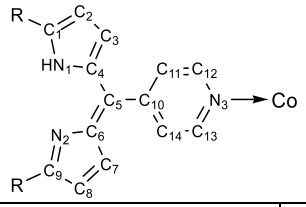		
	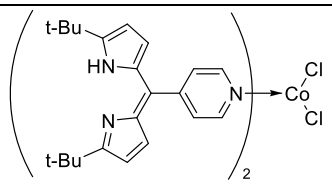 **14**	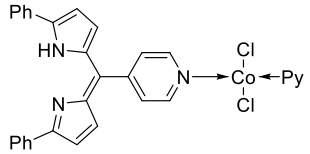 **18**
Dihedral angle py/dpm	74.85°	43.96
Distance C_5-C_{10} (Å)	1.497	1.473
C_{10}-C_{11}	1.377	1.395
C_{11}-C_{12}	1.329	1.364
C_{12}-N_3	1.325	1.352
N_3-C_{13}	1.329	1.344
C_{13}-C_{14}	1.387	1.370
C_{14}-C_{10}	1.392	1.415
Co-N_3	2.034	2.035

Table II-7: Comparison of dihedral angle and bond lengths between complex 14 and complex 18

These coordination tests gave several informations on the coordination of cobalt precursors with dipyrromethene ligands, and about the strategy we will have to set to get a bimetallic complex. Concerning **2** as ligand, the absence of substitution leads to a lack of control of the ligand number in the resulting complex. The mix of a “simple” cobalt salt with **2** will lead to a cobalt complex with three dipyrrin ligand, or two in the case of $Co(acac)_2$, with the chelation *via* the dipyrrin part. These complexes being not appropriate for our purpose of bimetallic compounds and catalysis, **2** was kept aside for potential other applications, like the complex **13**. Even if this complex is moisture- and air-sensitive, because of the strongly basic Cp* ligand, it is perfectly suitable as a precursor for a cobalt-lanthanide complex. As lanthanides tend to easily interact with heteroatom, and especially with oxygen, this complex either will not be involved in catalysis, but can be useful as proof of concept for highlighting the possibility of electron-transfer through the ligand.

For ligands **3** and **5**, the presence of *tert*-butyl or phenyl groups on the dipyrrin part leads to a preferential coordination of cobalt salts on the pyrdiyl part. To set the cobalt in the dipyrrin part, it will be necessary to first coordinate another metal on this pyridyl part, with a strong enough interaction, in order to block this coordination site. We expect that once this site occupied, the cobalt atom would have no other competitive coordination sites and will set in the dipyrrin part.

II.4. The cobalt-ruthenium bimetallic complexes

After having studied the behavior of different cobalt precursors with 5-(4-pyridyl)dipyrromethene ligands, we investigated which electron-transferring compounds we could use for the reductant part of the final complex. As said previously, we focused ourselves on divalent organolanthanides and photoactive polypyridyl ruthenium(II) (Figure II-21). The choice of these moieties has been motivated for several reasons:

- They both can be coordinated to a pyridine.

- Divalent lanthanides are known to be strong reductants able to transfer electron to redox non-innocent ligand. Bimetallic lanthanide-transition metal complexes have also been reported. The presence of the lanthanide in these complexes increases the stability of usually unstable intermediates, like Pd(IV).[63]

- Photosensitive polypyridyl ruthenium compounds (or ruthenium photosensitizers) are able to release an electron under light-excitation.[64] This electron can then be captured by a transition metal, like in dual photocatalytic system. One of the major group working on this kind of dual system is the group of MacMillan, that combine in their reaction medium a photosensitizer (ruthenium or iridium) with a transition metal in order to perform cross-coupling reactions.[65] With an electron released by photo-excitation, ruthenium photosensitizers allow a control of the reduction during the reaction.

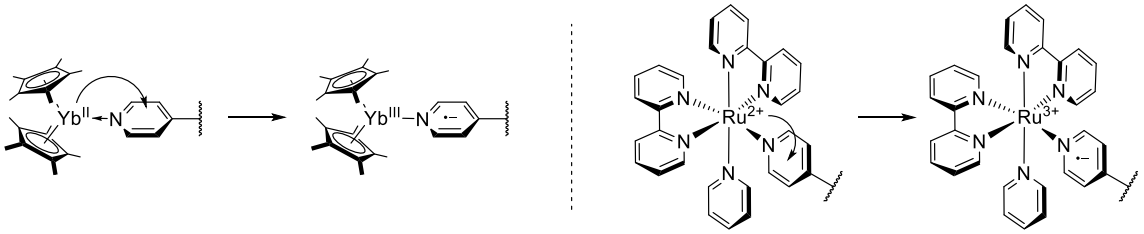

Figure II-21: Examples of coordinated organolanthanide (left) and polypyridyl ruthenium (right)

However, the use of these compounds as part of the complex implies restriction linked to their reactivity. Organometallic lanthanides compound as reductant part does not suit to develop a bimetallic catalyst, because of their easy interactions with heteroatoms, but it can be used to study the electron-transfer through the dipyrromethene ligand, if not the reduction process of the cobalt and the associated intermediates.

Concerning the use of ruthenium photosensitizers, they coordinate strongly to pyridine, preventing the decoordination of the reductant part from the complex. But ruthenium is able to transfer electrons in inter- and intramolecular way, contrary to lanthanides that proceed only by intramolecular electron-transfer.

Because of this effect, ruthenium photosensitizers can potentially lead to side-reactions due to the catch of the released electron by a substrate, as it can happen with unsaturated π systems.

We thus have two different organometallic species for the reductant part, each of them having different properties and different purposes: an organometallic divalent lanthanide can hardly be involved for reactions implying highly functionalized substrates, but can stabilize unstable states allowing the study of the potential active species; a ruthenium photosensitizer can transfer an electron *via* different mechanisms, but tolerates hard reaction conditions and functionalized substrates.

In the following part, we will only present our work with ruthenium photosensitizers as reductant part, insofar as the work with divalent lanthanides did not lead to substantial results for now.

II.4.1. The choice of the ruthenium precursor

Among all photosensitizers that were available, we decided to use a ruthenium polypyridyl species. In comparison with organic photosensitizers, the organometallic photosensitizers are more stable over time, and the ruthenium is one of the most studied transition metals for its photoactive properties. Moreover, the couple cobalt/ruthenium is a well-known couple, mainly used in the research for the split of water and carbon dioxide reduction. However, in bimetallic coupling reactions implying ruthenium photosensitizer, the ruthenium species is generally separated from the reactive transition metal. The classical employed ruthenium photosensitizer is $[Ru^{II}(bpy)_3],Cl_2$, discovered in 1936 by Burstall, and deeply studied since.[66] Several derivatives from $[Ru^{II}(bpy)_3]^{2+}$ have then been developed, in order to propose a wide range of photocatalysts with different photoluminescent properties (Figure II-22).[64,67]

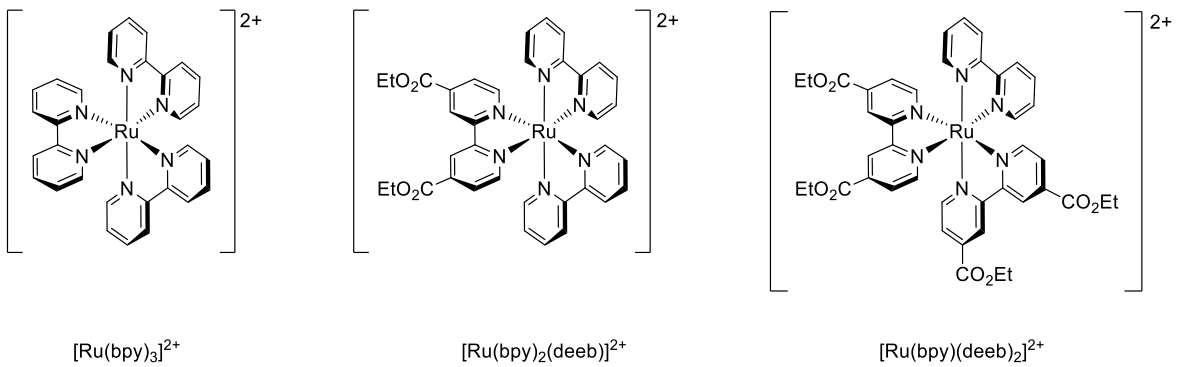

Figure II-22: Examples of *tris*(bipyridine) ruthenium(II)-type photosensitizers

The presence of three bipyridines leads to an equal distribution of the electronic density around the ruthenium center, and allows an equivalent distribution of the electron-transfer probability between each ligand. In our case, we wanted to preferentially transfer the electron on the pyridyl part. This pyridyl part being not conjugated to the dipyrrin part, we can consider its electronic properties is closed to an

unsubstituted pyridine. Considering this fact, the pyridyl part would not be more favored to have a more important distribution of the electron-transfer probability compared to the other pyridyl-type ligands. So, to increase the probability to transfer an electron to the ligand pyridyl part, it is necessary to disadvantage the probability of electron-transfer to the other pyridyl ligands, that is, to use electron-rich bipyridine, like alkyl-substituted bipyridines.[68]

For this reason, we decided to prepare the complex *bis*(4,4'-dimethyl-2,2'-bipyridine)ruthenium(II) chloride **19** as ruthenium species for the reductant part. This compound is prepared from the precursor $[RuCl_2(dmso)_4]$ **20**, by complexation of the bipyridine ligand in DMF at reflux, in presence of an excess of LiCl (Scheme II-20).[31] The excess of LiCl prevents from the formation of the complex *tris*(bipyridine)ruthenium(II) chloride by saturating the reaction medium in chloride anions, limiting the decoordination of the chlorine atom on the ruthenium center. The complex is then obtained as a black solid after precipitation by addition of acetone and wash of the solid with water and ether.

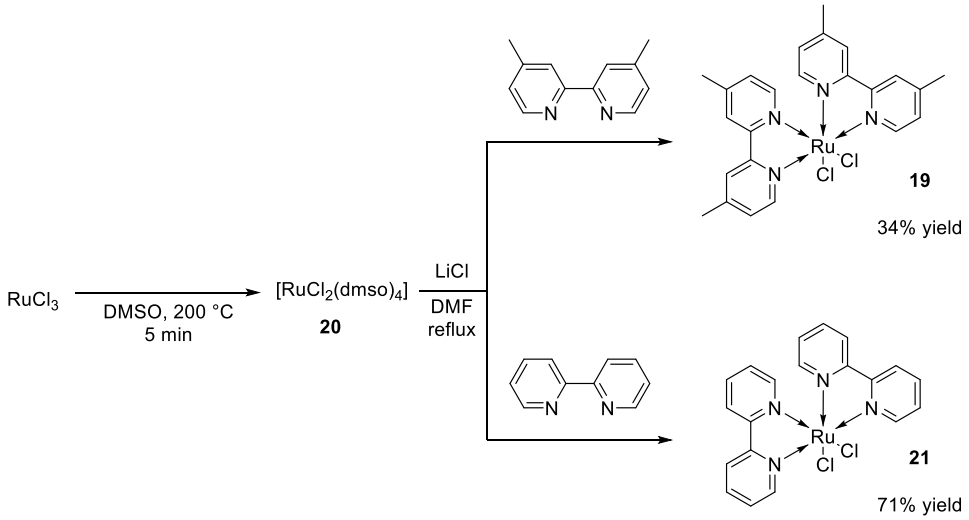

Scheme II-20: Synthesis of the *bis*(bipyridine)ruthenium(II) chloride precursors

Using the same protocol, we also synthesized the complex *bis*(2,2'-bipyridine)ruthenium(II) chloride **21**, to proceed to coordination tests of this kind of ruthenium precursor with the different dipyrromethenes ligands we have. The use of this precursor with unsubstituted bipyridine **21** allows also the possibility to observe, by comparison with **19**, the influence of the methyl groups on the reduction. Once this ruthenium precursor synthesized, we began our coordination tests. The main question remains the selectivity of the coordination site. Some ruthenium/5-heteroaryldipyrromethene complexes are reported in the literature, but none with a pyridyldipyrromethene derivative as ligand. It is noteworthy that ruthenium forms strong interactions with pyridyl ligand: Polypyridyl ruthenium complexes are indeed very stable. Considering this fact, we decided to assess the coordination regioselectivity of the ruthenium precursor **21** with **2**, which has two accessible coordination sites.

According to the literature, the coordination of a *bis* bipyridine ruthenium to an unsubstituted dipyrrin[69] proceeds by almost the same protocol than the coordination to a pyridine.[70] **21** and **2** have thus been solubilized in methanol and heated for 4 hours in the presence of triethylamine. The resulting reaction medium was then diluted with water and NH_4PF_6 was added. A black/brown precipitate formed and was collected by filtration and analyzed by ^{1}H NMR and mass spectroscopy. The NMR presents signals of unknown impurities, and the mass spectra highlighted the presence of at least two ruthenium complexes. By examining the mass and the fragment, we concluded that this reaction formed mainly two complexes: one with the ruthenium coordinated on the pyridyl part **22**, and another with the ruthenium coordinated on the dipyrrin part **23** (Scheme II-21).

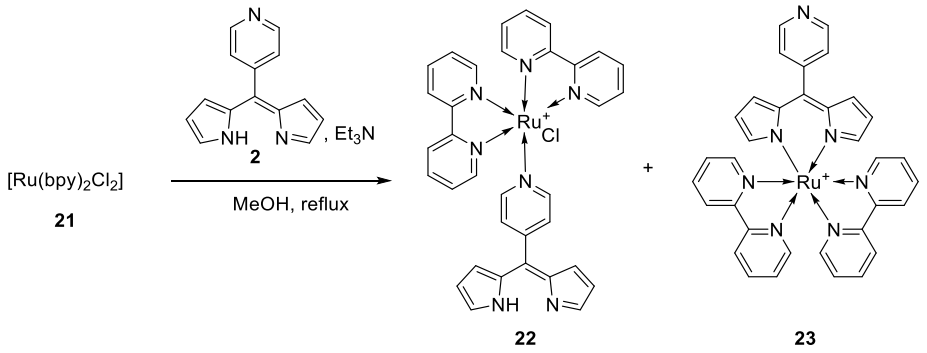

Scheme II-21: Test of the regioselectivity of the ruthenium coordination

II.4.2. Synthesis of the bimetallic cobalt-ruthenium complex

As **2** lead to several ruthenium complexes without control on the coordination regioselectivity, we decided to use **5** to form the expected cobalt-ruthenium complex: with two phenyl groups on position 1 and 9 of the dipyrrin, *bis*-bipyridine ruthenium complex can only coordinate to the pyridyl part. However, the main unknown point concerns the coordination of the cobalt in the dipyrrin part: according to our first test of coordination, the cobalt prefer to chelate on the pyridine, and according to the X-Ray structures, the position of the phenyl remains quite in the same plane than the dipyrrin part, suggesting that the conjugation between them restrains their rotation, preventing the insertion of a metal at this position. With the pyridyl part occupied by the ruthenium, we hoped to solve this problem.

Firstly, we managed to coordinate the ruthenium on the pyridyl part. Following the procedure used previously with **21** and **2**, **19** has been solubilized with **5** in methanol and the reaction medium has been heated at reflux for 4 hours, before being diluted by water. NH_4PF_6 was then added to proceed to the ion exchange, and precipitates the PF_6 salt (Scheme II-22). The black solid thus obtained has been washed several times with water and diethyl ether, to obtained the complex [(4,4'-Me_2-bpy)$_2$(**5**)Ru^{II}Cl],PF_6 **24**. As we did not succeed to have crystals, we analyzed it by ^{1}H NMR and mass spectroscopy. The signals of **5** and **19**

have been identified in by ^{1}H NMR, and the mass spectroscopy indicates clearly the mass of **24**, and its fragmentations.

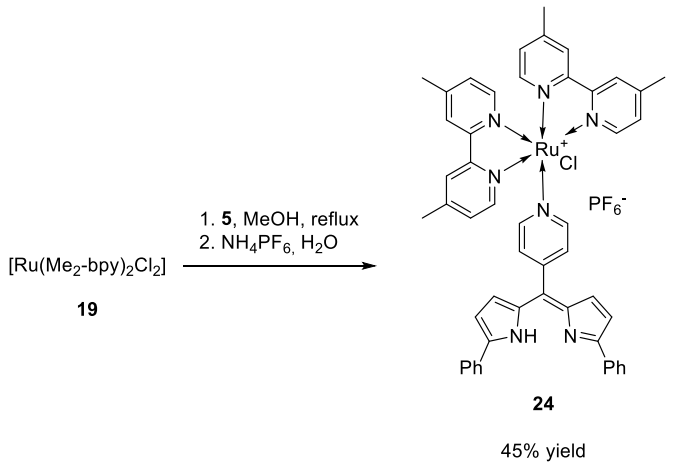

Scheme II-22: Synthesis of the ruthenium complex 24

For the coordination of the cobalt, we first tried with a classical and simple procedure. We decided to use *bis*-pyridine cobalt(II) chloride **17** as precursor, to take advantages of pyridines as proton scavengers and to satisfy the cobalt geometry as L ligand if necessary. **24** has been solubilized in acetonitrile, and **17**, in solution in acetonitrile, was added (Scheme II-23). After 3 days of stirring at room temperature, a red-brown precipitate was formed. After filtration and washing, the ^{1}H NMR presents paramagnetic signals. Moreover, the signal of the N–H proton of the dipyrrin part is no longer visible. Besides, the mass spectroscopy analysis also indicates the mass of the desired complex **25** including the ligand, the ruthenium part, the cobalt center and a pyridine ligand. The fragmentation is coherent with the expected structure, with first a loss of the pyridine, then the cobalt, and the ruthenium part. However, the mass also presents unknown products, corresponding to the mass of our complex with an oxygen atom. We thus did another NMR of **24**, and noted that the complex wasn't pure: other peaks were present, also in the aromatic area, making think that this product was impure, or partially oxidized with time.

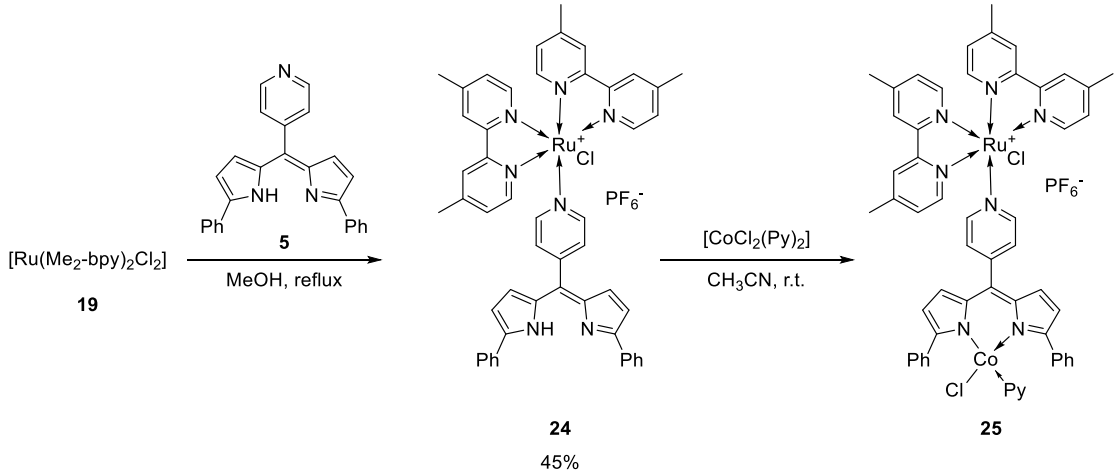

Scheme II-23: Preparation of the bimetallic Co/Ru complex 25

II.5. Conclusions and perspectives

In conclusion, we started a new project with the aim of developing a new family of bimetallic complexes based on 5-(4-pyridyl)dipyrromethene ligands, in order to discover new possibilities for cobalt-catalyzed cross-coupling reactions. To reach this goal, we synthesized three ligands: the 5-(4-pyridyl)dipyrromethene, the 1,9-di-*tert*-butyl-5-(4-pyridyl)dipyrromethene and the 1,9-diphenyl-5-(4-pyridyl)dipyrromethene, and worked on the optimization of their syntheses. The main optimization concern the oxidation step of this type of ligands: the classical used oxidants, which are DDQ or *p*-chloranil, do not allow a complete oxidation and leads to low yields. We replace the DDQ by manganese dioxide, bringing several improvements:

- The reaction can be realized in a concentrated solution, whereas DDQ, due to its low solubility, required important amount of solvents.
- The purification of the dipyrromethene is also simpler: performed into dichloromethane, a simple filtration allows removing the manganese salts, reagent and by-products. The dipyrromethene product is then obtained pure enough according to the ^{1}H NMR of the raw product.
- Manganese dioxide is less toxic than DDQ or *p*-chloranil.[58]

With the synthesized ligands, we managed to study the coordination of different cobalt salt precursors, to determine the regioselectivity of the coordination step for transition metals. We thus concluded that the presence of large group at the position 1 and 9 of the dipyrrin disfavors the coordination to the dipyrrin part, in favor of the coordination on the pyridyl part. However, by blocking the pyridyl part by another transition metal, a *bis*(bipyridine) ruthenium complex in our case, the cobalt coordinate to the dipyrrin part without any competition problem.

With this strategy, we succeeded to obtain as preliminary result a bimetallic cobalt-ruthenium complex, identified by mass spectroscopy and ^{1}H NMR.

For the following works on this project, the most important point would be to re-attempt the synthesis of the bimetallic complex already obtained, and to correctly characterize it. As the preliminary luminescence studies on this ruthenium complex shows a very weak emission, which has been confirmed by literature, it could be interesting also to replace the chloride X ligand bound to the ruthenium by a pyridine. Another option to remove this chloride ligand from the first coordination sphere would be to prepare a dipyrromethene with a 2,2'-bipyriyl moiety instead of the pyridyl part. The coordination of the ruthenium will be stronger, and the structure will be closer to the well-known *tris*-bipyridine ruthenium(II), and thus with potentially comparable properties.

Another path to explore would be also to change the cobalt center by another transition metal. Some preliminary works are ongoing in the laboratory with the nickel. For coordination, nickel(II) tends to be easier to work with, insofar as it does not change its oxidation degree, whereas cobalt(II) tends to oxidize into cobalt(III) when associated to dipyrrin ligands. This lead for example to the formation of complex like $[Co^{III}(dpm)_2(acac)]$ with cobalt, and $[Ni^{II}(dpm)(acac)]$ with nickel, which is more in accordance with our catalysis goal.

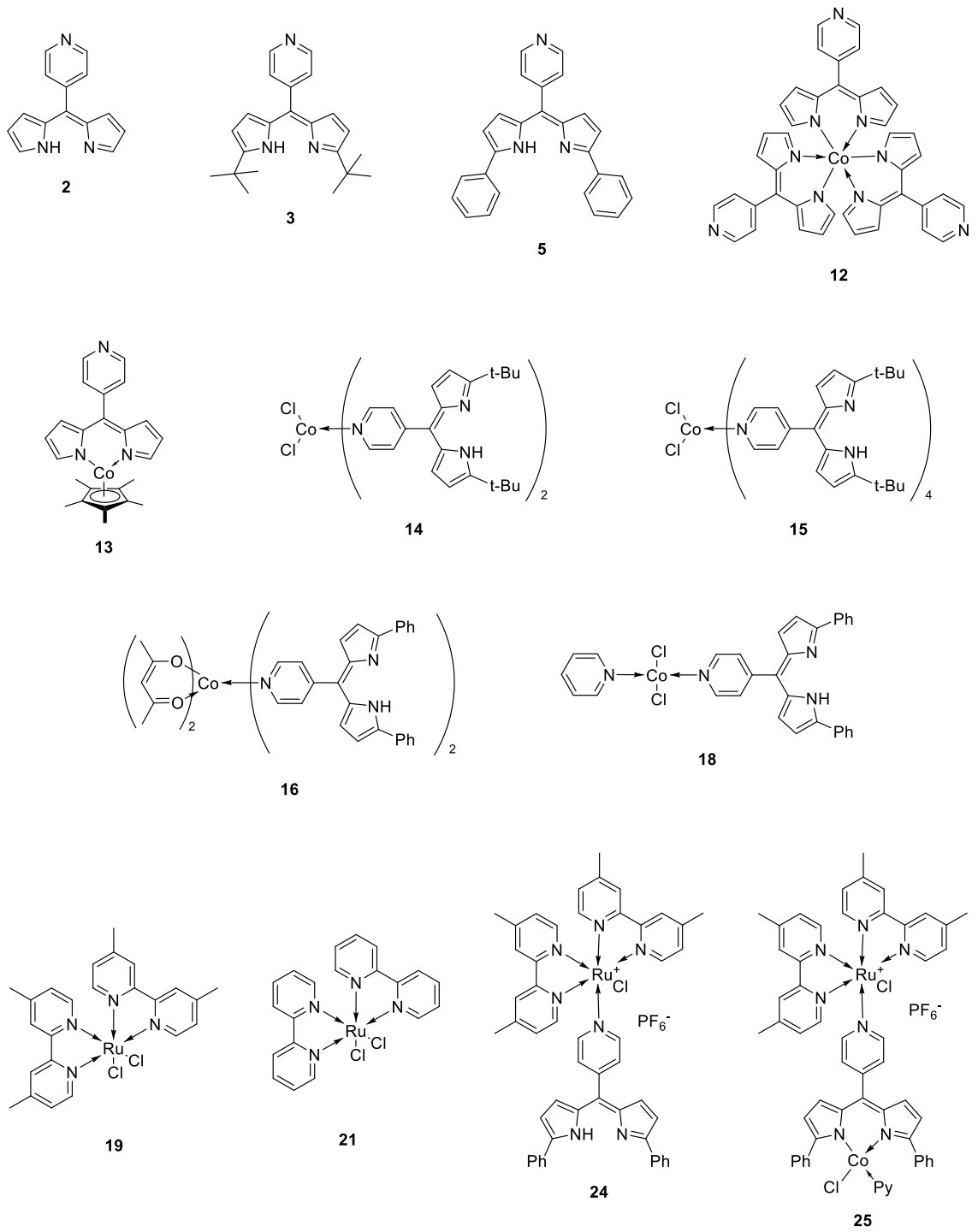

Figure II-23: List of ligands and molecules

Bibliography of part II

[1] R. Bonnett, D. C. Bradley, K. J. Fisher, *Chem. Commun.* **1968**, 886–887.

[2] R. Bonnett, D. C. Bradley, K. J. Fisher, I. F. Rendall, *J. Chem. Soc. A* **1971**, 1622–1627.

[3] L. Bourget-Merle, M. F. Lappert, J. R. Severn, *Chem. Rev.* **2002**, *102*, 3031–3066.

[4] T. R. Dugan, J. M. Goldberg, W. W. Brennessel, P. L. Holland, *Organometallics* **2012**, *31*, 1349–1360.

[5] C. Chen, T. R. Dugan, W. W. Brennessel, D. J. Weix, P. L. Holland, *J. Am. Chem. Soc.* **2014**, *136*, 945–955.

[6] J. M. Neely, M. J. Bezdek, P. J. Chirik, *ACS Cent. Sci.* **2016**, *2*, 935–942.

[7] J. V. Obligacion, S. P. Semproni, I. Pappas, P. J. Chirik, *J. Am. Chem. Soc.* **2016**, *138*, 10645–10653.

[8] J. V. Obligacion, M. J. Bezdek, P. J. Chirik, *J. Am. Chem. Soc.* **2017**, *139*, 2825–2832.

[9] C. H. Schuster, T. Diao, I. Pappas, P. J. Chirik, *ACS Catal.* **2016**, *6*, 2632–2636.

[10] J. V. Obligacion, J. M. Neely, A. N. Yazdani, I. Pappas, P. J. Chirik, *J. Am. Chem. Soc.* **2015**, *137*, 5855–5858.

[11] S. Krautwald, M. J. Bezdek, P. J. Chirik, *J. Am. Chem. Soc.* **2017**, *139*, 3868–3875.

[12] M. R. Friedfeld, M. Shevlin, G. W. Margulieux, L. C. Campeau, P. J. Chirik, *J. Am. Chem. Soc.* **2016**, *138*, 3314–3324.

[13] E. R. King, E. T. Hennessy, T. A. Betley, *J. Am. Chem. Soc.* **2011**, *133*, 4917–4923.

[14] E. R. King, G. T. Sazama, T. A. Betley, *J. Am. Chem. Soc.* **2012**, *134*, 17858–17861.

[15] E. T. Hennessy, R. Y. Liu, D. A. Iovan, R. A. Duncan, T. A. Betley, *Chem. Sci.* **2014**, *5*, 1526–1532.

[16] E. T. Hennessy, T. A. Betley, *Science (80-.).* **2013**, *340*, 591–595.

[17] V. Lyaskovskyy, B. De Bruin, *ACS Catal.* **2012**, *2*, 270–279.

[18] O. R. Luca, R. H. Crabtree, *Chem. Soc. Rev.* **2013**, *42*, 1440–1459.

[19] A. Winter, G. R. Newkome, U. S. Schubert, *ChemCatChem* **2011**, *3*, 1384–1406.

[20] A. M. W. Cargill Thompson, *Coord. Chem. Rev.* **1997**, *160*, 1–52.

[21] R. L. Webster, *Dalt. Trans.* **2017**, *46*, 4483–4498.

[22] D. A. Iovan, M. J. T. Wilding, Y. Baek, E. T. Hennessy, T. A. Betley, *Angew. Chem. Int. Ed.* **2017**, *56*, 15599–15602.

[23] F. Li, S. I. Yang, Y. Ciringh, J. Seth, C. H. Martin, D. L. Singh, D. Kim, R. R. Birge, D. F. Bocian, D. Holten, et al., *J. Am. Chem. Soc.* **1998**, *120*, 10001–10017.

[24] H. L. Kee, C. Kirmaiery, L. Yu, P. Thamyongkit, W. J. Youngblood, M. E. Calder, L. Ramos, B. C. Noll, D. F. Bocian, W. R. Scheldt, et al., *J. Phys. Chem. B* **2005**, *109*, 20433–20443.

[25] J. R. Pankhurst, N. L. Bell, M. Zegke, L. N. Platts, C. A. Lamfsus, L. Maron, L. S. Natrajan, S. Sproules, P. L. Arnold, J. B. Love, *Chem. Sci.* **2016**, *8*, 108–116.

[26] P. Rothemund, *J. Am. Chem. Soc.* **1935**, *57*, 2010–2011.

[27] P. Rothemund, *J. Am. Chem. Soc.* **1936**, *58*, 625–627.

[28] T. E. Wood, A. Thompson, *Chem. Rev.* **2007**, *107*, 1831–1861.

[29] C. Bruckner, V. Karunaratne, S. J. Rettig, D. Dolphin, *Can. J. Chem.* **1996**, *74*, 2182–2193.

[30] S. J. Smalley, M. R. Waterland, S. G. Telfer, *Inorg. Chem.* **2009**, *48*, 13–15.

[31] C. E. McCusker, J. K. McCusker, *Inorg. Chem.* **2011**, *50*, 1656–1669.

[32] A. Béziau, S. A. Baudron, D. Rasoloarison, M. W. Hosseini, *CrystEngComm* **2014**, *16*, 4973–4980.

[33] R. Toyoda, M. Tsuchiya, R. Sakamoto, R. Matsuoka, K. H. Wu, Y. Hattori, H. Nishihara, *Dalt. Trans.* **2015**, *44*, 15103–15106.

[34] A. Loudet, K. Burgess, *Chem. Rev.* **2007**, *107*, 4891–4932.

[35] H. Falk, F. Neufingerl, *Monatshefte für Chemie - Chem. Mon.* **1979**, *110*, 987–1001.

[36] L. Yu, K. Muthukumaran, I. V. Sazanovich, C. Kirmaier, E. Hindin, J. R. Diers, P. D. Boyle, D. F. Bocian, D. Holten, J. S. Lindsey, *Inorg. Chem.* **2003**, *42*, 6629–6647.

[37] S. Kusaka, R. Sakamoto, Y. Kitagawa, M. Okumura, H. Nishihara, *Chem. - An Asian J.* **2012**, *7*, 907–910.

[38] S. Kusaka, R. Sakamoto, H. Nishihara, *Inorg. Chem.* **2014**, *53*, 3275–3277.

[39] V. S. Thoi, J. R. Stork, D. Magde, S. M. Cohen, *Inorg. Chem.* **2006**, *45*, 10688–10697.

[40] S. R. Halper, M. R. Malachowski, H. M. Delaney, S. M. Cohen, *Inorg. Chem.* **2004**, *43*, 1242–1249.

[41] S. R. Halper, S. M. Cohen, *Inorg. Chem.* **2005**, *44*, 486–488.

[42] D. L. Murphy, M. R. Malachowski, C. F. Campana, S. M. Cohen, *Chem. Commun.* **2005**, 5506.

[43] N. A. M. Pereira, T. M. V. D. Pinho E Melo, *Org. Prep. Proced. Int.* **2014**, *46*, 183–213.

[44] J. P. NAGARKATTI, K. R. ASHLEY, *Synthesis (Stuttg).* **1974**, *1974*, 186–187.

[45] D. Gryko, J. S. Lindsey, *J. Org. Chem.* **2000**, *65*, 2249–2252.

[46] T. E. Wood, B. Berno, C. S. Beshara, A. Thompson, *J. Org. Chem.* **2006**, *71*, 2964–2971.

[47] W. H. Harman, T. D. Harris, D. E. Freedman, H. Fong, A. Chang, J. D. Rinehart, A. Ozarowski, M. T. Sougrati, F. Grandjean, G. J. Long, et al., *J. Am. Chem. Soc.* **2010**, *132*, 18115–18126.

[48] R. D. Rieth, N. P. Mankad, E. Calimano, J. P. Sadighi, *Org. Lett.* **2004**, *6*, 3981–3983.

[49] A. I. Mikhaleva, O. V. Petrova, L. N. Sobenina, *Chem. Heterocycl. Compd.* **2012**, *47*, 1367–1371.

[50] B. A. Trofimov, A. I. Mikhaleva, A. V. Ivanov, V. S. Shcherbakova, I. A. Ushakov, *Tetrahedron* **2015**, *71*, 124–128.

[51] J. Wen, R. Y. Zhang, S. Y. Chen, J. Zhang, X. Q. Yu, *J. Org. Chem.* **2012**, *77*, 766–771.

[52] A. Spaggiari, D. Vaccari, P. Davoli, F. Prati, *Synthesis (Stuttg).* **2006**, 995–998.

[53] S. E. Korostova, A. I. Mikhaleva, L. N. Sobenina, S. G. Shevchenko, V. V Shcherbakov, *Chem. Heterocycl. Compd.* **1985**, *21*, 1238–1241.

[54] C. Hansch, A. Leo, R. W. Taft, *Chem. Rev.* **1991**, *91*, 165–195.

[55] R. Orłowski, D. Gryko, D. T. Gryko, *Chem. Rev.* **2017**, *117*, 3102–3137.

[56] S. M. S. Ló, D. R. B. Ducatti, M. E. R. Duarte, S. M. W. Barreira, M. D. Noseda, A. G. Gonalves, *Tetrahedron Lett.* **2011**, *52*, 1441–1443.

[57] G. Cahiez, M. Alami, R. J. K. Taylor, M. Reid, J. S. Foot, in *Encycl. Reagents Org. Synth.*, John Wiley &

Sons, Ltd, Chichester, **2004**.

[58] B. F. O. Nascimento, A. M. d. A. Rocha Gonsalves, M. Pineiro, *Inorg. Chem. Commun.* **2010**, *13*, 395–398.

[59] C. Brückner, Y. Zhang, S. J. Rettig, D. Dolphin, *Inorganica Chim. Acta* **1997**, *263*, 279–286.

[60] E. A. Leushina, D. N. Gorbunov, D. A. Cheshkov, T. S. Kuchinskaya, A. V. Anisimov, A. L. Maksimov, M. V. Terenina, A. V. Khoroshutin, E. A. Karakhanov, *Russ. J. Org. Chem.* **2016**, *52*, 1625–1631.

[61] M. M. Clark, W. W. Brennessel, P. L. Holland, *Acta Crystallogr. Sect. E Struct. Reports Online* **2009**, *65*, m391–m391.

[62] K. Servaty, E. Cauët, F. Thomas, J. Lambermont, P. Gerbaux, J. De Winter, M. Ovaere, L. Volker, N. Vaeck, L. Van Meervelt, et al., *Dalt. Trans.* **2013**, *42*, 14188–14199.

[63] V. Goudy, A. Jaoul, M. Cordier, C. Clavaguéra, G. Nocton, *J. Am. Chem. Soc.* **2017**, *139*, 10633–10636.

[64] K. Teegardin, J. I. Day, J. Chan, J. Weaver, *Org. Process Res. Dev.* **2016**, *20*, 1156–1163.

[65] K. L. Skubi, T. R. Blum, T. P. Yoon, *Chem. Rev.* **2016**, *116*, 10035–10074.

[66] F. H. Burstall, *J. Chem. Soc.* **1936**, 173.

[67] M. D. Kärkäs, T. M. Laine, E. V. Johnston, B. Akermark, *Appl. Photosynth. - New Prog.* **2016**, DOI 10.5772/62272.

[68] J. Chambers, B. Eaves, D. Parker, R. Claxton, P. S. Ray, S. J. Slattery, *Inorganica Chim. Acta* **2006**, *359*, 2400–2406.

[69] G. Li, L. Ray, E. N. Glass, K. Kovnir, A. Khoroshutin, S. I. Gorelsky, M. Shatruk, *Inorg. Chem.* **2012**, *51*, 1614–1624.

[70] J. C. Curtis, J. S. Bernstein, R. H. Schmehl, T. J. Meyer, *Chem. Phys. Lett.* **1981**, *81*, 48–52.

General Conclusion and perspectives

To conclude, we worked on cobalt chemistry on two aspect: catalysis aspect, with the development of new catalytic reactions with a classical and known catalytic system: $CoBr_2$/bipyridine, and coordination aspect, with the design and the synthesis optimization of a new family of cobalt complexes.

For the first part, inspired by the works of Garg and Szostak on the activation of the C–N amidic bond with nickel, palladium and rhodium catalysts, we started to develop the cobalt activation of the amide function by applying the cobalt-catalyzed reductive cross-coupling conditions on distorted amides. With the aim of developing practical and synthetically interesting reactions, we worked on the use of *N*-Boc-protected amides as coupling partners, and succeeded to have promising preliminary results by coupling these amides with aryl bromides, forming the dissymmetric benzophenone product. Another interesting first result to develop further is the formation of a symmetric benzophenone from an activated benzamide. This reaction stands as a homo-coupling of an amide, with a decarbonylative step occurring before the reductive elimination. Finally, we developed the cobalt-catalyzed conversion of the amide function into ester, in mild conditions, and with a high tolerance for functionalized substrates. This reaction corresponds to a coupling between an amide and an alcohol. The coupling reaction has been realized with a wide scope of alcohols, and works even with weakly nucleophilic alcohol, like phenols or hexafluoroisopropanol. The reaction also worked on aliphatic amides as well as on benzamides. However, the reaction has also restrictions, like steric hindrance. Indeed, tertiary alcohols do not couple, and hindered alcohols, like 2-adamantanol, lead to relatively weak yields. This reaction works also on classical C–H activation directing group, allowing their transformation into esters in mild conditions and with correct yields.

For the second part, we managed to develop a new family of bimetallic complexes, based on a dipyrromethene ligands. The synthesis of the ditopic 5-(4-pyridyl)dipyrromethene ligand has firstly been optimized. The oxidation step, generally realized with DDQ, and giving poor yield in the case of this ligand, can be realized with MnO_2 with a total conversion of the substrate, a very good yield and a more simple reaction process. Then, we prepared two variation of this ligand: the 1,9-di(*ter*-butyl)-5-(4-pyridyl)dipyrromethene and the 1,9-(diphenyl)-5-(4-pyridyl)dipyrromethene. With each of these ligands, we attempted several coordination of cobalt salts and precursors. It appeared that with our two substituted dipyrromethenes, cobalt(II) salts coordinate preferentially on the pyridyl part. On the contrary, in the case of the unsubstituted dipyrromethene, cobalt(II) salts coordinate on the dipyrrin part, leading, for cobalt(II) halides or cobalt(II) acetate, to *tris*(dipyrrin) Cobalt(III) complexes or, for cobalt(II) acetyacetonate, to

bis(dipyrrin) acetylacetonate cobalt(III) complex. With the precursor $[Cp^*Co^{II}Cl]_2$, we nevertheless managed to obtain a heteroleptic dipyrrin/Cp* cobalt(II) complex, with the pyridyl part free. Concerning the 1,9-(diphenyl)-5-(4-pyridyl)dipyrromethene, it has been possible to prevent the cobalt complexation on the pyridyl part by blocking this part. By firstly coordinating a *bis*(bipyridine)ruthenium(II) chloride moiety on the pyridyl part, the cobalt precursor coordinates easily, in mild conditions, to the dipyrrin part, leading to the bimetallic cobalt/ruthenium complex. This complex still have to be studied, as for its luminescent properties, and its potential applications in catalysis.

To finish, it would be interesting to cross these two part of this thesis by studying the potential reactivity of cobalt/ruthenium dipyrrin complexes toward activated amide. It could lead to a photo-induced activation of the amide function and the development of cobalt-catalyzed cross-coupling reaction involving amides without an excess of metallic reducing species.

Moreover, as the cobalt is involved in the conjugation of the dipyrrin part, its stability is enhanced. Adding to that the potential steric hindrance of the ligand near the cobalt center, and it could also be possible, in a first time, to recover the decarbonylation step of the amide activation reaction after the insertion of the metal into the C–N amidic bond and, in a second time, to constrain the decoordination of the carbonyl ligand.

Another possibility to enlarge the reactivity of these complexes would be to change the substitution of the dipyrromethene ligand. The problem with the actual system is that it requires bulky substituents to force the ruthenium photosensitizer to coordinate to the pyridine part. However, with another bulkier photosensitizer, it would be possible to have access to less hindered dipyrrin part, but still hindered enough to avoid the coordination of several dipyrrin to one cobalt. For example, the zinc(II) tetraphenylporphyrin (ZnTPP) can be used as photosensitizer and is too bulky to coordinate to the dipyrrin part. The combination of this photosensitizer with a 1,9-dimethyl or 1,9-diethyl substitution on the dipyrrin part and $Co(acac)_2$ as cobalt source could lead to a complex $(acac)Co^{II}$(dpm-Py)(ZnTPP) with a weak steric hinderance near the cobalt center, and thus allowing the approach of bulkier substrates.

The finality of these projects would be to develop a set of combinations between photosensitizers, 5-pyridyldipyrromethene ligands and cobalt sources to be able to react selectively with different amide substrates and couple them electrophilic partners or radical partners.

Experimental Part

General information

All solvents and chemicals were obtained commercially and used as received, unless specified. NMR spectra were recorded on a Bruker AC-300 SY spectrometer operating at 300.0 MHz for ^{1}H and 75.0 MHz for 13C or a Bruker Advance DPX 400 instrument operating at 400.0 MHz for ^{1}H and 101.0 MHz for ^{13}C, and are internally referenced to residual solvents signal. HR-MS analyses were carried out with a quadrupol time-of-flight mass spectrometer (Q-TOF premier) equipped with a Z-spray electrospray source (Waters, Saint-Quentin-en-Yvelines, France). Solutions were infused into the ESI source with a syringe pump at an infusion rate of 10µL.min-1. Ion source parameters were adjusted as followed: the cone voltage (Vcone) at 25 V, the capillary voltage was set to 3.0 kV. Typical values for the other source parameters were 4 V for the extraction cone and 2.1 V for the ion guide. Source and desolvation temperatures were set to 80 °C and 250 °C, respectively. Nitrogen was used as both nebulizing and desolvation gas. Argon was used as the collision gas at a flow of 0.26 mL.min-1, corresponding to a pressure of 4.10-3 mbar. The accurate mass and the elemental composition for all ions were obtained using the instrument MassLynx software. Gas chromatopgraphy (GC) was performed on a Perichrom PR2100 2317 Series gas chromatograph equipped with a split-mode, capillary injection system and flame ionization detectors using a SGE apolar IDBP1 (25m x 0.33mm) column. Column chromatography was performed on silica gel with 60, 40-63 µm. Single crystals were mounted on a Kapton loop using a Paratone N oil. An APEX II CCD BRUKER detector and a graphite Mo-Kα monochromator were used for the data acquisition. All measurements were done at 150 K and a refinement method was used for solving the structure. The structure resolution was accomplished using athe SHELXT-2014 program and the refinement was done with SHELXL-2014 program. The structure solution and the refinement were achieved with the PLATON software. Finally, pictures of the compound structure were obtained using the MERCURY software. During the refinement steps, all atoms- except hydrogens- were refined anisotropically. The position of hydrogens was determined using residual electronic densities, which are calculated by a Fourier difference. Finally, in order to obtain a complete refinement, a weighting step followed by multiples loops of refinement was done.

Part I. Reactivity of cobalt catalyst with non-planar amides

Amides were prepared following procedures described in the literature. *N*-Boc-*N*-methyl amides substrates were prepared by following the procedure described in the literature, employing HBTU (1 equivalent) instead of EDC/HOBt.

The semi-decarbonylative reductive homocoupling of amides

Typical procedure for the optimization of the semi-decarbonylative homocoupling of amides: a 20 mL reaction tube was charged with *N*-Boc-*N*-phenyl-benzamide (0.5 mmol, 149 mg), bipyridine (0.20 mmol, 31.2 mg), manganese powder (1.5 mmol, 82.4 mg), $CoBr_2$ (0;10 mmol, 21.8 mg), DMF (2.25 mL), pyridine (0.25 mL) and dodecane (20 µL) as internal standard. Then, TMSCl (0.32 mmol, 40 µL) was added to the reaction medium and the tube was sealed and placed into a heated aluminum bloc under stirring. The tube was stirred 60 °C. After 30 minutes, a sample of the reaction medium is taken, neutralized with $NH_4Cl_{aq.sat}$ and filtered through a pad of $MgSO_4$. The resulting organic solution is analyzed by GC-FID.

The reductive cross-coupling between amides and aryl halides

Typical procedure for the optimization of the reductive cross-coupling between amides and aryl halides: a 20 mL reaction tube was charged with *N*-Boc-*N*-phenyl-benzamide (0.5 mmol, 149 mg), 4-methylphenyl halide (2.0 mmol), manganese powder (1.5 mmol, 82.4 mg), $CoBr_2$ (0;10 mmol, 21.8 mg), DMF (2.25 mL), pyridine (0.25 mL) and dodecane (20 µL) as internal standard. Then, TMSCl (0.32 mmol, 40 µL) was added to the reaction medium and the tube was sealed and placed into a heated aluminum bloc under stirring. The tube was stirred 60 °C. After 30 minutes, a sample of the reaction medium is taken, neutralized with $NH_4Cl_{aq.sat}$ and filtered through a pad of $MgSO_4$. The collected organic solution is analyzed by GC-FID.

The cobalt-catalyzed amide-to-ester conversion

Typical procedure for amide conversion into ester: a 20 mL reaction tube was charged with *N*-Boc-amide (1.0 mmol), bipyridine (0.10 mmol, 15,6 mg), manganese powder (1.0 mmol, 54,9 mg), $CoBr_2$ (0;050 mmol, 10.9 mg), alcohol (1.2 mmol), DMF (4.6 mL) and pyridine (0.4 mL). Then, TMSCl (0.32 mmol, 40 µL) was added to the reaction medium and the tube was sealed and placed into a heated aluminum bloc under stirring. The tube was stirred at indicated temperature for 20 h. After cooling to room temperature, the reaction medium was diluted with Et_2O and filtered through a pad of silica gel. The resulting organic layer was washed with HCl (1 N) and with LiCl aqueous solution (5 %), three times, and dried over $MgSO_4$,

filtered and evaporated. Unless specified, the crude product was purified by flash chromatography (Petroleum Ether/diethyl ether, 100:0 to 90:10) and characterized by NMR (^{1}H, ^{13}C).

Procedure for the one-pot-two-steps amide conversion onto ester: a 20 mL reaction tube was charged with *N*-Boc benzamide (1.0 mmol), Boc_2O (1.2 mmol, 261, 9 mg), DMAP (0.5 mmol, 61.1 mg), DMF (2.0 mL) and pyridine (0.4 mL). The tube was sealed and placed into a heated aluminum bloc under stirring. The reaction medium was stirred at 60 °C for 5 h. Then, the resulting solution was added to a solution of $CoBr_2$ (0.050 mmol, 10.9 mg), bipyridine (0.10 mmol, 15.6 mg), manganese powder (1.0 mmol, 54.9 mg), alcohol (1.2 mmol) in DMF (2.6 mL, activated with TMSCl (0.32 mmol, 40 µL) in a tube. The tube was stirred at 60 °C for 20 h. After cooling to room temperature, dodecane (25 µL) was added and an aliquot of the reaction medium was diluted with Et_2O and filtered through a pad of silica gel. The resulting sample was analyzed by GC-FID.

Procedure for the gram-scale synthesis of (*S*)-3,7-dimethyloct-6-en-1-yl 4-methoxybenzoate (48): a 50 mL reaction tube was charge with *tert*-butyl 4-methoxylbenzoyl(methyl)carbamate (10 mmol, .65 g), bipyridine (0.20 mmol, 31 mg), manganese powder (10 mmol, 550 mg), $CoBr_2$ (0.10 mmol, 22 mg), *L*-β-citronellol (12 mmol, 2.2 mL), DMF (9.2 mL) and pyridine (0.8 mL). Then, TMSCl (traces) was added to the reaction medium and the tube was sealed and placed into a heated aluminum bloc under stirring. The tube was stirred at 60 °C for 20 h. After cooling to room temperature, the reaction medium was diluted with Et_2O and filtered through a pad of silica gel. The resulting organic layer was washed with HCl (1 N) and with LiCl aqueous solution (5 %), three times, and dried over $MgSO_4$, filtered and evaporated. The crude product was purified by flash chromatography (Petroleum Ether/Et_2O, 100:0 to 90:10). 2.2 g of (*S*)-3,7-dimethyloct-6-en-1-yl 4-methoxybenzoate was obtained as a colorless oil (76 %). **^{1}H NMR** (300 MHz, $CDCl_3$) δ 7;98 (d, *J* = 8.9 Hz, 2H), 6.89 (d, *J* = 8.9 Hz, 2H), 5.09 (t, *J* = 7.1 Hz, 1H), 4.39 – 4.25 (m, 2H), 3.82 (s, 3H), 2.09 – 1.91 (m, 2H), 1.85 – 1.73 (m, 1H), 1.67 (s, 3H), 1.71 – 1.47 (m, 2H), 1.59 (s, 3H), 1.46 – 1.32 (m, 1H), 1.30 – 1.15 (m, 1H), 0.96 (d, *J* = 6.4 Hz, 3H); **^{13}C NMR** (75 MHz, CDCl3) δ 166.3, 163.2, 131.5, 131.2, 124.6, 122.9, 113.5, 63.1, 55.3, 37.0, 35.5, 29.5, 25.7, 25.4, 19.5, 17.6; **HRMS** ESI-P (Q-TOF LiCl) *m/z* calcd. for $C_{18}H_{27}O_3$ $[M]^+$: 291.1960, found: 291.1975.

Optimization of the reaction

I. Products descriptions

a. N,N-bis substituted benzamide derivatives:

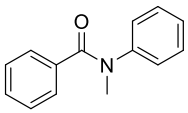

***N*-methyl-*N*-phenylbenzamide** [1934-92-5] (**1**): **^{1}H NMR** (300 MHz, $CDCl_3$) δ 7.28 – 7.22 (m, 2H), 7.18 – 7.00 (m, 6H), 7.00 – 6.93 (m, 2H), 3.42 (s, 3H); **^{13}C NMR** (75 MHz, $CDCl_3$) δ 170.6, 144.8, 135.9, 129.6, 129.1, 128.7, 127.7, 126.9, 126.5, 38.4.

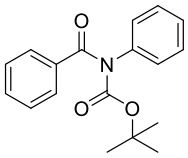

***tert*-butyl benzoyl(phenyl)carbamate** [101137-69-3] **(2)**: **^{1}H NMR** (300 MHz, $CDCl_3$) δ 7.74 (dt, *J* = 8.6, 1.9 Hz, 2H), 7.57 – 7.50 (m, 1H), 7.48 – 7.40 (m, 4H), 7.38 – 7.31 (m, 1H), 7.30 – 7.25 (m, 2H), 1.23 (s, 9H); **^{13}C NMR** (75 MHz, $CDCl_3$) δ 172.8, 153.3, 139.1, 137.0, 131.8, 129.2, 128.3, 128.1, 128.0, 127.8, 83.5, 27.5.

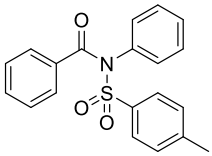

***N*-phenyl-*N*-tosylbenzamide** [74542-54-4] (**11**): **^{1}H NMR** (300 MHz, $CDCl_3$) δ 7.82 (t, *J* = 7.0 Hz, 2H), 7.44 (d, *J* = 7.0 Hz, 2H), 7.36 – 7.23 (m, 6H), 7.16 (dd, *J* = 8.8, 5.8 Hz, 4H), 2.45 (s, 3H); **^{13}C NMR** (75 MHz, $CDCl_3$) δ 169.9, 137.4, 135.2, 133.6, 131.8, 130.4, 129.6, 129.5, 129.3, 129.1, 129.1, 128.6, 128.0, 21.8.

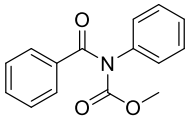

Methyl benzoyl(phenyl)carbamate (**12**): **^{1}H NMR** (300 MHz, $CDCl_3$) δ 7.88 – 7.60 (m, 2H), 7.56 – 7.31 (m, 6H), 7.27 (d, *J* = 7.3 Hz, 2H), 3.66 (s, 3H); **^{13}C NMR** (75 MHz, $CDCl_3$) δ 172.2, 155.3, 138.7, 135.6, 132.1, 129.4, 128.4, 128.4, 128.0, 127.3, 53.9.

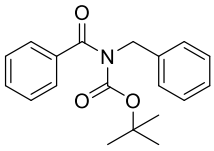

***tert*-butyl benzoyl(benzyl)carbamate** [85909-02-0] (**13**): **^{1}H NMR** (300 MHz, $CDCl_3$) δ 7.59 – 7.52 (m, 2H), 7.51 – 7.41 (m, 3H), 7.40 – 7.31 (m, 4H), 7.30 – 7.23 (m, 1H), 5.03 (s, 2H), 1.14 (s, 9H); **^{13}C NMR** (75 MHz, $CDCl_3$) δ 173.0, 153.5, 137.9, 137.8, 131.1, 128.5, 128.2, 128.1, 127.5, 127.5, 83.1, 48.9, 27.4.

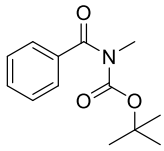

***tert*-butyl benzoyl(methyl)carbamate** (*Angew. Chem. Int. Ed.*, **2016**, *128*, 8860-8864) (**14**): **^{1}H NMR** (300 MHz, $CDCl_3$) δ 7.35 – 7.28 (m, 2H), 7.28 – 7.21 (m, 1H), 7.17 (t, *J* = 7.4 Hz, 2H), 3.10 (s, 3H), 0.95 (s, 9H); **^{13}C NMR** (75 MHz, $CDCl_3$) δ 173.1, 153.2, 137.8, 130.6, 127.8, 127.2, 82.5, 32.3, 27.1.

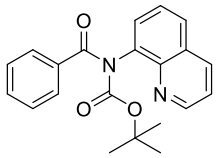

***tert*-butyl benzoyl(quinolin-8-yl)carbamate** (**53**): **^{1}H NMR** (300 MHz, $CDCl_3$) δ 8.87 (dd, *J* = 4.2, 1.6 Hz, 1H), 8.11 (dd, *J* = 8.3, 1.6 Hz, 1H), 8.03 – 7.94 (m, 2H), 7.79 (d, *J* = 8.3 Hz, 1H), 7.71 (dd, *J* = 7.3, 1.1 Hz, 1H), 7.61 – 7.42 (m, 4H), 7.35 (dd, *J* = 8.3, 4.2 Hz, 1H), 1.24 (s, 9H); **^{13}C NMR** (75 MHz, $CDCl_3$) δ 173.5, 153.5, 150.5, 144.1, 137.5, 137.2, 136.2, 131.5, 129.2, 129.1, 128.6, 128.4, 128.1, 126.3, 121.7, 83.2, 27.5.

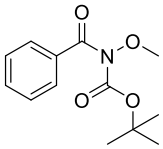

***tert*-butyl benzoyl(methoxy)carbamate** (**54**): To a solution of *N*-methoxybenzamide (5 mmol, 755.6 mg) and DMAP (1 mmol, 122.2 mg) in acetonitrile (2.5 mL) was added a solution of Boc_2O (6 mmol, 1.31 g) in acetonitrile (2.5 mL) dropwise. The resulting solution was heated at 50°C during 20 h under stirring. The medium was quenched with an aqueous solution of Na_2CO_3 (sat.) and extracted with AcOEt three times. The combined organic layers were dried over $MgSO_4$, filtered and concentrated. The residue was purified using flash chromatography (Eluent Pentane/AcOEt, 100:0 to 80:20). **^{1}H NMR** (300 MHz, $CDCl_3$) δ 7.61 – 7.54 (m, 2H), 7.49 (t, *J* = 7.4 Hz, 1H), 7.39 (t, *J* = 7.4 Hz, 2H), 3.87 (s, 3H), 1.28 (s, 9H); **^{13}C NMR** (75 MHz, $CDCl_3$) δ 168.9, 150.6, 135.5, 131.7, 128.1, 128.0, 84.7, 64.0, 27.5.

b. Obtained esters:

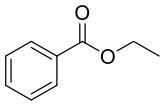

Ethyl benzoate [93-89-0] (**10**): **^{1}H NMR** (300 MHz, $CDCl_3$) δ 8.05 (d, *J* = 7.3 Hz, 2H), 7.55 (t, *J* = 7.3 Hz, 1H), 7.43 (t, *J* = 7.3 Hz, 2H), 4.38 (q, *J* = 7.1 Hz, 2H), 1.39 (t, *J* = 7.1 Hz, 3H); **^{13}C NMR** (75 MHz, $CDCl_3$) δ 166.6, 132.8, 130.5, 129.5, 128.3, 60.9, 14.3.

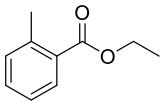

Ethyl 2-methylbenzoate [87-24-1] (**15**): **Yield**: 72.6 mg, 88%; **^{1}H NMR** (400 MHz, $CDCl_3$) δ 7.84 (dd, *J* = 8.1, 1.4 Hz, 1H), 7.32 (td, *J* = 7.5, 1.4 Hz, 1H), 7.19 – 7.14 (m, 2H), 4.29 (q, *J* = 7.1 Hz, 2H), 2.53 (s, 3H), 1.32 (t, *J* = 7.1 Hz, 3H); **^{13}C NMR** (101 MHz, $CDCl_3$) δ 183.7, 140.0, 131.8, 131.6, 130.5, 125.7, 114.7, 60.7, 21.7, 14.3.

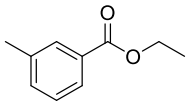

Ethyl 3-methylbenzoate [120-33-2] (**16**): **Yield**: 50.4 mg, 61%; **^{1}H NMR** (400 MHz, $CDCl_3$) δ 7.80 – 7.71 (m, 2H), 7.28 – 7.17 (m, 2H), 4.27 (q, *J* = 7.1 Hz, 2H), 2.29 (s, 3H), 1.29 (t, *J* = 7.1 Hz, 3H); **^{13}C NMR** (101 MHz, $CDCl_3$) δ 166.8, 138.1, 133.6, 130.4, 130.1, 128.2, 126.7, 60.9, 21.3, 14.3.

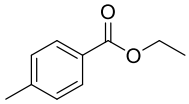

Ethyl 4-methylbenzoate [94-08-6] (**17**): **Yield**: 60.7 mg, 74%; **^{1}H NMR** (400 MHz, $CDCl_3$) δ 7.84 (d, *J* = 8.1 Hz, 2H), 7.12 (d, *J* = 8.1 Hz, 2H), 4.25 (q, *J* = 7.1 Hz, 2H), 2.29 (s, 3H), 1.28 (t, *J* = 7.1 Hz, 3H); **^{13}C NMR** (101 MHz, $CDCl_3$) δ 166.7, 143.4, 129.6, 129.0, 127.8, 60.7, 21.6, 14.3.

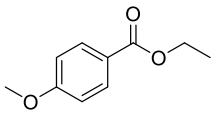

Ethyl 4-methoxybenzoate [94-30-4] (**18**): **Yield**: 78.9 mg, 88%; **^{1}H NMR** (300 MHz, $CDCl_3$) δ 7.99 (d, *J* = 8.8 Hz, 2H), 6.90 (d, *J* = 8.8 Hz, 2H), 4.33 (q, *J* = 7.1 Hz, 2H), 3.84 (s, 3H), 1.37 (t, *J* = 7.1 Hz, 3H); **^{13}C NMR** (75 MHz, $CDCl_3$) δ 166.4, 163.2, 131.5, 122.9, 113.5, 60.6, 55.4, 14.4.

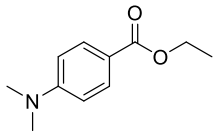

Ethyl 4-dimethylaminobenzoate [10287-53-3] (**19**): purified by flash chromatography (Petroleum Ether/AcOEt, 100:0 to 90:10) **Yield**: 84.8 mg, 88%; **^{1}H NMR** (400 MHz, $CDCl_3$) δ 7.83 (d, *J* = 9.0 Hz, 2H), 6.57 (d, *J* = 9.0 Hz, 2H), 4.23 (q, *J* = 7.1 Hz, 2H), 2.92 (s, 6H), 1.27 (t, *J* = 7.1 Hz, 3H); **^{13}C NMR** (101 MHz, $CDCl_3$) δ 167.0, 153.0, 131.2, 111.0, 60.1, 40.2, 14.5.

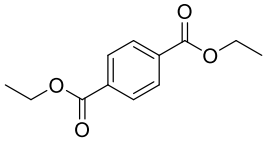

Diethyl terephthalate [636-09-9] (**20**): **Yield**: 47.3 mg, 63%; **^{1}H NMR** (300 MHz, $CDCl_3$) δ 8.08 (s, 4H), 4.39 (q, *J* = 7.1 Hz, 4H), 1.40 (t, *J* = 7.1 Hz, 6H); **^{13}C NMR** (75 MHz, $CDCl_3$) δ 165.8, 134.1, 129.4, 61.4, 14.3.

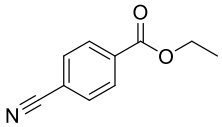

Ethyl 4-cyanobenzoate [7153-22-2] (**21**): **Yield**: 66.9 mg, 76%; **^{1}H NMR** (300 MHz, $CDCl_3$) δ 8.14 (d, *J* = 8.3 Hz, 2H), 7.74 (d, *J* = 8.3 Hz, 2H), 4.41 (q, *J* = 7.1 Hz, 2H), 1.41 (t, *J* = 7.1 Hz, 3H); **^{13}C NMR** (75 MHz, $CDCl_3$) δ 164.9, 134.3, 132.2, 130.1, 118.0, 116.2, 61.8, 14.2.

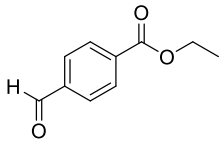

Ethyl 4-formylbenzoate [6287-86-1] (**22**): **Yield**: 83.1 mg, 93%; **^{1}H NMR** (300 MHz, $CDCl_3$) δ 8.19 (d, $J_{A\text{-}B}$ = 8.5 Hz, 2H), 8.15 (d, $J_{A\text{-}B}$ = 8.5 Hz, 2H), 4.42 (q, *J* = 7.1 Hz, 2H), 1.43 (t, *J* = 7.1 Hz, 3H); **^{13}C NMR** (75 MHz, $CDCl_3$) δ 171.2, 165.7, 135.1, 132.9, 130.1, 129.6, 61.6, 14.3.

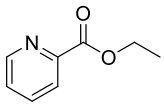

Ethyl picolinate [2524-52-9] (**23**): purified by flash chromatography ($CHCl_3$/MeOH, 95:5) **Yield**: 54.4 mg, 72%; **^{1}H NMR** (300 MHz, $CDCl_3$) δ 8.70 (d, *J* = 4.0 Hz, 1H), 8.07 (d, *J* = 7.8 Hz, 1H), 7.78 (t, *J* = 7.8 Hz, 1H), 7.47 – 7.37 (m, 1H), 4.42 (q, *J* = 7.1 Hz, 2H), 1.38 (t, *J* = 7.1 Hz, 3H); **^{13}C NMR** (75 MHz, $CDCl_3$) δ 165.1, 149.8, 148.1, 137.0, 126.8, 125.1, 61.9, 14.3.

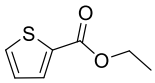

Ethyl thiophene-2-carboxylate [2810-04-0] (**24**): **Yield**: 62.3 mg, 80%; **^{1}H NMR** (400 MHz, $CDCl_3$) δ 7.70 (dd, *J* = 3.8, 1.2 Hz, 1H), 7.44 (dd, *J* = 5.0, 1.2 Hz, 1H), 6.99 (dd, *J* = 5.0, 3.8 Hz, 1H), 4.26 (q, *J* = 7.1 Hz, 2H), 1.28 (t, *J* = 7.1 Hz, 3H); **^{13}C NMR** (101 MHz, $CDCl_3$) δ 162.3, 134.1, 133.3, 132.2, 127.7, 61.1, 14.3.

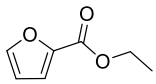

Ethyl furan-2-carboxylate [614-99-3] (**25**): **Yield**: 56.2 mg, 80%; **^{1}H NMR** (300 MHz, $CDCl_3$) δ 7.60 – 7.52 (m, 1H), 7.16 (d, *J* = 3.5 Hz, 1H), 6.49 (dd, *J* = 3.5, 1.7 Hz, 1H), 4.35 (q, *J* = 7.1 Hz, 2H), 1.36 (t, *J* = 7.1 Hz, 3H); **^{13}C NMR** (75 MHz, $CDCl_3$) δ 158.8, 146.2, 144.8, 117.8, 111.8, 61.0, 14.3.

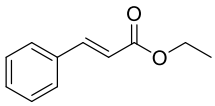

Ethyl cinnamate [4192-77-2] (**26**): **Yield**: 70.6 mg, 80%; **^{1}H NMR** (300 MHz, $CDCl_3$) δ 7.69 (d, *J* = 16.0 Hz, 1H), 7.51 (dd, *J* = 6.5, 2.9 Hz, 2H), 7.41 – 7.33 (m, 3H), 6.44 (d, *J* = 16.0 Hz, 1H), 4.26 (q, *J* = 7.1 Hz, 2H), 1.33 (t, *J* = 7.1 Hz, 3H); **^{13}C NMR** (75 MHz, $CDCl_3$) δ 167.0, 144.6, 134.4, 130.2, 128.9, 128.0, 118.2, 60.5, 14.3.

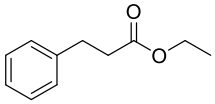

Ethyl 3-phenylpropanoate [2021-28-5] (**27**): **Yield**: 68,0 mg, 76%; **^{1}H NMR** (300 MHz, $CDCl_3$) δ 7.36 – 7.18 (m, 5H), 4.15 (qd, *J* = 7.1, 3.5 Hz, 2H), 3.02 – 2.92 (m, 2H), 2.64 (td, *J* = 7.8, 3.2 Hz, 2H), 1.25 (td, *J* = 7.1, 3.5 Hz, 3H); **^{13}C NMR** (75 MHz, $CDCl_3$) δ 172.9, 140.6, 128.5, 128.3, 126.2, 60.4, 36.0, 31.0, 14.2.

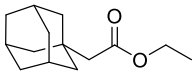

Ethyl 2-(adamantan-1-yl)acetate [15782-66-8] (**28**): **Yield**: 24.5 mg, 22%, **^{1}H NMR** (300 MHz, $CDCl_3$) δ 4.11 (q, *J* = 7.1, 2H), 2.06 (d, *J* = 5.7 Hz, 2H), 1.97 (s, 3H), 1.74 – 1.60 (m, 12H), 1.26 (t, *J* = 7.1 Hz, 3H); **^{13}C NMR** (75 MHz, $CDCl_3$) δ 171.8, 59.8, 49.0, 42.4, 36.8, 32.8, 28.6, 14.4.

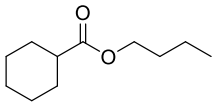

Butyl cyclohexanecarboxylate [6553-81-7] (**29**): **Yield**: 83.7 mg, 91%, **^{1}H NMR** (300 MHz, $CDCl_3$) δ 4.18 – 3.96 (m, 2H), 2.25 (tt, *J* = 11.1, 3.6 Hz, 1H), 1.94 – 1.51 (m, 6H), 1.48 – 1.14 (m, 7H), 0.90 (t, *J* = 7.3 Hz, 3H); **^{13}C NMR** (75 MHz, $CDCl_3$) δ 176.1, 63.9, 43.2, 30.7, 29.0, 25.8, 25.4, 19.1, 13.6.

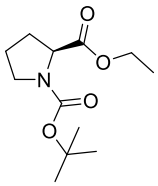

1-(*tert*-butyl)-2-ethyl-(*S*)-pyrrolidine-1,2-dicarboxylate [135097-23-3] (**30**): **Yield**: 64.4 mg, 53%, mixture of rotamers was described, **^{1}H NMR** (300 MHz, $CDCl_3$) δ 4.34 – 4.07 (m, 3H), 3.61 – 3.30 (m, 2H), 2.30 – 2.09 (m, 1H), 2.04 – 1.75 (m, 3H), 1.54 – 1.34 (m, 9H), 1.32 – 1.21 (m, 3H); **^{13}C NMR** (75 MHz, $CDCl_3$) δ 173.3, 153.9, 79;8, 77.2, 60.8, 59.2, 58.9, 46.5, 46.3, 30.9, 29.9, 28.4, 29.3, 24.3, 23.6, 14.3.

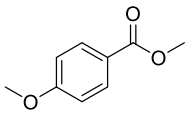

Methyl 4-methoxybenzoate [121-98-2] (**31**): **Yield**: 132.8 mg, 80%; **^{1}H NMR** (300 MHz, $CDCl_3$) δ 7.97 (d, *J* = 9.0 Hz, 2H), 6.88 (d, *J* = 9.0 Hz, 2H), 3.85 (s, 3H), 3.81 (s, 3H); **^{13}C NMR** (75 MHz, $CDCl_3$) δ 166.8, 163.3, 131.5, 122.5, 113.5, 55.3, 51.8.

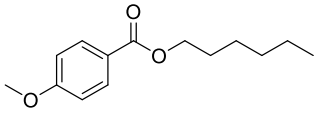

Hexyl 4-methoxybenzoate [81542-09-8] (**32**): **Yield**: 189.3 mg, 80%; **^{1}H NMR** (300 MHz, $CDCl_3$) δ 7.98 (d, *J* = 8.9 Hz, 2H), 6.89 (d, *J* = 8.9 Hz, 2H), 4.27 (t, *J* = 6.7 Hz, 2H), 3.82 (s, 3H), 1.80 – 1.66 (m, 2H), 1.50 – 1.38 (m, 2H), 1.36 – 1.25 (m, 4H), 0.89 (t, *J* = 6.9 Hz, 3H); **^{13}C NMR** (75 MHz, $CDCl_3$) δ 166.4, 163.2, 131.5, 122.9, 113.5, 64.8, 55.3, 31.5, 28.7, 25.7, 22.5, 14.0.

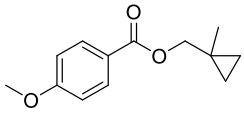

(1-methylcyclopropyl)methyl 4-methoxybenzoate (**33**): **Yield**: 190.5 mg, 86%; **^{1}H NMR** (300 MHz, $CDCl_3$) δ 8.01 (d, *J* = 8.9 Hz, 2H), 6.90 (d, *J* = 8.9 Hz, 2H), 4.08 (s, 2H), 3.82 (s, 3H), 1.19 (s, 3H), 0.58 – 0.47 (m, 2H), 0.46 – 0.35 (m, 2H); **^{13}C NMR** (75 MHz, $CDCl_3$) δ 166.4, 163.2, 131.5, 122.9, 113.5, 72.2, 55.3, 21.1, 15.4, 11.3; **HRMS** ESI-P (Q-TOF LiCl) *m/z* calcd. for $C_{13}H_{16}O_3$ $[MLi]^+$: 227.1259, found: 227.1258

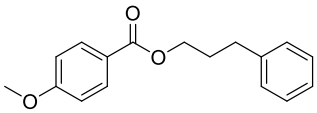

3-phenylpropyl 4-methoxybenzoate [104330-37-2] (**34**): **Yield**: 240.0 mg, 89%; **^{1}H NMR** (300 MHz, $CDCl_3$) δ 8.06 (d, *J* = 8.9 Hz, 2H), 7.39 – 7.31 (m, 2H), 7.29 – 7.21 (m, 3H), 6.96 (d, *J* = 8.9 Hz, 2H), 4.36 (t, *J* = 6.5 Hz, 2H), 3.86 (s, 3H), 2.83 (t, *J* = 7.6 Hz, 2H), 2.20 – 2.07 (m, 2H); **^{13}C NMR** (75 MHz, $CDCl_3$) δ 166.3, 163.4, 141.3, 131.6, 128.5, 128.5, 126.1, 122.8, 113.6, 64.0, 55.4, 32.4, 30.4.

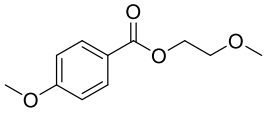

2-methoxyethyl 4-methoxybenzoate [5154-50-3] (**35**): **Yield**: 205.9 mg, 98%; **^{1}H NMR** (300 MHz, $CDCl_3$) δ 7.98 (d, *J* = 8.9 Hz, 2H), 6.87 (d, *J* = 8.9 Hz, 2H), 4.44 – 4.36 (m, 2H), 3.80 (s, 3H), 3.70 – 3.64 (m, 2H), 3.38 (s, 3H); **^{13}C NMR** (75 MHz, $CDCl_3$) δ 166.2, 163.4, 131.7, 122.4, 113.5, 70.6, 63.7, 59.0, 55.3.

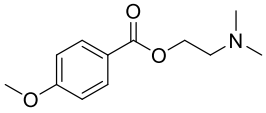

2-(dimethylamino)ethyl 4-methoxybenzoate [38152-19-1] (**36**): purified by flash chromatography (AcOEt/MeOH, 90:10) **Yield**: 224.2 mg, 99%; **^{1}H NMR** (300 MHz, $CDCl_3$) δ 7.94 (d, *J* = 8.8 Hz, 2H), 6.84 (d, *J* = 8.8 Hz, 2H), 4.34 (t, *J* = 5.8 Hz, 2H), 3.77 (s, 3H), 2.65 (t, *J* = 5.8 Hz, 2H), 2.28 (s, 6H); **^{13}C NMR** (75 MHz, $CDCl_3$) δ 166.2, 163.3, 131.6, 122.5, 113.5, 62.6, 57.8, 55.3, 45.7.

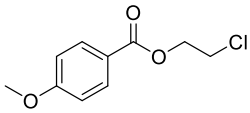

2-chloroethyl 4-methoxybenzoate [5452-06-2] (**37**): **Yield**: 77.6 mg, 53%; **^{1}H NMR** (300 MHz, $CDCl_3$) δ 8.02 (d, *J* = 8.9 Hz, 2H), 6.93 (d, *J* = 8.9 Hz, 2H), 4.59 – 4.49 (m, 2H), 3.87 (s, 3H), 3.85 – 3.77 (m, 2H); **^{13}C NMR** (75 MHz, $CDCl_3$) δ 165.9, 163.6, 131.8, 122.0, 113.7, 64.2, 55.4, 41.8.

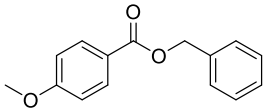

Benzyl 4-methoxybenzoate [6316-54-7] (**38**): **Yield**: 201.0 mg, 83%; **^{1}H NMR** (300 MHz, $CDCl_3$) δ 8.08 (d, *J* = 8.9 Hz, 2H), 7.51 – 7.35 (m, 5H), 6.94 (d, *J* = 8.9 Hz, 2H), 5.37 (s, 2H), 3.84 (s, 3H); **^{13}C NMR** (75 MHz, $CDCl_3$) δ 166.2, 163.5, 136.4, 131.8, 128.6, 128.2, 128.1, 122.6, 113.7, 66.4, 55.4.

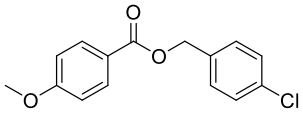

4-chlorobenzyl 4-methoxybenzoate [108939-24-8] (**39**): **Yield**: 221.7 mg, 80%; **^{1}H NMR** (300 MHz, $CDCl_3$) δ 8.03 (d, *J* = 9.0 Hz, 2H), 7.42 – 7.32 (m, 4H), 6.92 (d, *J* = 9.0 Hz, 2H), 5.30 (s, 2H), 3.86 (s, 3H); **^{13}C NMR** (75 MHz, $CDCl_3$) δ 166.0, 163.5, 134.8, 134.0, 131.7, 129.5, 128.8, 122.3, 113.7, 65.6, 55.4.

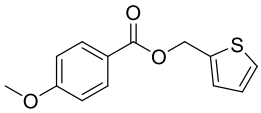

Thiophen-2-ylmethyl 4-methoxybenzoate (**40**): **Yield**: 210.6 mg, 85%; **^{1}H NMR** (300 MHz, $CDCl_3$) δ 8.03 (d, *J* = 8.9 Hz, 2H), 7.33 (dd, *J* = 5.1, 1.1 Hz, 1H), 7.17 (d, *J* = 3.4 Hz, 1H), 7.00 (dd, *J* = 5.1, 3.4 Hz, 1H), 6.91 (d, *J* = 8.9 Hz, 2H), 5.49 (s, 2H), 3.82 (s, 3H); **^{13}C NMR** (75 MHz, $CDCl_3$) δ 166.0, 163.5, 138.3, 131.8, 128.1, 126.8, 126.8, 122.3, 113.6, 60.8, 55.4; **HRMS** ESI-P (Q-TOF LiCl) *m/z* calcd. for $C_{13}H_{12}LiO_3S$ $[MLi]^+$: 255.0667, found: 255.0662.

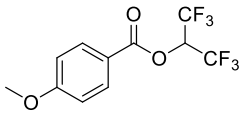

1,1,1,3,3,3-hexafluoropropan-2-yl 4-methoxybenzoate [1431386-96-7] (**41**): **Yield**: 72.0 mg, 26%; **^{1}H NMR** (300 MHz, $CDCl_3$) δ 8.08 (d, *J* = 9.0 Hz, 2H), 6.98 (d, *J* = 9.0 Hz, 2H), 6.01 (hept, J^{3}_{H-F} = 6.1 Hz, 1H), 3.90 (s, 3H); **^{13}C NMR** (75 MHz, $CDCl_3$) δ 164.8, 162.8, 132.7, 120.67 (q, J^{1}_{C-F} = 282.2 Hz), 118.9, 114.1, 66.7 (hept, J^{2}_{C-F} = 34.4 Hz), 55.6.

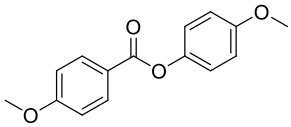

4-methoxyphenyl 4-methoxybenzoate [60127-34-6] (**42**): the product was contaminated by 10% of *O*-Boc-4-methoxyphenok, **Yield**: 45.1 mg, 35%, **^{1}H NMR** (300 MHz, $CDCl_3$) δ 8.24-8.06 (m, 2H), 7.17-7.06 (m, 2H), 7.02-6.95 (m, 2H), 6.95-6.89 (m, 2H), 3.89 (s, 3H), 3.82 (s, 3H); **^{13}C NMR** (75 MHz, $CDCl_3$) δ 163.8, 157.2, 144.5, 132.2, 130.0, 122.5, 122.0, 114.5, 113.8, 55.6, 55.5.

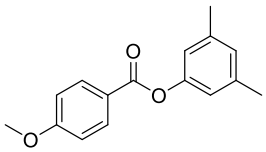

3,5-dimethylphenyl 4-methoxybenzoate (*Org. Biomol. Chem.*, **2016**, 14, 3869-3872) (**43**): **Yield**: 100.1 mg, 39%; **^{1}H NMR** (300 MHz, $CDCl_3$) δ 8.17 (d, *J* = 8.9 Hz, 2H), 7.00 (d, *J* = 8.9 Hz, 2H), 6.92 (s, 1H), 6.85 (s, 2H), 3.90 (s, 3H), 2.36 (s, 6H); **^{13}C NMR** (75 MHz, $CDCl_3$) δ 165.1, 163.8, 151.0, 139.3, 132.2, 127.5, 122.0, 119.4, 113.8, 55.5, 21.3.

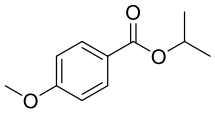

Isopropyl 4-methoxybenzoate [6938-38-1] (**44**): **Yield**: 133.4 mg, 69%; **^{1}H NMR** (300 MHz, $CDCl_3$) δ 7.98 (d, *J* = 8.9 Hz, 2H), 6.89 (d, *J* = 8.9 Hz, 2H), 5.21 (hept, *J* = 6.3 Hz, 1H), 3.83 (s, 3H), 1.34 (d, *J* = 6.3 Hz, 6H); **^{13}C NMR** (75 MHz, $CDCl_3$) δ 165.8, 163.1, 131.5, 123.3, 113.4, 67.9, 55.3, 22.0.

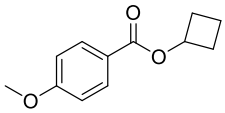

Cyclobutyl 4-methoxybenzoate (**45**): **Yield**: 195.5 mg, 95%; **^{1}H NMR** (300 MHz, $CDCl_3$) δ 7.97 (d, *J* = 8.9 Hz, 2H), 6.88 (d, *J* = 8.9 Hz, 2H), 5.24 – 5.10 (m, 1H), 3.81 (s, 3H), 2.49 – 2.35 (m, 2H), 2.26 – 2.10 (m, 2H), 1.90 – 1.75 (m, 1H), 1.66 (qd, *J* = 10.4, 5.2 Hz, 1H); **^{13}C NMR** (75 MHz, $CDCl_3$) δ 165.7, 163.3, 131.5, 122.8, 113.5, 69.0, 55.3, 30.4, 13.6; **HRMS** ESI-P (Q-TOF LiCl) *m/z* calcd. for $C_{12}H_{15}O_3$ $[MH]^+$: 207.1021, found: 207.1013.

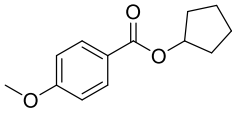

Cyclopentyl 4-methoxybenzoate [5421-02-2] (**46**): **Yield**: 149.4 mg, 68%; **^{1}H NMR** (300 MHz, $CDCl_3$) δ 7.96 (d, *J* = 8.9 Hz, 2H), 6.88 (d, *J* = 8.9 Hz, 2H), 5.41 – 5.32 (m, 1H), 3.82 (s, 3H), 2.02 – 1.88 (m, 2H), 1.88 – 1.73 (m, 4H), 1.70 – 1.55 (m, 2H); **^{13}C NMR** (75 MHz, $CDCl_3$) δ 166.1, 163.1, 131.4, 123.3, 113.4, 77.3, 55.3, 32.8, 23.8.

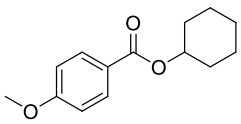

Cyclohexyl 4-methoxybenzoate [7464-48-4] (**47**): **Yield**: 153.3 mg, 65%; **^{1}H NMR** (300 MHz, $CDCl_3$) δ 7.99 (d, *J* = 8.9 Hz, 2H), 6.89 (d, *J* = 8.9 Hz, 2H), 5.05 – 4.93 (m, 1H), 3.82 (s, 3H), 1.98 – 1.86 (m, 2H), 1.83 – 1.70 (m, 2H), 1.64 – 1.28 (m, 6H); **^{13}C NMR** (75 MHz, $CDCl_3$) δ 165.7, 163.1, 131.5, 123.4, 113.4, 72.60, 55.3, 31.7, 25.5, 23.7.

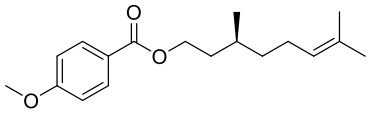

(*S*)-3,7-dimethyloct-6-en-1-yl 4-methoxybenzoate (**48**): **Yield**: 254.3 mg, 88%; **^{1}H NMR** (300 MHz, $CDCl_3$) δ 7.98 (d, *J* = 8.9 Hz, 2H), 6.89 (d, *J* = 8.9 Hz, 2H), 5.09 (t, *J* = 7.1 Hz, 1H), 4.39 – 4.25 (m, 2H), 3.82 (s, 3H), 2.09 – 1.91 (m, 2H), 1.85 – 1.73 (m, 1H), 1.67 (s, *J* = 9.6 Hz, 3H), 1.71 – 1.47 (m, 2H), 1.59 (s, 3H), 1.46 – 1.32 (m, 1H), 1.30 – 1.15 (m, 1H), 0.96 (d, *J* = 6.4 Hz, 3H); **^{13}C NMR** (75 MHz, $CDCl_3$) δ 166.3, 163.2, 131.5, 131.2, 124.6, 122.9, 113.5, 63.1, 55.3, 37.0, 35.5, 29.5, 25.7, 25.4, 19.5, 17.6; **HRMS** ESI-P (Q-TOF LiCl) *m/z* calcd. for $C_{18}H_{27}O_3$ $[M]^+$: 291.1960, found: 291.1975.

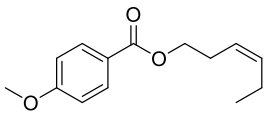

(Z)-hex-3-en-1-yl 4-methoxybenzoate (**49**): **Yield**: 189 mg, 81%; **^{1}H NMR** (300 MHz, $CDCl_3$) δ 7.98 (d, *J* = 8.9, 2H), 6.89 (d, *J* = 8.9 Hz, 2H), 5.66 – 5.31 (m, 2H), 4.27 (t, *J* = 6.9 Hz, 2H), 3.82 (s, 3H), 2.55 – 2.37 (m, 2H), 2.23 – 1.93 (m, 2H), 0.96 (t, *J* = 7.5 Hz, 3H); **^{13}C NMR** (75 MHz, $CDCl_3$) δ 166.3, 163.3, 134.5, 131.5, 123.8, 122.8, 113.5, 64.1, 55.3, 26.9, 20.6, 14.2; **HRMS** ESI-P (Q-TOF LiCl) *m/z* calcd. for $C_{14}H_{18}LiO_3$ $[MLi]^+$: 241.1416, found: 241.1409.

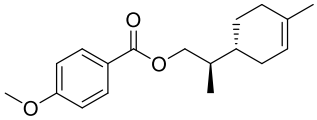

(*R*)-2-((*R*)-4-methylcyclohex-3-en-1-yl)propyl 4-methoxybenzoate (**50**): The product was obtained as a mixture of diastereoisomeres which was already contained in the initial alcohol. **Yield**: 236.5 mg, 82%; **^{1}H NMR** (300 MHz, $CDCl_3$) δ 7.98 (d, *J* = 8.9 Hz, 2H), 6.89 (d, *J* = 8.9 Hz, 2H), 5.36 (s, 1H), 4.28 (ddd, *J* = 10.8, 5.5, 1.9 Hz, 1H), 4.14 (dd, *J* = 10.8, 6.9 Hz, 1H), 3.81 (s, 3H), 2.10 – 1.92 (m, 3H), 1.91 – 1.72 (m, 3H), 1.62 (s, 4H), 1.45 – 1.24 (m, 1H), 1.00 (t, J = 6.8 Hz, 3H); **^{13}C NMR** (75 MHz, $CDCl_3$) δ 166.4, 163.2, 133.9, 133.9, 131.5, 122.9, 120.6, 120.5, 113.5, 67.9, 67.7, 55.3, 37.0, 37.0, 35.8, 35.7, 30.6, 30.5, 29.6, 28.0, 27.0, 25.7, 23.4, 14.2, 13.9; **HRMS** ESI-P (Q-TOF LiCl) *m/z* calcd. for $C_{18}H_{24}O_3Li$ $[MLi]^+$: 295.1880, found: 295.1876.

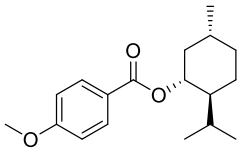

(1*R*,2*S*,5*R*)-2-isopropyl-5-methylcyclohexyl 4-methoxybenzoate [50465-27-5] (**51**): **Yield**: 140.8 mg, 49%; **^{1}H NMR** (300 MHz, $CDCl_3$) δ 8.00 (d, *J* = 8.9 Hz, 2H), 6.91 (d, *J* = 8.9 Hz, 2H), 4.90 (td, *J* = 10.8, 4.4 Hz, 1H), 3.84 (s, 3H), 2.12 (d, *J* = 11.5 Hz, 1H), 1.96 (dtd, *J* = 13.9, 6.9, 2.7 Hz, 1H), 1.72 (d, *J* = 11.5 Hz, 2H), 1.62 – 1.45 (m, 3H), 1.22 – 1.02 (m, 2H), 0.92 (dd, *J* = 6.9, 2.7 Hz, 6H), 0.79 (d, *J* = 6.9 Hz, 3H); **^{13}C NMR** (75 MHz, $CDCl_3$) δ 165.8, 163.2, 131.5, 123.3, 113.5, 74.4, 55.4, 47.3, 41.0, 34.3, 31.4, 26.5, 23.7, 22.1, 20.8, 16.6.

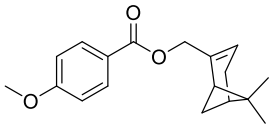

((1*R*,5*S*)-6,6-dimethylbicyclo[3.1.1]hept-2-en-2-yl)methyl 4-methoxybenzoate (**52**): **Yield**: 122.6 mg, 43%; **^{1}H NMR** (300 MHz, $CDCl_3$) δ 7.99 (d, *J* = 8.9 Hz, 2H), 6.91 (d, *J* = 8.9 Hz, 2H), 5.68 – 5.60 (m, 1H), 4.66 (d, *J* = 1.3 Hz, 2H), 3.84 (s, 3H), 2.42 (dt, *J* = 8.7, 5.6 Hz, 1H), 2.30 (d, *J* = 8.7 Hz, 2H), 2.24 – 2.17 (m, 1H), 2.12 (s, 1H), 1.29 (s, 3H), 1.23 (d, J = 8.7 Hz, 1H), 0.87 (s, 3H); **^{13}C NMR** (75 MHz, $CDCl_3$) δ 166.2, 163.3, 143.2, 131.6, 122.8, 121.4, 113.6, 67.2, 55.4, 43.6, 40.7, 38.1, 31.5, 31.3, 26.2, 21.2; **HRMS** ESI-P (Q-TOF LiCl) *m/z* calcd. for $C_{18}H_{22}LiO_3$ $[MLi]^+$: 293.1729, found: 293.1738.

Part II. Development of new cobalt catalysts with dipyrromethene ligands

Synthesis of pyrroles

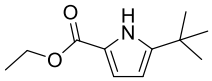

Synthesis of Ethyl 5-*tert*-butyl-1H-pyrrole-2-carboxylate [125261-17-8] (**7**): In a 2 L round-bottom flask under nitrogen atmosphere, ethyl pyrrole-2-carboxylate (20 g, 0.144 mol, 1.0 equiv.) was solubilized in DCE (1.2 L). $AlCl_3$ (40.3 g, 0.29 mol, 2.1 equiv.) was added in one portion, followed by *tert*-butyl chloride (15.8 mL, 0.14 mmol, 1.0 equiv.). The reaction medium was stirred at room temperature for 2 hours. Then the reaction medium was neutralized with $NaHCO_{3\ aq.\ sat.}$ and extracted with Et_2O. The aqueous phase was extracted twice with Et_2O, and the organic phases were reunited, dried over $MgSO_4$, filtered and evaporated. The raw product obtained is dried under vacuum and did not undergo any further purification. The product was obtained as a brown solid. **Yield**: 28 g, 99%. **^{1}H NMR** (300 MHz, $CDCl_3$): δ 9.07 (s, 1H), 6.82 (dd, *J* = 3.7, 2.6 Hz, 1H), 6.01 (dd, *J* = 3.7, 2.6 Hz, 1H), 4.31 (q, *J* = 7.1 Hz, 2H), 1.39 – 1.29 (m, 12H).

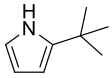

Synthesis of 2-*tert*-butyl pyrrole [5398-58-3] (**4**): In a 500 round-bottom flask, **7** (14 g, 71.7 mmol, 1.0 equiv.) and NaOH (14.3 g, 358.5 mmol, 5.0 equiv.) were solubilized in ethylene glycol (140 mL) and the reaction medium was then refluxed at 200 °C for 6 hours. The reaction medium was then cooled at room temperature, diluted with water (170 mL) and extracted with DCM. The organic phase was dried over MgSO4, filtered and evaporated. The raw product **4** was obtained as a crystalline light-brown solid. **Yield**: 6.08 g, 69%. **^{1}H NMR** (300 MHz, $CDCl_3$): δ 8.02 (s, 1H), 6.71 (td, *J* = 2.7, 1.7 Hz, 1H), 6.16 (q, *J* = 2.7 Hz, 1H), 5.98 (td, *J* = 3.2, 1.7 Hz, 2H), 1.33 (s, 9H).

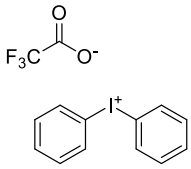

Synthesis of diphenyliodonium triflate [66003-76-7] (**8**): In a 250 mL round-bottom flask, mCPBA (11.1 g, 43 mmol) was solubilized in DCM (150 mL). Iodobenzene (4.3 mL, 38 mmol) was then added, followed by benzene (3.8 mL, 43 mmol). Triflic acid (10 mL, 114 mmol) was then added dropwise to the round-bottom flask. The reaction medium was stirred at room temperature during 10 minutes and then evaporated. The residue was suspended in Et_2O and the solution was stored for 1 hour at +4 °C. The solid was filtered, washed with Et_2O and dried under air. The product is obtained as a beige solid. **Yield**: 15.8 g, 97%. **^{1}H NMR** (300 MHz, DMSO-d6): δ 8.26 (d, *J* = 7.6 Hz, 2H), 7.68 (t, *J* = 7.4 Hz, 2H), 7.54 (dd, *J* = 7.6, 7.4 Hz, 2H).

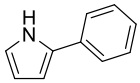

Synthesis of 2-phenylpyrrole [3042-22-6] (**6**): A 250 mL round-bottom flask was charged with NaOH (20.7 mmol, 830 mg), **8** (13.8 mmol, 5.9 g) and pyrrole (75 mL). The reaction medium was stirred at 80 °C overnight and then evaporated under vacuum to recover the excess of pyrrole. The residue was diluted in ethyl acetate and washed with $NaCl_{aq.sat.}$ and water. The organic solution was dried with $MgSO_4$ and evaporated. The crude product was then purified by flash

chromatography. 2-phenylpyrrole was obtained pure as a beige solid. **Yield**: 1.32 g, 67%. **^{1}H NMR** ($CDCl_3$, 300 MHz): δ 8.45 (s, 1H), 7.49 (dd, *J* = 8.2 Hz, 1.2 Hz, 2H), 7.41 – 7.34 (m, 2H), 7.22 (tt, *J* = 6.7, 1.2 Hz, 1H), 6.88 (td, *J* = 2.7, 1.5 Hz, 1H), 6.54 (ddd, *J* = 4.0, 2.7, 1.5 Hz, 1H), 6.32 (q, *J* = 2.7 Hs, 1H).

Dipyrromethenes syntheses

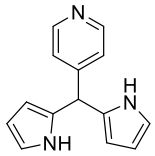

Synthesis of 5-(4-pyridyl)dipyrromethane [52073-75-3] (**1**): In a 250 mL Schlenk tube, 4-pyridinecarboxaldehyde (2.9 mL, 31.0 mmol, 1.0 equiv.) was mixed with pyrrole (30 mL, 434 mmol, 14 equiv.) and the reaction medium was stirred at 90 °C overnight. The excess of pyrrole was then evaporated under vacuum and the residue was purified through chromatography on alumina (DCM/AcOEt, 100:0 to 0:100) to afford product **1** as a grey solid. **Yield**: 3.15 g, 45%. **^{1}H NMR** (300 MHz, $CDCl_3$) δ 8.51 (d, *J* = 6.0 Hz, 2H), 8.07 (s, 2H), 7.14 (d, *J* = 6.0 Hz, 2H), 6.74 (q, *J* = 2.5 Hz, 2H), 6.18 (q, *J* = 2.5 Hz, 2H), 5.90 (s, 2H), 5.46 (s, 1H).

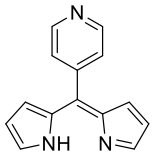

Synthesis of 5-(4-pyridyl)dipyrromethene (**2**): In a 100 mL round-bottom flask, **1** (223 mg, 1 mmol, 1.0 equiv.) was solubilized in DCM (15 mL). MnO_2 (435 mg, 5.0 mmol, 5.0 equiv.) was added and the reaction medium was stirred at 40°C overnight. The reaction medium was filtered over a pad of silica and the resulting solution was evaporated, affording **2** as a brown solid. **Yield**: 182 mg, 82%. **^{1}H NMR** (300 MHz, $CDCl_3$): δ 8.73 (dd, *J* = 4.4, 1.6 Hz, 2H), 7.68 (s, 2H), 7.42 (dd, *J* = 4.4, 1.6 Hz, 2H), 6.52 (dd, *J* = 4.2, 0.9 Hz, 2H), 6.42 (dd, *J* = 4.2, 1.4 Hz, 2H); **^{13}C NMR** (75 Hz, $CDCl_3$) δ 149.3, 145.2, 144.6, 140.1, 138.1, 128.2, 125.2, 118.3.

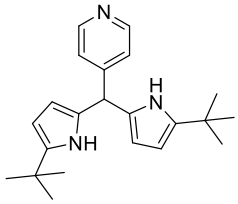

Synthesis of 1,9-di-*tert*-butyl-5-(4-pyridyl)dipyrromethane (**10**): In a 250 mL Schlenk tube, and 4-pyridinecarboxaldehyde (0.4 mL, 4.25 mmol, 1.0 equiv.) and **4** (6.08 g, 49.4 mmol, 11.6 equiv.) were heated at 90 °C under stirring overnight. The reaction medium was then cooled at room temperature, diluted with DCM and chromatographed on alumina (DCM/AcOEt, 100:0 to 80/20). The product fraction and the pyrrole fraction were collected and evaporated. The crude product of the pyrrole fraction was sublimated to recover the excess of **4** (1.26 g, 10.2 mmol, 21%). The product fraction was evaporated to afford **10** as a yellow solid. **Yield**: 827 mg, 58%. **^{1}H NMR** (300 MHz, DMSO-d6) δ 10.31 (s, 2H), 8.45 (d, *J* = 5.7 Hz, 2H), 7.06 (d, *J* = 5.7 Hz, 2H), 5.58 (t, *J* = 2.8 Hz, 2H), 5.39 (t, *J* = 2.8 Hz, 2H), 5.31 (s, 1H), 1.20, (s, 18H).

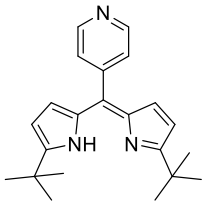

Synthesis of 1,9-di-*tert*-butyl-5-(4-pyridyl)dipyrromethene (**3**): In a 250 mL round-bottom flask, **10** (400 mg, 1.19 mmol, 1.0 equiv.) was solubilized in a mixture DCM/toluene (40 mL/30 mL) and DDQ (298 mg, 1.31 mmol, 1.1 equiv.) was added. The reaction medium was stirred overnight at room temperature and then filtered. The resulting solution was purifying by chromatography to afford **3** as a dark yellow solid. **Yield**: 143 mg, 36%. **^{1}H NMR** (300 MHz, CD_2Cl_2) δ 8.71 (d, *J* = 5.0 Hz, 2H), 7.48 – 7.37 (m, 2H), 6.47 (d, *J* = 4.2

Hz, 2H), 6.36 (d, *J* = 4.2 Hz, 2H), 1.43 (s, 18H); **^{13}C NMR** (75 MHz, CD_2Cl_2) δ 167.2, 149.2, 145.1, 138.4, 135.4, 127.7, 125.3, 114.7, 33.35, 29.5.

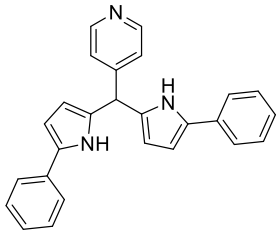

Synthesis of 1,9-diphenyl-5-(4-pyridyl)dipyrromethane (**11**): In a 100 mL round-bottom flask, 4-pyridinecarboxaldehyde (158 µL, 1.68 mmol, 1.0 equiv.) and **6** (1.2 g, 8.38 mmol, 5.0 equiv.) were suspended in toluene (893 µL, 8.38 mmol, 5.0 equiv.) and the mixture was stirred at 90 °C overnight. The solvent was then evaporated and the raw product was purified by chromatography on basic alumina (DCM/AcOEt, 100:0 to 60:40) to give **11** as a fuchsia solid. **Yield**: 580 mg, 92%. **^{1}H NMR** (300 MHz, $CDCl_3$) δ 8.58 – 8.51 (m, 2H), 7.45 – 7.40 (m, 4H), 7.36 – 7.29 (m, 6H), 7.22 – 7.15 (m, 4H), 6.50 – 6.44 (m, 2H), 5.96 (t, *J* = 2.8Hz, 2H), 5.52 (s, 1H); **^{13}C NMR** (75 MHz, $CDCl_3$) δ 150.9, 149.8, 132.5, 132.4, 131.7, 128.9, 126.3, 123.7, 109.8, 106.2, 43.8.

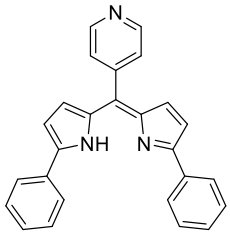

Synthesis of 1,9-diphenyl-5-(4-pyridyl)dipyrromethene (**5**): **Oxidation with DDQ**: In a 50 mL round-bottom flask, **11** (580 mg, 1.54 mmol, 1.0 equiv.) was solubilized in a mixture $CHCl_3$/toluene (38 mL/6 mL) and DDQ (420 mg, 1.85 mmol, 1.2 equiv.) was added. The mixture was then stirred at room temperature for 1 hour. The reaction medium was filtered on a pad of celite® and the pad was washed with $CHCl_3$. The resulting solution was evaporated. The crude product was then purified by chromatography on silica (petroleum ether/AcOEt, 90:10 to 0:100) to afford **5** as a fuchsia solid. **Yield**: 86,7 mg, 15%. **Oxidation with MnO_2**: In a 100 mL Schlenk tube, **11** (708 mg, 1.89 mmol, 1.0 equiv.) was solubilized in DCM (30 mL). MnO_2 (822 mg, 9.45 mmol, 5.0 equiv.) was added and the reaction mixture was stirred at 40 °C for 24 hours. The reaction medium was cooled to room temperature and filtered on a pad of celite®. The collected solution was evaporated, and **5** was obtained as a fushia/green solid. **Yield**: 474 mg, 67%. **^{1}H NMR** (300 MHz, $CDCl_3$) δ 8.76 (dd, *J* = 4.4 Hz, 2H), 7.97 – 7.90 (m, 4H), 7.55 – 7.41 (m, 8H), 6.87 (d, *J* = 4.3 Hz, 2H), 6.65 (d, *J* = 4.3 Hz, 2H); **^{13}C NMR** (75 MHz, $CDCl_3$) δ 154.9, 145.3, 141.1, 135.7, 132.8, 129.3, 129.2,129.1, 126.3, 125.4, 123.8, 116.3.

Tests of cobalt complexation

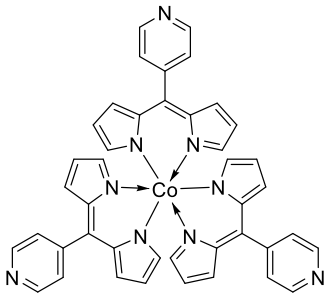

Synthesis of *tris*(5-(4-pyridyl)dipyrrin)cobalt(III) complex (**12**): In a 20 mL tube, **2** (1.33 g, 6.0 mmol, 3.0 equiv.) was solubilized in DCM (6 mL). A solution of $CoCl_2$ (260 mg, 2.0 mmol, 1.0 equiv.) in ACN (6 mL) was then added and the reaction mixture was then stirred at room temperature overnight. A precipitate was formed. The reaction medium was filtered and the solid was washed with Et_2O.

Mass spectrum:

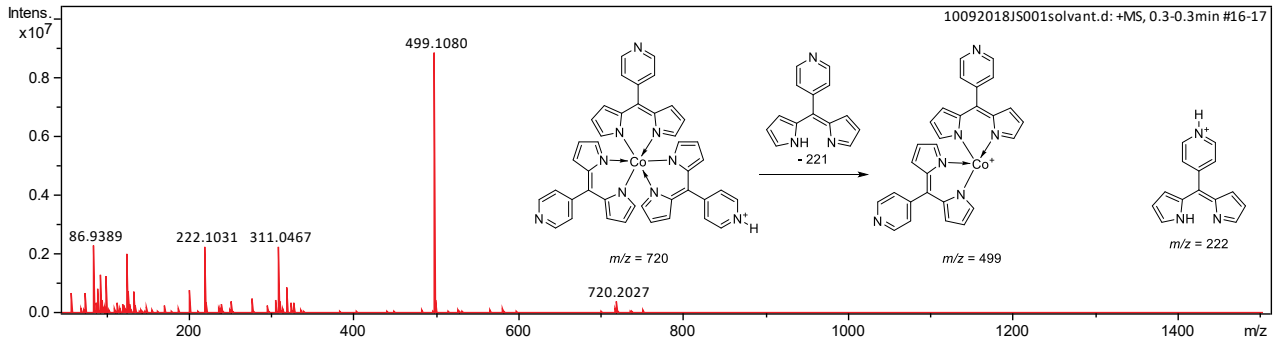

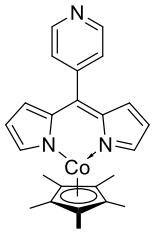

Synthesis of (pentamethylcyclopentadienyl)(5-(4-pyridyl)dipyrrin)cobalt(II) complex (**13**): In glovebox. In a 50 mL flask, $[Cp^*CoCl]_2$ (160 mg, 0.350 mmol) was solubilized in 5 mL ACN. A solution of **2** (155 mg, 0.700 mmol) in 5 mL ACN was then added dropwise. The reaction medium was stirred at room temperature for 2 hours and then stored at +4 °C overnight. Red crystals formed. The reaction medium was filtered and stored again at +4 °C overnight for new crystallization. This procedure was reproduce a third time, to finally obtained, after having brought each lot of crystals together, 167 mg of **13** as red crystals suitable for X-Ray diffraction. **Yield**: 167 mg, 58%.

Crystallographic data:

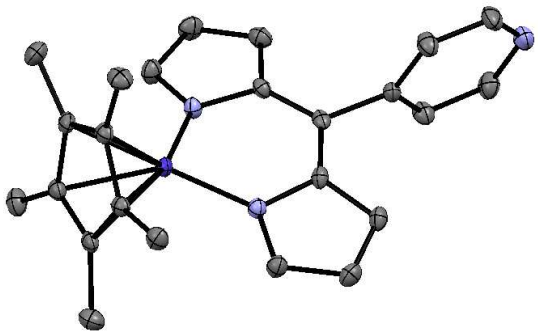

Molecular formula	'$C_{24}H_{25}CoN_3$'	a(Å)	6.8489(2)
Molecular weight	414.40	b(Å)	9.6733(3)
Crystal habit	red blue plate	c(Å)	15.3536(5)
Crystal dimensions(mm)	0.300x0.260x0.020	a(°)	84.828(2)
Crystal system	triclinic	b(°)	89.915(2)
Space group	P -1	g(°)	74.369(2)
		V(Å^3)	975.32(5)

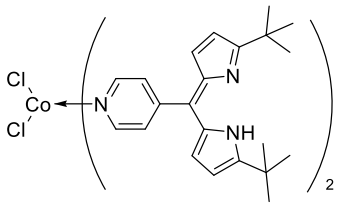

Synthesis of complex 14: In a 5 mL flask, $CoCl_2$ (64.9 mg, 0.5 mmol, 1.0 equiv.) was solubilized in ACN (2 mL). A solution of **3** (167 mg, 0.5 mmol, 1.0 equiv.) was then added dropwise. A green precipitate appeared The reaction medium was stored at +4 °C overnight. Green crystals, suitable for X-ray diffraction, appeared.

Crystallographic data:

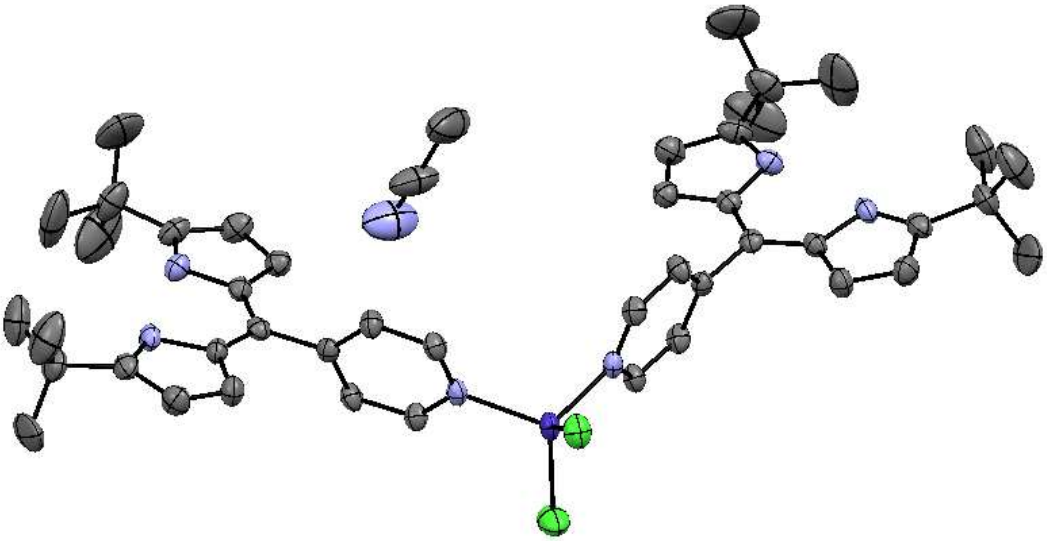

Molecular formula	'$C_{44}H_{54}Cl_2CoN_6$, 2(C_2H_3N)'	a(Å)	46.597(3)
Molecular weight	878.87	b(Å)	10.0778(4)
Crystal habit	green needle	c(Å)	10.6919(6)
Crystal dimensions(mm)	0.400x0.060x0.060	a(°)	90
Crystal system	orthorhombic	b(°)	90
Space group	C m c 21	g(°)	90
		V(Å3)	5020.9(5)V(Å3)

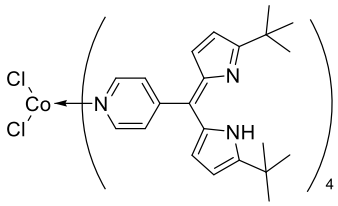

Synthesis of 15: in a 100 mL round-bottom flask, **14** was solubilized in ACN (20 mL) and the solution was left open-flask for slow evaporation. After a week, the solvent was completely evaporated, and red crystals, suitable for X-Ray diffraction, appeared in the flask.

Crystallographic data:

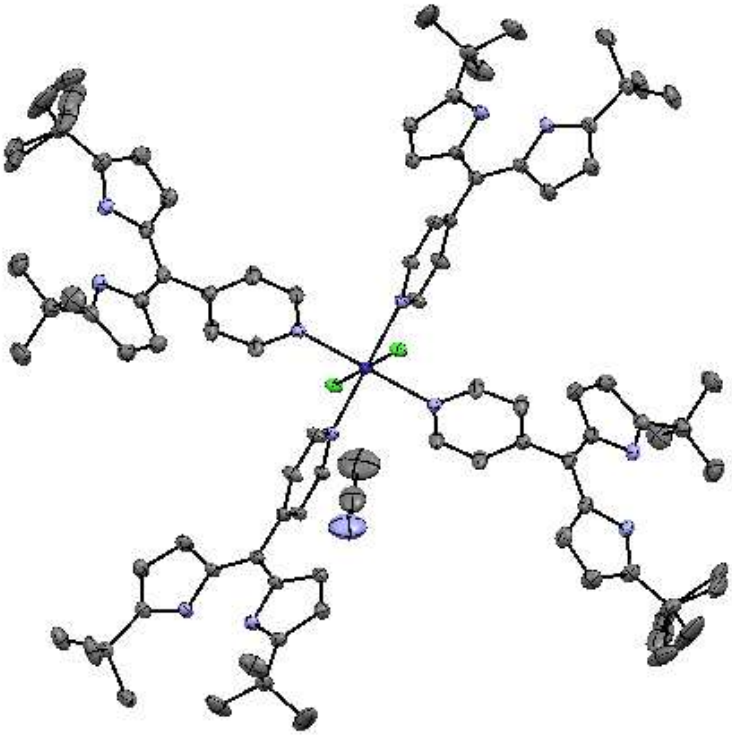

Molecular formula	'C88 H108 Cl2 Co N12,	a(Å)	14.8193(5)
2(C2 H3 N)'		b(Å)	11.2740(3)
Molecular weight	1545.80	c(Å)	26.7475(9)
Crystal habit	orange needle	a(°)	90
Crystal dimensions(mm)	0.320x0.260x0.120	b(°)	94.838(2)
Crystal system	monoclinic	g(°)	90
Space group	P 21/n	V(Å3)	4452.9(2)

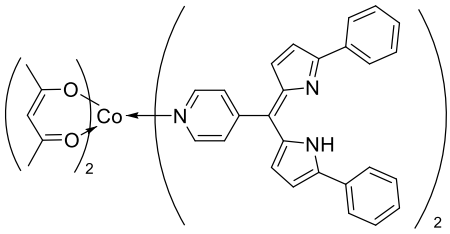

Synthesis of complex 16: In a 5 mL flask, $Co(acac)_2$ (35 mg, 0.14 mmol, 1.0 equiv.) was solubilized in THF (1 mL). A solution of **5** (50 mg, 0.13 mmol, 1.0 equiv.) was then added dropwise. The reaction medium was stirred at room temperature for 3 hours, and then stored at +4 °C overnight. Dark crystals, suitable for X-ray diffraction, appeared.

Crystallographic data:

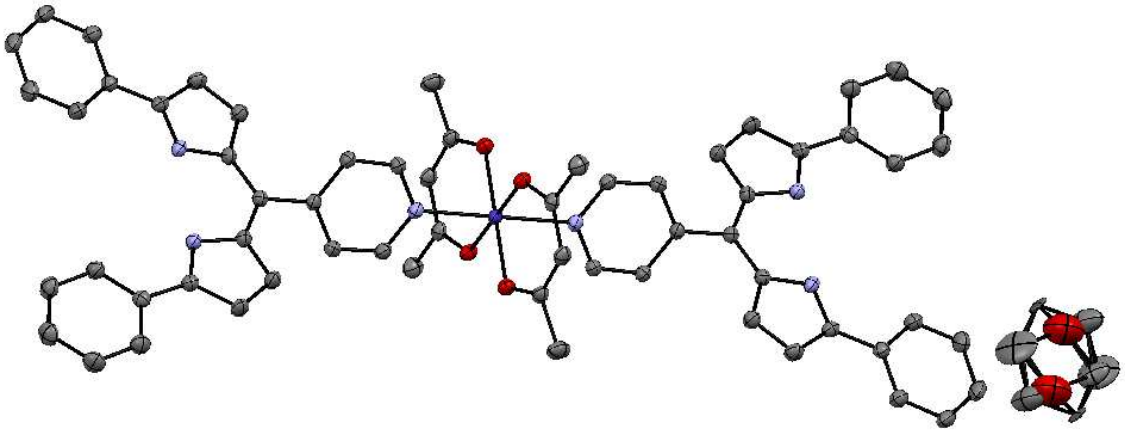

Molecular formula 'C_{62} H_{52} Co N_6 O_4, C_4 H_8 O'	a(Å) 7.8713(4)
Molecular weight 1076.13	b(Å) 11.8319(6)
Crystal habit black block	c(Å) 15.2066(7)
Crystal dimensions(mm) 0.400x0.220x0.200	α(°) 98.184(1)
Crystal system triclinic	β(°) 103.247(1)
Space group P -1	γ(°) 98.606(1)
	V(Å^3) 1339.87(11)

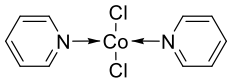

Synthesis of complex 17: In a 100 mL round-bottom flask, $CoCl_2$ (1.3 g, 10.0 mmol, 1.0 equiv.) was solubilized in ACN (30 mL). Pyridine (1.61 mL, 20.0 mL, 2.0 equiv.) was then added to the solution and the reaction medium was stirred at room temperature for 2 hours. A blue precipitate appeared. The reaction medium was filtered and the solid was washed with Et_2O. the blue solid turned then to purple and was dried under vacuum. Suitable crystals for X-ray diffraction were obtained by slow diffusion Et_2O into a solution of the product in ACN. The structure of **17** has been confirmed by comparison of the cell parameters in the database.

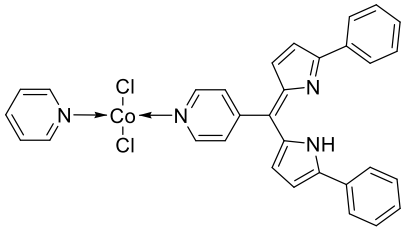

Synthesis of complex 18: In a 5 mL flask, **17** (46 mg, 0.16 mmol, 1.0 equiv.) was solubilized in THF (1 mL). A solution of **5** (60 mg, 0.16 mmol, 1.0 equiv.) was then added dropwise. The reaction medium was stirred at room temperature for 3 hours, and then stored at +4 °C overnight. Dark crystals, suitable for X-ray diffraction, appeared. **Yield**: 45 mg, 48%

Crystallographic data:

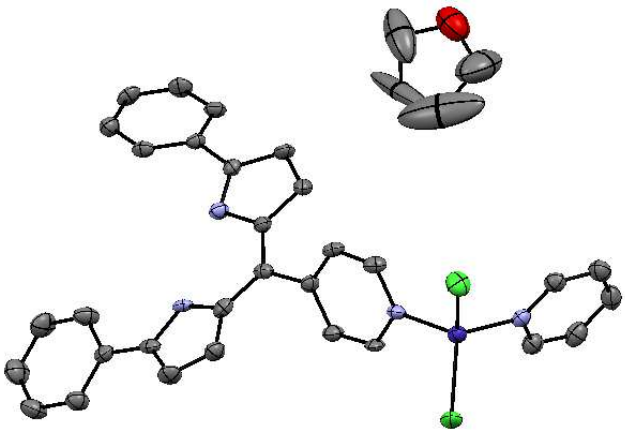

Molecular formula 'C_{31} H_{24} Cl_2 Co N_4, C_4 H_8 O'	a(Å) 7.9752(10)
Molecular weight 654.47	b(Å) 12.4381(17)
Crystal habit black plate	c(Å) 16.951(3)
Crystal dimensions(mm) 0.100x0.080x0.010	α(°) 83.851(5)
Crystal system triclinic	β(°) 81.963(4)
Space group P -1	γ(°) 72.426(8)
	V(Å^3) 1583.5(4)

Synthesis of complex [Ru(dmso)$_4$Cl$_2$] (**20**): In a 50 mL Schlenk tube, $RuCl_3$•xH_2O (1.0 g) was solubilized in DMSO (5 mL) and stirred at 180 °C for 5 minutes. The reaction medium was then cooled to room temperature, diluted with acetone (20 mL) and stored at +4 °C overnight. A yellow precipitate formed. The solution was filtered and **20** was obtained as a yellow crystalline solid. **Yield**: 1.01 g.

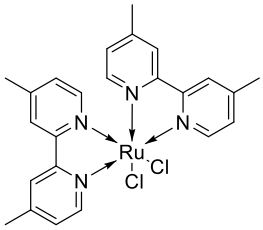

Synthesis of *bis*(4,4'-dimethyl-2,2'-bipyridine)ruthenium(II) dichloride (**19**): In a Schlenk tube, **20** (1.01 g, 2.08 mmol, 1.0 equiv.), 4,4'-dimethyl-2,2'-bipyridine (806 mg, 4.38 mmol, 2.1 equiv.) and LiCl (4.6g, 109 mmol, 52 equiv.) were suspended in degassed DMF (23 mL). The mixture was then stirred at 150 °C for 4 hours. The reaction medium was cooled at room temperature, diluted with acetone (100 mL) and stored overnight at +4 °C. The solution was filtered and the solid was washed with water and Et_2O. The solid was then dried under vacuum. **19** was obtained as a black solid.

Yield: 381 mg, 34%. **1H NMR** (300 MHz, DMSO-d6) δ 9.77 (d, *J* = 6.0 Hz, 2H), 8.50 – 8.44 (m, 2H), 8.35 – 8.29 (m, 2H), 7.59 (d, *j* = 6.3 Hz, 2H), 7.31 (d, *J* = 6.0 Hz, 2H), 6.92 (d, *J* = 6.3 Hz, 2H), 2.62 (s, 6H), 2.34 (s, 6H).

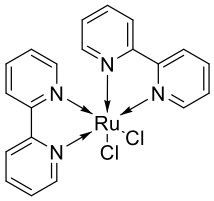

Synthesis of *bis*(2,2'-bipyridine)ruthenium(II) dichloride (**21**): In a Schlenk tube, **20** (400 mg, 0.83 mmol, 1.0 equiv.), 2,2'-bipyridine (270 mg, 1.73 mmol, 2.1 equiv.) and LiCl (1.82 g, 43.0 mmol, 51 equiv.) were suspended in degassed DMF (9 mL). The mixture was then stirred at 150 °C for 4 hours. The reaction medium was cooled at room temperature, diluted with acetone (40 mL) and stored overnight at +4 °C. The solution was filtered and the solid was washed with water and Et_2O. The solid was then dried under vacuum. **21** was obtained as a black solid. **Yield**: 287 mg, 71%. **^{1}H NMR** (300 MHz, DMSO-d6) δ 9.97 (d, *J* = 5.0 Hz, 2H), 8.64 (d, *J* = 8.0 Hz, 2H), 8.49 (d, *J* = 8.1 Hz, 2H), 8.07 (td, *J* = 8.1, 1.4 Hz, 2H), 7.81 – 7.74 (m, 2H), 7.72 – 7.64 (m, 2H), 7.52 (d, *J* = 5.5 Hz, 2H), 7.14 – 7.07 (m, 2H).

Complexation reaction between 2 and 21: In a 20 mL tube, **2** (131 mg, 0.59 mmol, 1.0 equiv.) and **21** (287 mg, 0.59 mmol, 1.0 equiv.) were solubilized in EtOH (15 mL) with triethylamine (0.5 mL). The reaction medium was stirred overnight at 100 °C. The reaction mixture was then cooled to room temperature and a solution of NH_4PF_6 (967 mg, 5.9 mmol, 10 equiv.) in EtOH (2 mL) was added. The reaction mixture was stirred at room temperature for 1 hour and then stored at +4 °C overnight. The resulting solution was filtered and the solid obtained was washed with water and ethanol. The black solid obtained gave unclear ^{1}H NMR. Mass spectroscopy revealed the presence of different products: **22** and **23.**

<u>Mass spectrum:</u>

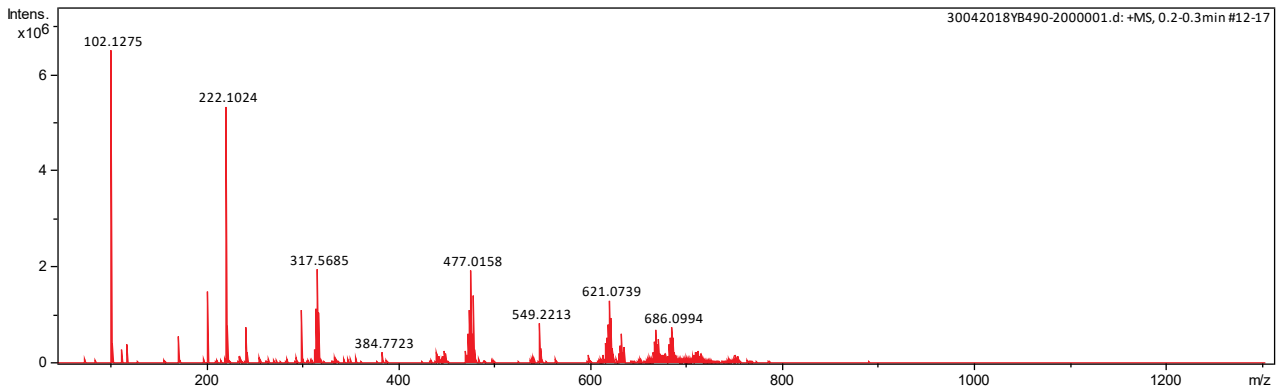

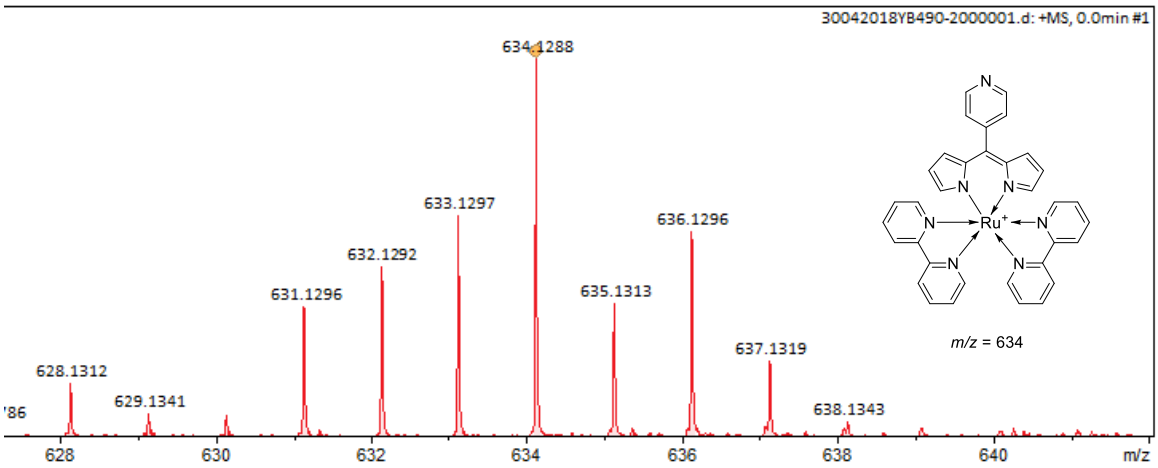
30042018YB490-2000001.d: +MS, 0.0min #1
634.1288
633.1297
632.1292
631.1296
636.1296
635.1313
637.1319
628.1312
629.1341
638.1343
m/z = 634
m/z

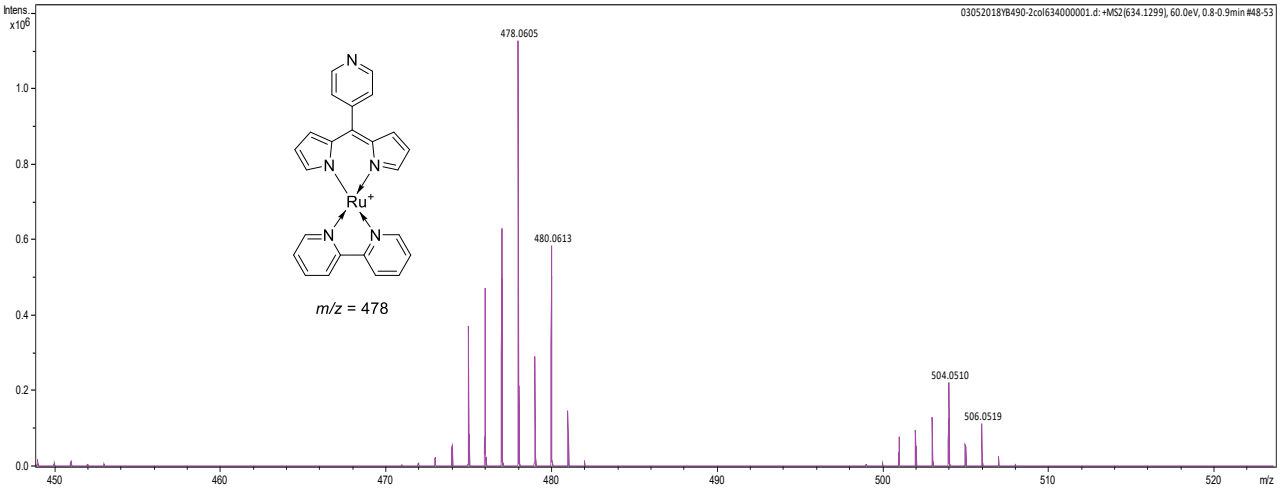
Intens.
x10^6
478.0605
480.0613
504.0510
506.0519
m/z = 478
m/z

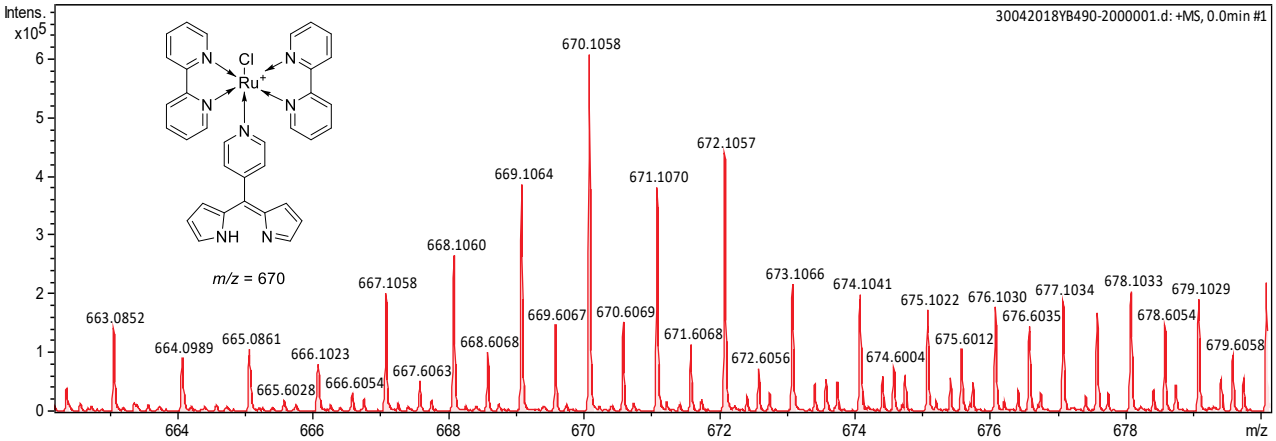
Intens.
x10^5
30042018YB490-2000001.d: +MS, 0.0min #1
670.1058
672.1057
669.1064
671.1070
668.1060
667.1058
673.1066
674.1041
675.1022
676.1030
677.1034
678.1033
679.1029
678.6054
676.6035
675.6012
674.6004
673.6056
671.6068
670.6069
669.6067
668.6068
667.6063
666.6054
666.1023
665.6028
665.0861
664.0989
663.0852
679.6058
m/z = 670
m/z

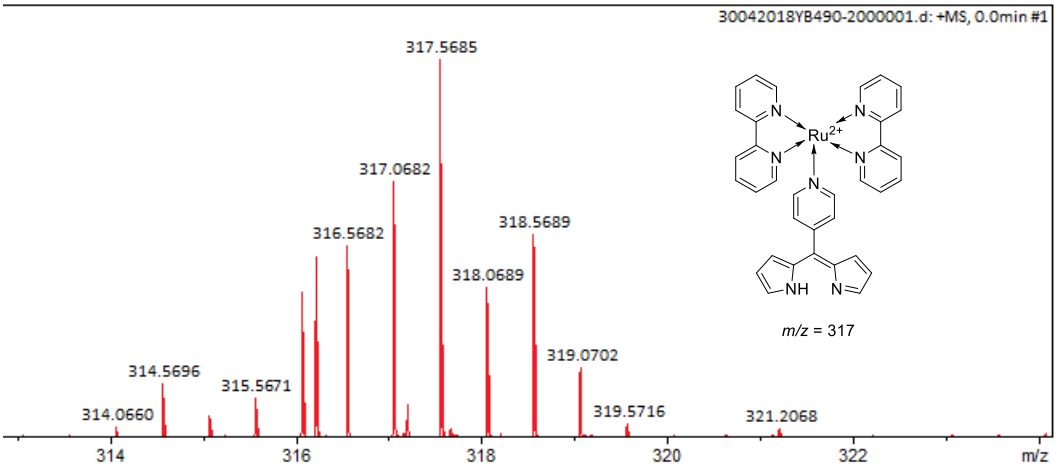
30042018YB490-2000001.d: +MS, 0.0min #1
317.5685
317.0682
316.5682
318.5689
318.0689
319.0702
314.5696
315.5671
314.0660
319.5716
321.2068
m/z = 317
m/z

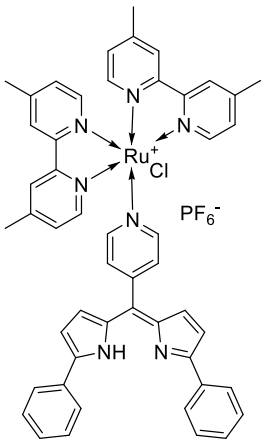

Synthesis of complex 24: In a 100 mL Schlenk tube under nitrogen atmosphere, **5** (59 mg, 0.158 mmol, 1.0 equiv.) and **19** (85 mg, 0.157 mmol, 1.0 equiv.) were solubilized in MeOH (26 mL). Under cover of light, the reaction medium was stirred at 75 °C for 2 hours and cooled to room temperature. The solvent was partially evaporated, and a solution of NH_4PF_6 (257 mg, 1.58 mmol, 10 equiv.) in water (10 mL) was added ad the reaction medium was stirred at room temperature for 2 hours. The solution was then filtered and the solid was washed with water and MeOH and dried under vacuum. **24** was obtained as a black solid. **Yield**: 73 mg, 45%. **^{1}H NMR** (300 MHz, CD_3CN) δ 13.58 (s, NH), 9.78 (d, *J* = 6.1 Hz, 1H), 8.74 (s, 2H), 8.55 (d, *J* = 5.0 Hz, 1H), 8.38 (s, 1H), 8.32 – 8.16 (m, 3H), 7.97 (d, *J* = 6.7 Hz, 4H), 7.70 (d, *J* = 5.4 Hz, 1H), 7.64 (d, *j* = 5.4 Hz, 1H), 7.61 – 7.43 (m, 8H), 7.41 – 7.31 (m, 2H), 7.06 (dd, *J* = 12.9, 4.2 Hz, 2H), 6.96 (d, *J* = 2.2 Hz, 2H), 6.62 (s, 2H), 2.66 (d, *J* = 5.8 Hz, 6H), 2.46 (d, *J* = 7.2 Hz, 6H).

Mass spectrum:

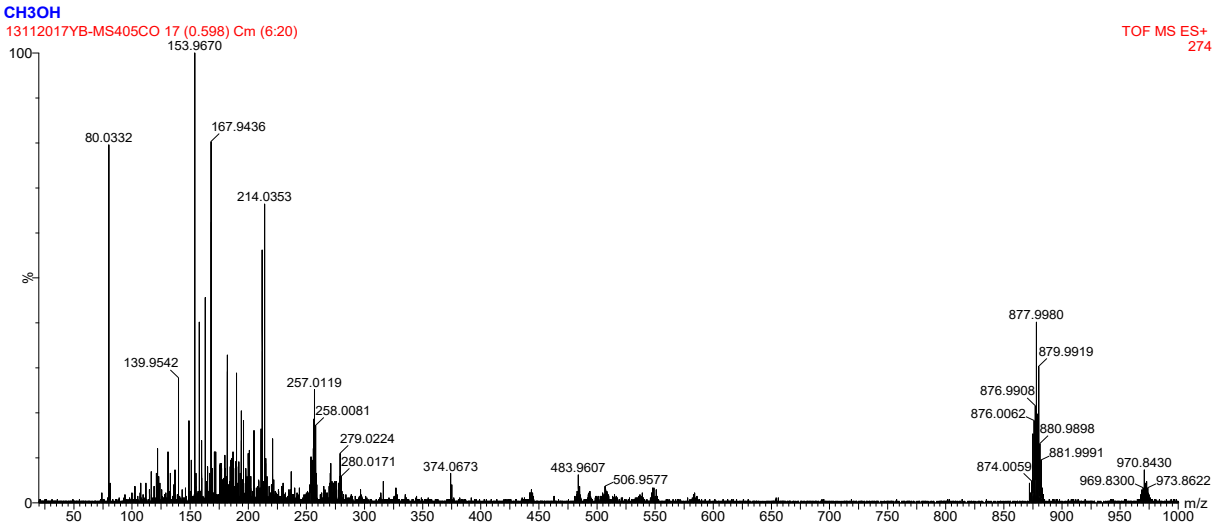

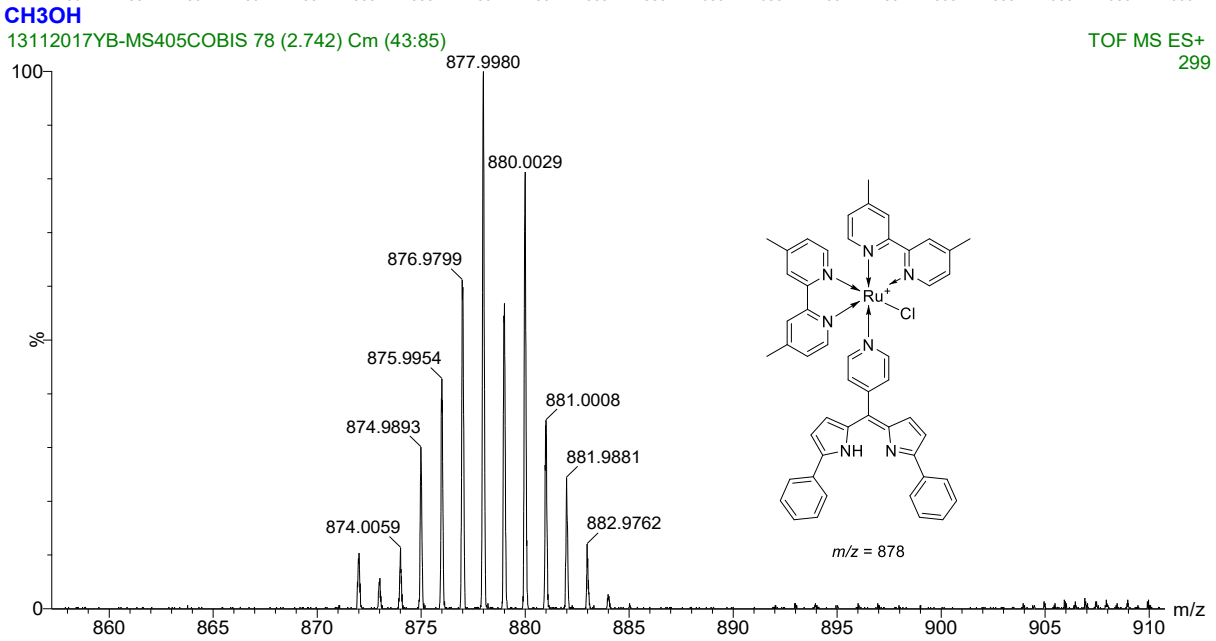

Synthesis of complex 25: In a 20 mL tube, **17** (15.8 mg, 0.0548 mmol, 1.0 equiv.) and **24** (56.0 mg,, 0.0548 mmol, 1.0 equiv.) were solubilized in acetonitrile and the reaction mixture was stirred at room temperature for 3 days. A red powder appeared. The tube was centrifugated, the solution was filtered and **25** was obtained as a red solid.

Mass spectrum:

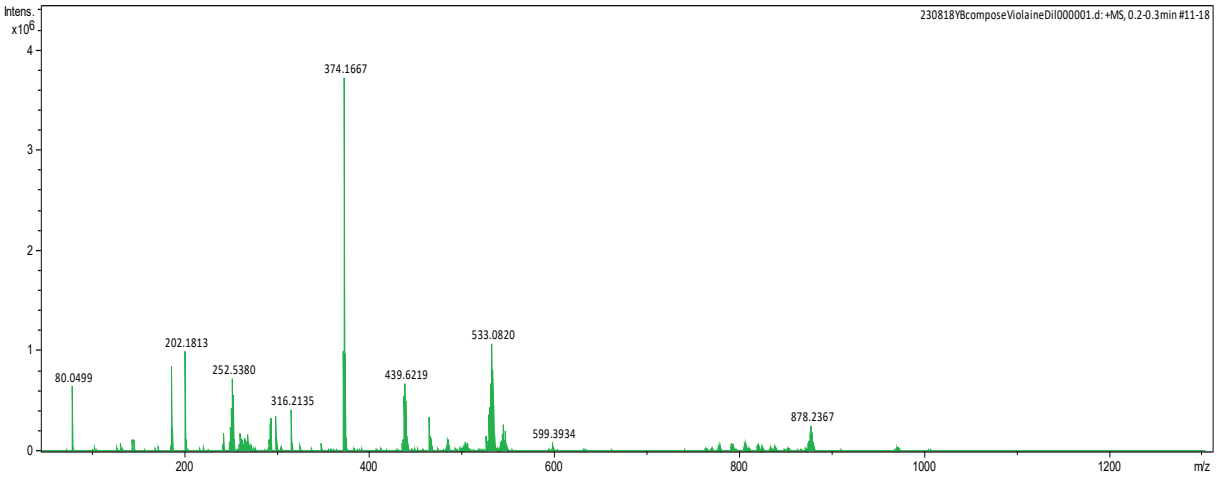

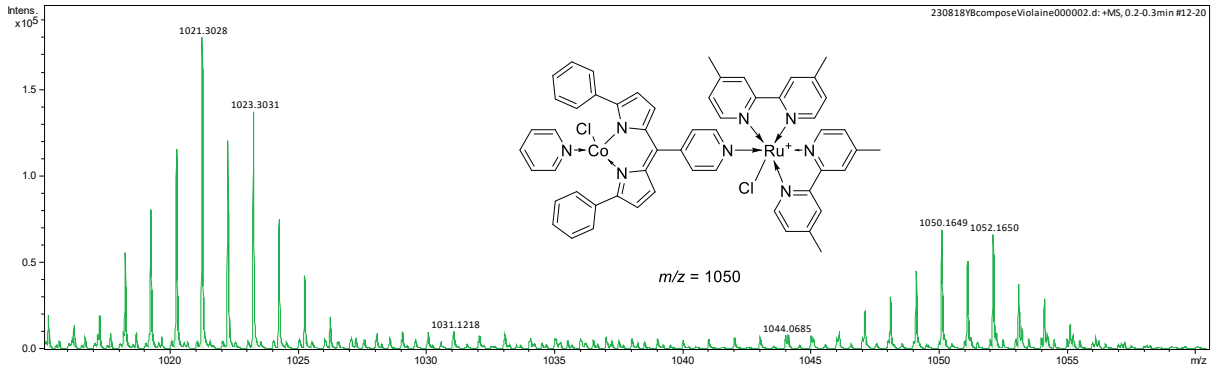

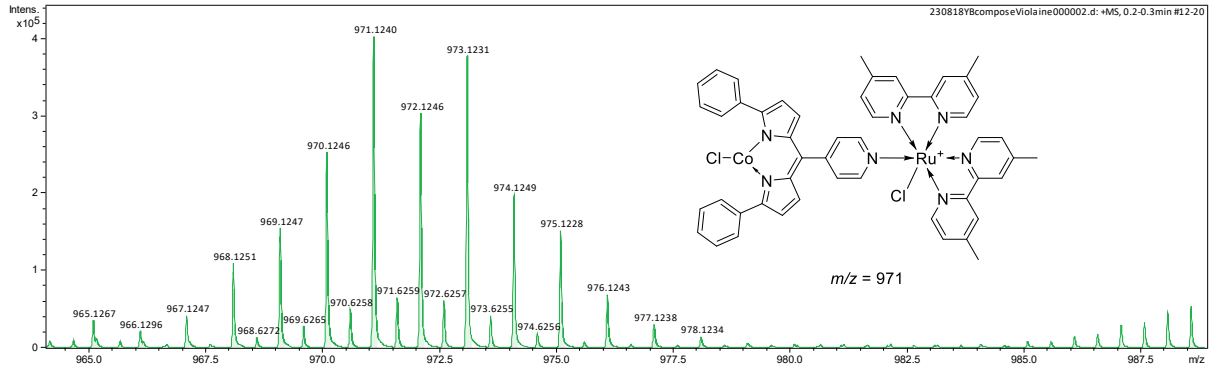

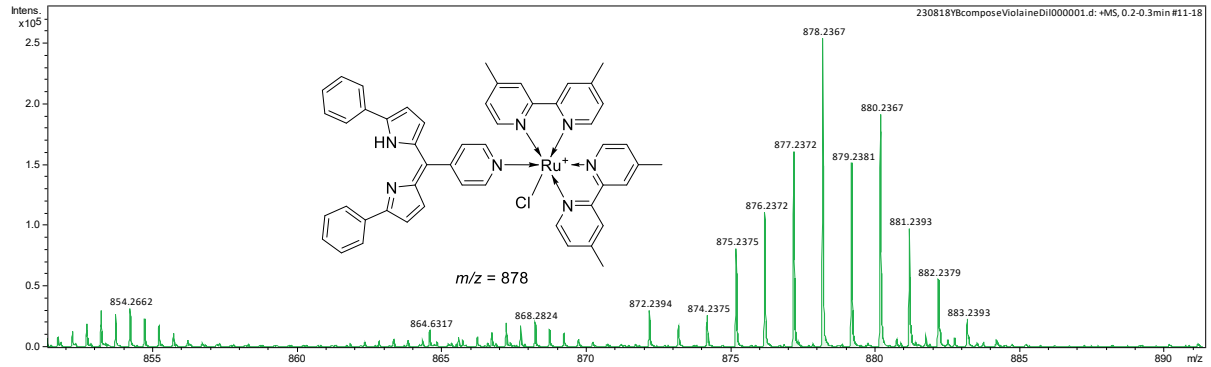

ÉCOLE DOCTORALE
Sciences chimiques : molécules, matériaux, instrumentation et biosystèmes

Titre : Complexes de cobalt à ligands *N*-hétérocycliques pour la catalyse

Mots clés : Cobalt, Couplage croisé, Ligands *N*-hétérocycliques, Catalyse

Résumé : Ces travaux de thèse se partage en deux parties distinctes : d'une part, les travaux concernant l'insertion du cobalt dans la liaison C(O)–N d'amide non-planaire, et les réactions de catalyse qui en découlent, et d'autre part, le développement d'une nouvelle famille de complexes de cobalt, basé sur ligand 5-(4-pyridyl)dipyrrométhène et ses dérivés.
Dans la première partie, qui concerne la catalyse au cobalt avec les dérivés d'amides, la réactivité de différents sels et complexes de cobalt avec les amides non-planaires a été étudiés. L'insertion du cobalt se fait en présence de bipyridine en tant que ligand, dans le DMF, avec du manganèse métallique en tant que système réducteur. L'optimisation des réactions de conversion des amides secondaires en esters et les couplages réducteurs entre amides et iodoaryles est ensuite décrite.
Dans la seconde partie, concernant la chimie de coordination du cobalt, le développement de. complexes cobalt-dipyrrométhène est présenté. Dans un premier temps, l'optimisation de la synthèse des 5-(4pyridyl)dipyrrométhène décrite, suivi de tests de complexation avec différents précurseurs de cobalt. Le ligand ayant deux sites de coordination, la coordination sélective d'un métal de transition sur un des sites dépends principalement de l'encombrement du site "dipyrrométhène". Si ce site est suffisamment encombré, le cobalt se chélate préférentiellementsur la partie pyridine. Pour forcer la coordination du cobalt dans la partie dirpyrrin, il est nécessaire de bloquer la partie pyridyl. En coordinant un précurseur de ruthénium photosensible sur la pyridine avant le cobalt, il est possbile d'obtenir un complexe bimétallique cobalt-ruthenium, permettant la photoréduction du cobalt, et donc potentiellement le développement d'une catalyse au cobalt sans réducteur métallique

Title : Cobalt complexes with *N*-heterocyclic ligands for catalysis

Keywords : Cobalt, Cross-coupling, *N*-heterocyclic ligands, Catalysis

Abstract : This thesis is divided in two distinct part: on one side, the works concerning the cobalt insertion into the C(O)–N bond of non-planar amides, and the resulting reactions, and on the other side, the development of a new family of cobalt complexes, based on the 5-(4-pyridyl)dipyrromethene ligand and its derivatives.
In the first part, concerning cobalt catalysis with amide derivatives, the reactivity of different cobalt precursors and complexes toward non-planar amides has been studied. The insertion of the cobalt can be realized en presence of bipyridine as ligand, en DMF, with manganese powder as reductant system. The otpimization of the amide-to-ester conversion and the reductive cross-coupling between amides and iodo-aryl is then described.
In the second part, concerning the coordination Chemistry of cobalt, the development of cobalt -dipyrromethene complexes is presented. Firstly, the optimization of the 5-(4-pyridyl)dipyrromethene synthesis is described, followed by complexation tests with different cobalt precursors. With two coordination sites on the ligand, the selective coordination of a transition metal on one of the sites depends mainly on the dipyrrin hindrance. If this part is hindered enough, cobalt chelate preferentially on the pyridyl part. To force the cobalt coordination on the dipyrrin part, it is necessary to occupied the pyridyl part. By coordinating a photoensitive ruthenium precursor on the pyridine, it is possible to obtain un bimetallic cobalt-ruthenium complex, allowing the cobalt photoreduction, and potentially the development of a cobalt catalysis without metallic reductant.

Université Paris-Saclay
Espace Technologique / Immeuble Discovery
Route de l'Orme aux Merisiers RD 128 / 91190 Saint-Aubin, France